Computer Modeling of the Side Impact Penetration of Dummies of Various Sizes into Padding
NTIS, August 1983

EDC Library Ref. No. 1091

DISCLAIMER

PB85-161206

August 1983
Final Report

DOT HS 806 669

U.S. Department
of Transportation
National Highway
Traffic Safety
Administration

Computer Modeling of the Side Impact Penetration of Dummies of Various Sizes Into Padding

MGA Research Corp.
58 Sonwill Drive
Buffalo, N.Y. 14225

Contract No. DTNH22-82-C-07047

TECHNICAL REPORT STANDARD TITLE PAGE

1. Report No.	2. Government Accession No.	3. Recipient's Catalog No.
DOT HS 806 669	PB85 161206/AS	

4. Title and Subtitle	5. Report Date
Computer Modeling of the Side Impact Penetration of Dummies of Various Sizes into Padding	August 1983
	6. Performing Organization Code

7. Author(s)	8. Performing Organization Report No.
David J. Segal	G37-V-3

9. Performing Organization Name and Address	10. Work Unit No.
MGA Research Corporation 58 Sonwil Drive Buffalo, NY 14225	11. Contract or Grant No. DTNH22-82-C-07047
	13. Type of Report and Period Covered Final Report 6/82 - 8/83
12. Sponsoring Agency Name and Address U. S. Department of Transportation National Highway Traffic Safety Administration Washington, D. C. 20590	14. Sponsoring Agency Code

15. Supplementary Notes

Contract Technical Manager: Dr. Carl Clark

16. Abstract

Experimental research to improve protection levels offered to automobile occupants in lateral collisions has focused on the study of responses of the 50th percentile male as a result of the availability of the Side Impact Dummy of that size. The question of the suitability of protective measures developed for the 50th percentile male for other occupant sizes is of concern. Hence, a major objective of this study was to analytically evaluate injury potential of a broad range of occupant sizes in lateral collisions in combination with various types of padding.

Two computer models were used in the study. The first was a one-dimensional lumped mass model that was used on a desk top computer to make over 120 parameter study runs. The CAL-3D crash victim simulation was also configured to represent an occupant in a lateral collision with intruding door motion.

Results of the study generally indicate that padding on the interior of the door surface is beneficial to all occupant sizes and, in fact, reduces injury severity measures more for smaller occupants than for larger. Both side impact models have been shown to be very useful in the study of side impact events and also compare favorably with experimental results.

17. Key Words	18. Distribution Statement
Side Impact Lateral Impact Computer Modeling Automobile Occupant Safety	Document is available to the public through the National Technical Information Service Springfield, Virginia 22151

19. Security Classif. (of this report)	20. Security Classif. (of this page)	21. No. of Pages	22. Price
None	None		

Form DOT F 1700.7 (8-69)

TABLE OF CONTENTS

LIST OF FIGURES

LIST OF FIGURES (Contd.)

LIST OF FIGURES (Contd.)

1. INTRODUCTION

During the past ten years, a substantial amount of effort within the highway safety community has been directed toward the problem of lateral impacts in which the front of a striking vehicle contacts the passenger compartment of a struck vehicle. A major undertaking in this area has been the development of means to assess occupant injury levels that occur during a crash test. This has resulted in development of the Side Impact Dummy (SID). The Side Impact Dummy provides the means to measure selected responses with which an injury model then operates to produce an AIS (Abbreviated Injury Scale) level by which the severity of the collision to the struck vehicle occupant in judged.

The SID, as developed, is intended to represent the median of the male population, i.e., the 50th percentile male. Test and development programs seeking to identify means of increasing the protection levels offered to occupants in lateral collisions have utilized this dummy as the basis for assessing injury. Because side impact dummies of other sizes are not available, the knowledge gained in testing with the 50th percentile male dummy is generally applied to the population as a whole.

The question can, however, be raised as to whether or not such test results apply to other occupant sizes, particularly the extremes. That is, if a protective system is developed based on 50th percentile male responses, does that system also offer protection, and if so, to what relative levels, for large adult males, small adult females and children?

The primary object of this study was to develop means of answering this question and, indeed, to explore the protection levels offered to four different occupant sizes by different paddings. Implicit in this primary objective was the sub-objective of developing procedures for simulating any sized occupant in lateral collisions based on our knowledge of the behavior of the 50th percentile SID dummy. An additional, and significant, intent of the

study was to develop means of simulating the side impact event with both a simplified lumped mass dynamics program and with the CAL-3D Crash Victim Simulation program.

The availability of representations of occupant dynamics in lateral collisions with both simple and complex computer programs is of significant benefit to the highway safety researcher. In general, a great many runs can be made with a modest effort with the simplified lumped mass model. Results are generally indicative of trends in injury resulting from wide variations of parameters. Thus, such a representation is generally useful as one aspect of benefit/cost modeling or studies. The CAL-3D representation, on the other hand, is not likely to be used when large numbers of runs covering wide variations in parameters is desired. Rather, this complex model is better utilized to check the reasonableness of simplified model results, and to investigate specific areas or problems of interest.

The project involved three principle areas of effort. These were: development of model representations of occupants in side impacts, verification of the models by comparison with test results, and use of the models to study effects of occupant size and padding on injury measures. This first area included a literature review to identify previously used approaches and data for model input and verification. A means of scaling 50th percentile data to other occupant sizes was also established. It should be mentioned that this model development activity did not consist of any computer program development. Existing computer programs were utilized. A lumped mass program called SMDYN (Spring Mass DYNamics) was used on an in-house, desk top computer while the CAL-3D as maintained by NHTSA on the McAuto Timesharing Service was used in conjunction with the User Convenience Package (Ref. 4). Model Development consisted only of defining the representation of masses and connectivity, with suitable data, to describe the side impact event.

Verification of the models was accomplished by comparing predicted results against comparable test results. We should emphasize that this was

not an attempt at rigorous validation of the models because a complete definition of the test conditions, to the detail needed for model validation, was unavailable. Rather, the verification effort attempted to demonstrate the reasonableness of the model results based on reasonable estimates of undefined test parameters. Use of the models consisted of more than 120 runs with the lumped mass model and 16 runs with the CAL-3D. The principal parameters varied included striking car impact speed, struck car occupant size and padding acting between the struck car door and occupant.

The remainder of this report is organized into six major sections. The next summarizes conclusions and recommendations resulting from the study. This is followed by a discussion of modeling approaches and modeling data sources. Sections 4 and 5 describe development and use of the lumped mass and CAL-3D models, respectively. Section 6 presents model verification comparisons and evaluations of the consistency of predictions between models. The last numbered section then summarizes significant points resulting from the study. Appendix A contains an interim report summarizing the results of the literature review conducted for the study. Appendix B provides a concise summary of the results of the lumped mass model parameter study and Appendix C documents the input data used to model various sized occupants with the CAL-3D model. Lastly, Appendix D contains a listing of the lumped mass model computer program used in the study.

2. CONCLUSIONS AND RECOMMENDATIONS

This section summarizes the conclusions developed as a result of the study described herein and presents a number of recommendations for expanding upon the results obtained.

2.1 Conclusions

1. Both the CAL-3D and lumped mass representations of the side impact occupant developed and used in the study have been verified as being reasonable predictors of side impact phenomena for adult occupants over the range of conditions studied.

   Both models predict trends which are evident in experimental results and are generally within reasonable levels of agreement in terms of peak values, injury measures, etc. The CAL-3D model appears to be better at matching the general character of struck rib response, at evaluating variations in occupant spacing from the door surface and in predicting child responses. Attempts at predicting head responses with the lumped mass model were not generally successful. This appears to require a model with more realistic connectivity like the CAL-3D which did a good job of matching experimental head responses. More effort needs to be devoted to understanding the results seen in modeling the child in this study.

2. The effects of including padding between the occupant and the interior door surface appears to be twofold as based on the results of the parameter study. First, the inclusion of padding results in a reduction of severity measures for all occupants. Second, padding helps to reduce the spread in severity measures across occupant sizes. That is, it results

in more consistent severity measures across the occupant population. Padding appears to offer incrementally more benefit to smaller occupants in that the reductions in severity measures were greater than for larger occupants.

The addition of three inches of padding to an unpadded door resulted in a slightly greater incremental benefit than did the addition of a second three inches of padding. The greatest reduction in severity measures occurred when padding was added without reduction of the initial gap between the occupant and door surface. If the inclusion of padding is assumed to reduce this gap, injury severity measures were reduced but not quite as much as if the gap were maintained. It should be emphasized that this effect was found to be much less significant than the presence of padding. That is, padding results in significant reductions in severity measures, even if the initial gap between the occupant and door surface is reduced.

3. In general, the smaller occupants sustained higher severity measures for the same collision conditions. This trend was very clear and consistent from both models for the adult occupants. The results obtained when simulating the child occupant were not always consistent with this trend nor consistent between the models. It is not fully understood whether this results from the data used to simulate the child or whether effects of the significantly larger gap simulated with the smaller occupant tend to confuse the trends. In any case, padding consistently reduced severity measures more for the smaller occupants than the larger.

4. In this study, striking vehicle impact speed was used as the primary measure of impact severity. Occupant injury severity

measures increased strongly with impact speed as would be expected. Generally, accident data analyses make use of vehicle velocity change as a basis for evaluating accident severity as it can be calculated with less physical evidence from the accident scene. Based on results of the parameter study, it appears that occupant injury severity in side impacts is a function of both struck vehicle velocity change and impacting vehicle speed. The striking vehicle speed is significant in these cases because it directly affects the velocity of the intruding door which contacts the occupant. More investigation of this dual dependence appears to be desirable.

5. The substantial number of computer simulation conducted with output of multiple injury indicies led to the opportunity of trying to identify relationships between injury indicies. Results from this study indicate that a definite relationship exists between AIS and CSI, which are calculated independently. While substantial scatter exists in cross plots of AIS and CSI, it appears that an AIS level of 2 corresponds approximately to a CSI level of 1000.

6. Results of this study indicate that both the lumped mass and CAL-3D models are useful in the study of side impact phenomena. The agreement achieved between the two models and with test results generally support the use of the simple lumped mass model to obtain a basic understanding of trends, and of the influence and the interaction amongst parameters. The ease of use of this model, in conjunction with its predictive capability, make it particularly well suited for those situations where a large number of runs covering a broad spectrum of parameter variations is to be made.

On the other hand, the CAL-3D model, being much more general, is much better suited to specific studies in which the general, overall response of the occupant is of interest. Furthermore, it is felt that the CAL-3D model or suitable test data should be used to confirm the general responses of the lumped mass model as different ranges of conditions are simulated.

2.2 Recommendations

1. Additional effort should be directed toward validation of the models used in this study. Although model comparisons with test results generally confirm that both models predict trends and general levels observed in tests, rigorous validation has not been undertaken due to lack of necessary test parameter data. It is recommended that, as additional testing projects are undertaking utilizing the SID dummy, consideration be given to developing sufficient detail in test and parameter definition in conjunction with the test activities to allow subsequent validation of side impact models.

2. The variations in padding explored in this study consisted only of padding thickness and of the spacing between it and the occupant. Additional studies should be undertaken to explore the effects of basic padding characteristics such as density or saturation pressure on occupant injury measures. With such an effort, trade-offs between padding thickness and stiffness could be evaluated to result in an optimum padding.

3. In its current configuration, the CAL-3D model of side impact occupant response requires prior knowledge and specification of the intruding door motion. As the success of this approach in conjunction with a separate rib segment has now been demonstrated, it appears worthwhile to eliminate this

restriction on door motion. The CAL-3D can be configured, using existing program options, to simulate the entire side impact event, including structural collapse of a striking car and struck door. A limited effort should be undertaken to develop and evaluate the practicality of this option.

4. The relationship of struck side occupant severity measures to striking car impact speed and struck car velocity change should be further explored. Parameter study results indicate that struck car velocity change, by itself, may not be a totally satisfactory indicator of accident severity. That is, a given velocity change to the struck vehicle can be produced by many combinations of stricking vehicle weight and speed. Higher impact speeds impose a higher velocity of the intruding door at contact with the occupant and consequently result in higher injury indicies.

   The parameter study contained only a very limited range of conditions for which this effect could be explored as it was designed for other purposes. Hence, it is not known whether occupant injury indicies are strongly related to both accident severity measures over a wide range of conditions. This should be studied further.

5. Additional effort should be directed toward study and verification of the simulated child responses. In some cases, unexpected behavior was observed. It is not known whether this resulted from the data representing the child or from other factors, one of which may have been the sizable increase in gap between the child and door due to the smaller lateral dimensions.

3. MODELING APPROACHES AND DATA

An early task within the program involved a review of pertinent literature for the purpose of assisting side impact model development and verification activites. This literature review attempted to identify information applicable to the following general areas:

- Modeling Approaches
- Modeling Parameters
- Model Development and Verification Data

An interim report was prepared (and is included as Appendix A) describing the results of this literature review and its impact on the project. In this section, each of the three areas listed above is discussed as related specifically to the activities undertaken and the application of information to the project.

3.1 Modeling Approaches

Two general modeling approaches were employed to simulate side impact events. The first was a lumped mass one-dimensional model in which discrete masses, representing various parts of an occupant and vehicle, were connected by non-linear force-deflection characteristics and dampers. The second approach involved use of the CAL-3D Crash Victim Simulation to model an automobile occupant involved in a lateral collision. It should be noted that in each case, an existing computer program was used. Development of modeling approaches was limited to defining input data sets for the systems to be simulated.

These two approaches were both used for the following reasons. The lumped mass approach is very easy to implement and relatively inexpensive to use. Thus it offers the potential for widespread use in support of, for example, benefit/cost studies. But, because lumped mass models greatly

simplify a complex system and are based to a significant extent on parameter estimates derived from test matching, legitimate concern exists as to the overall validity of the approach for conditions other than those utilized in model development.

The CAL-3D CVS is a very complex rigid body dynamics model that allows a rather detailed representation of an automobile occupant by a number of segments connected by pin or ball joints. In conjunction with this three-dimensional body dynamics model, a contact model that produces forces acting on segments through interference between ellipsoids and planes or ellipsoids and other ellipsoids provides the major interface between the occupant and the vehicle interior.

The CAL-3D allows a much more realistic representation of the automobile occupant than does a lumped mass model. The side impact event is, at a minimum, two-dimensional in terms of the motion of the occupant. Substantial rotation of the head and upper torso generally occurs which cannot be accurately accounted for with a one-dimensional representation. Furthermore, the connectivity between segments is automatically handled by specification of appropriate joints. Thus, the CAL-3D representation of the occupant in a lateral collision is expected to be more realistic over a wider range of conditions than is the lumped mass representation.

Development of each of these modeling representations (i.e., input data sets) is discussed in some detail in later sections. An important consideration in establishing modeling requirements is the means used to determine an injury severity. In addition to traditional injury severity measures of peak chest acceleration and chest severity index (CSI), an injury model relating an abbreviated injury scale number to struck rib response and occupant age was used in the study. The specific model was as follows:

$$AIS = 0.0768(V) + 0.053(AGE) - 1.89$$

where:

ΔV is the maximum velocity change of the struck rib versus the far side rib.

AGE is the age of the occupant in years.

This specific injury model was provided by the CTM as the best available at the time of the study being the current version of the work of Ref. 2.

Since the response of the struck rib is the major factor in this injury model, the implication with respect to a modeling approach is that the dynamics of the struck rib, as a minimum, must be calculated. Consequently, a separate rib mass and its interaction with the torso had to be modeled.

Note that the velocity change in the injury model is that of the struck rib relative to the far side rib. A procedure has been developed to analytically determine the response of the far rib based on the acceleration of the struck rib (Ref. 2). This approach, based on digital convolution theory, approximates the far rib acceleration with the following equation:

$$a_f(t) = \sum_{n=1}^{45} h'(n)\, a_s\,(t-n)$$

where:

a_f is the calculated acceleration of the far rib at time t.

a_s is the known acceleration of the struck rib at time t-n.

$h'(n)$ is an array of empirically based coefficients (Table 3-1)

Table 3-1

COEFFICIENTS OF "AVERAGED FINITE IMPULSE RESPONSES"

DERIVED FROM SIX LATERAL IMPACT TESTS

Term	Coefficient	Term	Coefficient	Term	Coefficient
1	0.46193	16	-0.02970	31	0.02379
2	-0.71032	17	0.01949	32	-0.00313
3	0.10809	18	0.03948	33	-0.00831
4	0.46534	19	0.13491	34	-0.04094
5	-0.11179	20	0.10206	35	-0.00038
6	0.02809	21	0.08549	36	0.02501
7	-0.38776	22	0.00164	37	0.00253
8	0.32800	23	-0.02334	38	-0.01502
9	0.29154	24	0.08463	39	-0.02452
10	-0.01035	25	0.07260	40	-0.02127
11	-0.08155	26	0.04146	41	0.00518
12	-0.04710	27	0.00164	42	0.00676
13	0.16269	28	-0.04284	43	-0.02821
14	0.14598	29	-0.03330	44	-0.03638
15	0.10515	30	0.04419	45	-0.02782

Using this approach, only the struck rib had been modeled dynamically. The maximum velocity change required for injury prediction is then obtained by approximating the far side rib acceleration from the struck rib acceleration and integrating both to obtain velocity. Both the CAL-3D and the lumped mass modeling approaches made use of this procedure to determine an AIS severity measure for the conditions simulated.

3.2 Model Parameters

Data needed to fully define and execute side impact simulation models included information to represent the vehicles involved in the collision, the occupants within the struck car and the padding material between the occupant and inner door surface. Contained in this section is a discussion of the data used within the program and the sources of that data.

3.2.1 Vehicle Data

The lumped mass modeling approach included simulation of the entire side impact event including structural collapse of both vehicles. As is described in more detail in the following section, the representation of the vehicles used within the project was based on the side impact sled facility developed by Dynamic Science, Inc. (Ref. 2). This facility simulated lateral collisions with a target sled buck containing a moving door structure whose motion relative to the target sled was controlled by programmed energy absorption units. The moving door structure was directly impacted by a striking vehicle bogie whose structural crush properties were simulated with a honeycomb material.

Using this sled facility as a basis for defining vehicle modeling requirements, three discrete vehicle masses were simulated. These were the striking vehicle, the struck vehicle door and the remainder of the struck vehicle. Force-deflection characteristics acting between the striking vehicle

and the struck vehicle door and between the door and remainder of the struck vehicle completed the information necessary for simulation of vehicle structural crash response.

These necessary data were either available directly from Ref. 2 or were derived from information obtained therein. The baseline vehicle component weights used were:

- striking vehicle - 2357 lbs.
- struck vehicle door - 165 lbs.
- struck vehicle - 2248 lbs.

The force-deflection properties acting between vehicle masses are illustrated in Figure 3-1.

The remaining vehicle properties needed consisted of interior door surface crush characteristics for the baseline vehicle condition. Ref. 3 contains summaries of tests conducted to obtain such data. Interior stiffness tests were performed by forcing rigid body forms into the interior door structure of a VW Rabbit. A number of tests were performed on vehicle doors that had previously been impacted and deformed into the passenger compartment. An impacting vehicle was also secured to the struck vehicle door. Thus, the test configuration closely duplicates the actual crash environment as door force-deflection characteristics were obtained from already deformed (from the outside) door structures backed up by the striking vehicle front structure.

Static tests at various levels of door intrusion were reported in Ref. 3. For purposes of the reported project, door structure crush properties at the upper torso and pelvis levels measured at the medium door intrusion level (13.5 inches) were used to represent the baseline condition to be simulated. Force-deflection properties actually used are shown in Figure 3-2. Note that these properties represent the door structure only. Padding

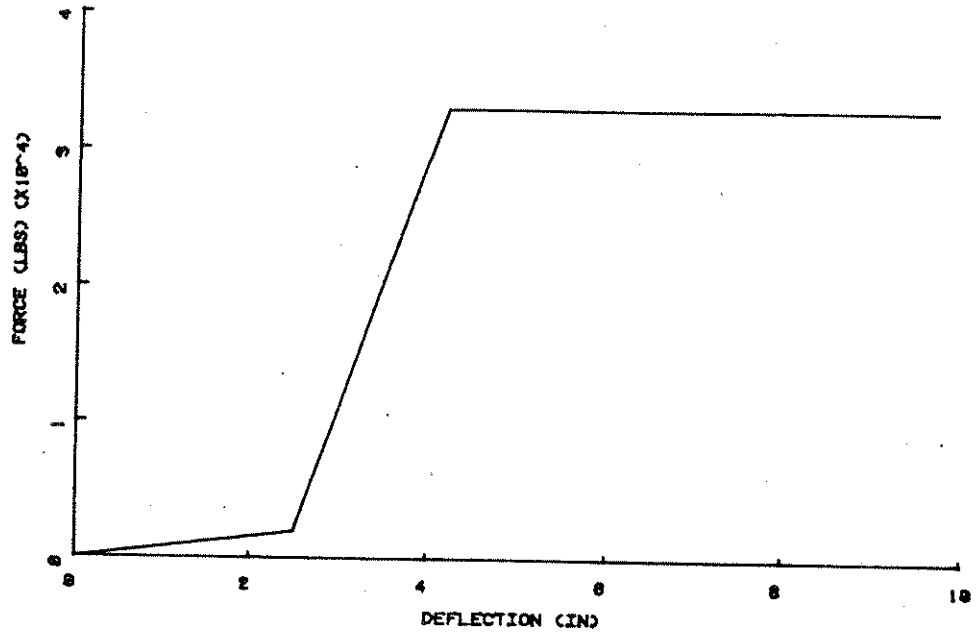

a) Bullet Vehicle Structural Crush

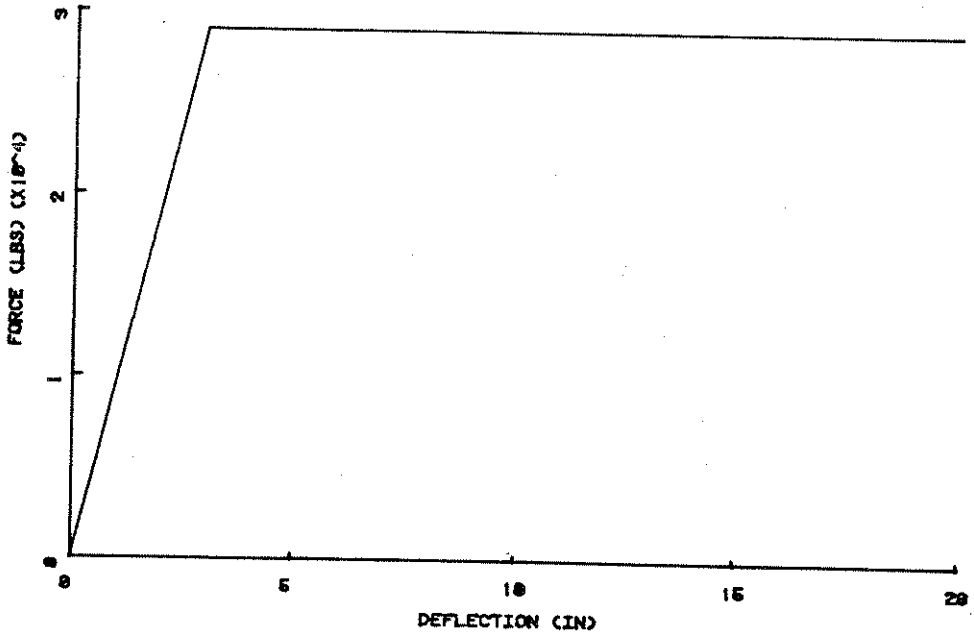

b) Target Vehicle Door Crush

Figure 3-1 SIMULATED VEHICLE STRUCTURAL FORCE-DEFLECTION PROPERTIES

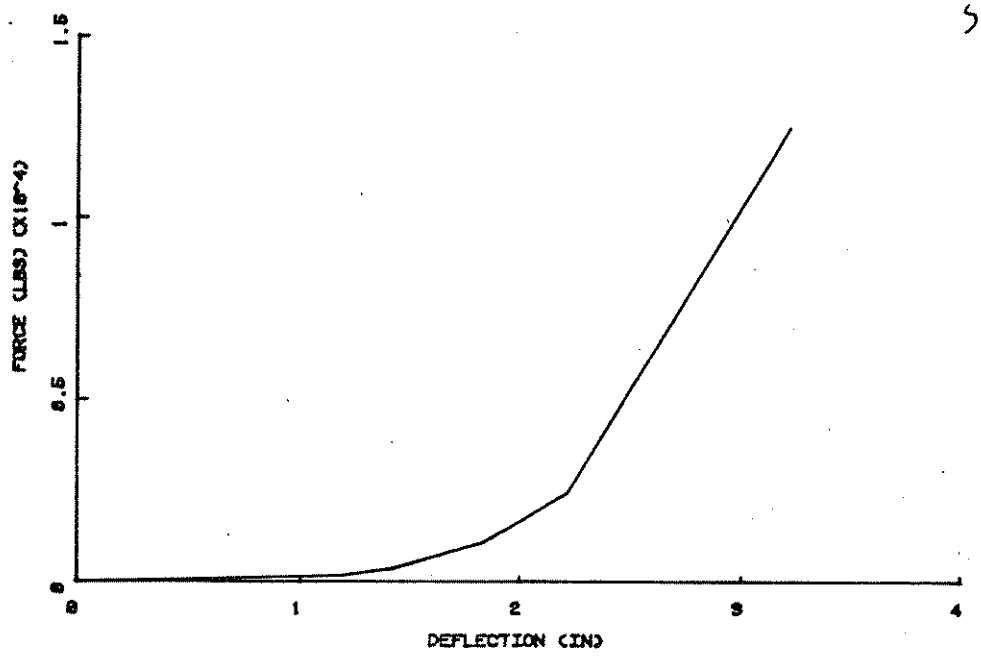

a) Upper Door Area

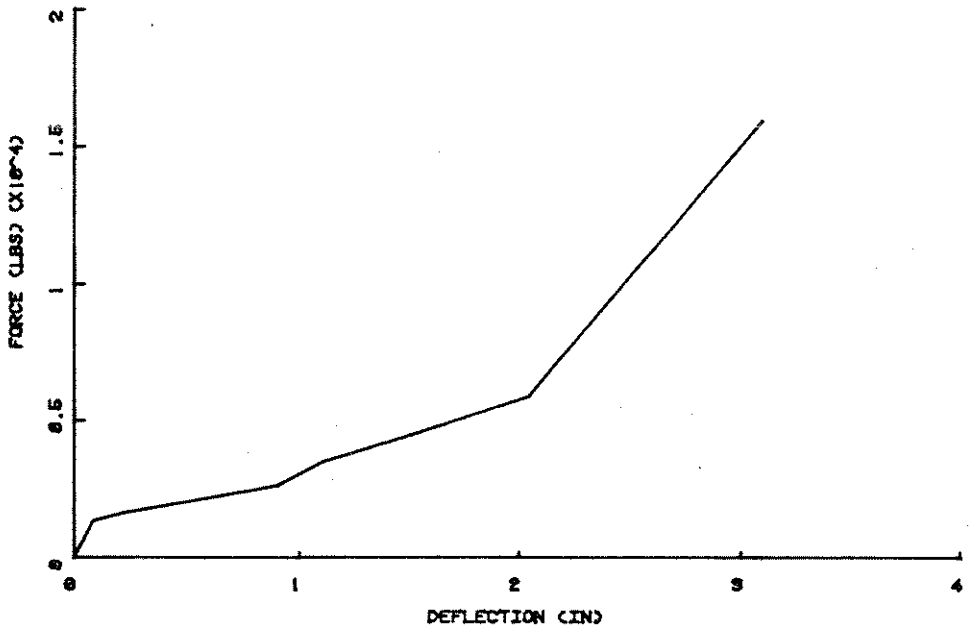

b) Lower Door Area

Figure 3-2 SIMULATED INTERIOR DOOR STRUCTURE FORCE-DEFLECTION PROPERTIES

material properties and dummy skin properties were added to those shown to represent the total force-deflection characteristics acting between the door and occupant as appropriate.

3.2.2 Occupant Parameters

A major objective of the project was to study the differences in protection levels offered by padding to occupants of various sizes in lateral collisions. Thus, the ability to model different sized occupants was fundamental to the study.

Initial efforts with respect to developing mathematical descriptions of a vehicle occupant for the study were concentrated on the 50th percentile male occupant size. In particular, a definition of the properties of the SID dummy, developed specifically for side impact situations, was needed as a starting point. The SID dummy is based on the Part 572 50th percentile male dummy but has a completely different upper torso structure. Principle data requirements for the lumped mass modeling approach consisted of:

- Segment weight distribution
- Pelvis and upper torso external skin and padding force-deflection properties
- Effective force-deflection properties acting between the rib segment and the spinal segment

Data required for the CAL-3D modeling approach consisted of the above items plus all additional data (e.g., segment moments of inertia, joint properties and locations, etc.) required by the CAL-3D. This additional data was available in the form of an existing 50th percentile male data set on the User Convenience Package Data Library (Ref. 4) and was used generally unmodified.

In reviewing available literature, only a very limited amount of information was found to describe the needed characteristics of the SID dummy. Pelvis padding and skin force-deflection properties of a Part 572 dummy are presented in Ref. 5. Force-deflection properties needed for the thorax (both external padding and rib motion properties) were reported in Ref. 6. However, these data reflected an early model SID which did not contain recent modifications to the rib and torso structure.

As a result, it was decided to make certain static force-deflection measurements on a recent SID at MGA in order to be sure that those used in the subsequent modeling activities were from an up-to-date SID. A SID dummy was provided by NHTSA and compression tests were made on the foam and skin material external to the rib structure and on the rib structure relative to the spinal structure. Photographs of the test setups are shown in Figure 3-3 and resulting force-deflection data are illustrated in Figure 3-4.

Pelvis foam and skin external force-deflection properties were reported in Ref. 5 and were therefore not measured at MGA. The data, taken from that reference, are illustrated in Figure 3-5. Damping characteristics of the SID torso damper were obtained from Ref. 6. In that reference, an average damping coefficient of 5.03 lb. sec/in was determined from impact tests on a damper unit. Hence, this value was used in all 50th percentile male simulations.

While disassembled for static testing, the SID upper thorax structure was weighed both complete and separated into rib and spinal elements. These measurements resulted in weights of 26 pounds for each of the elements. We should note that these data provided a reference for subsequent modeling activities, but, for a number of reasons, as are discussed later, were not used exactly in either the lumped mass or CAL-3D representations.

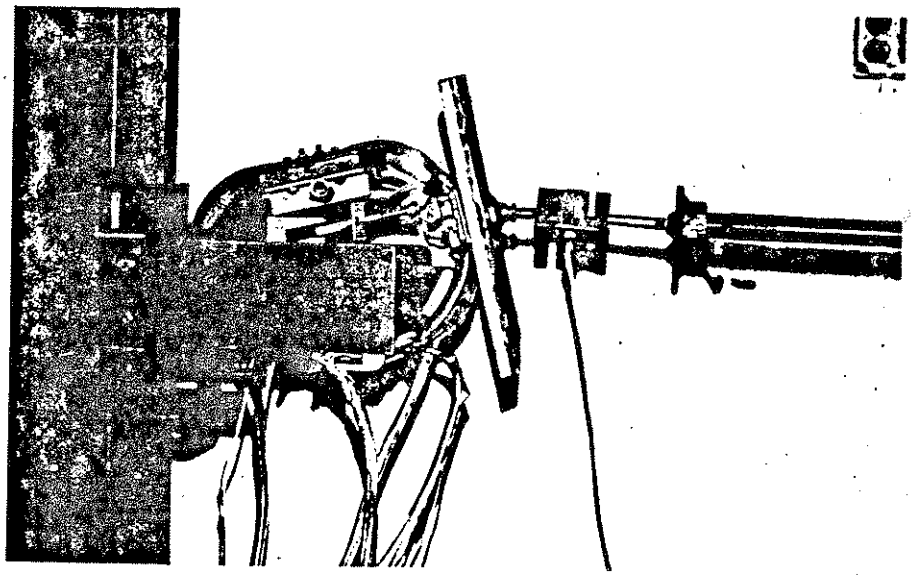

a) Rib to Torso Stiffness

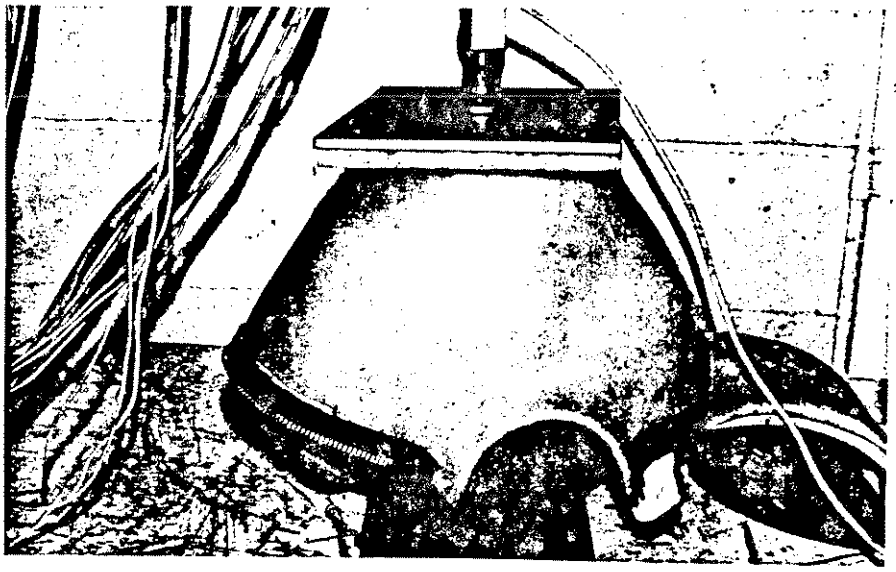

b) External Foam & Skin Stiffness

Figure 3-3 PHOTOGRAPHS OF TEST SETUP

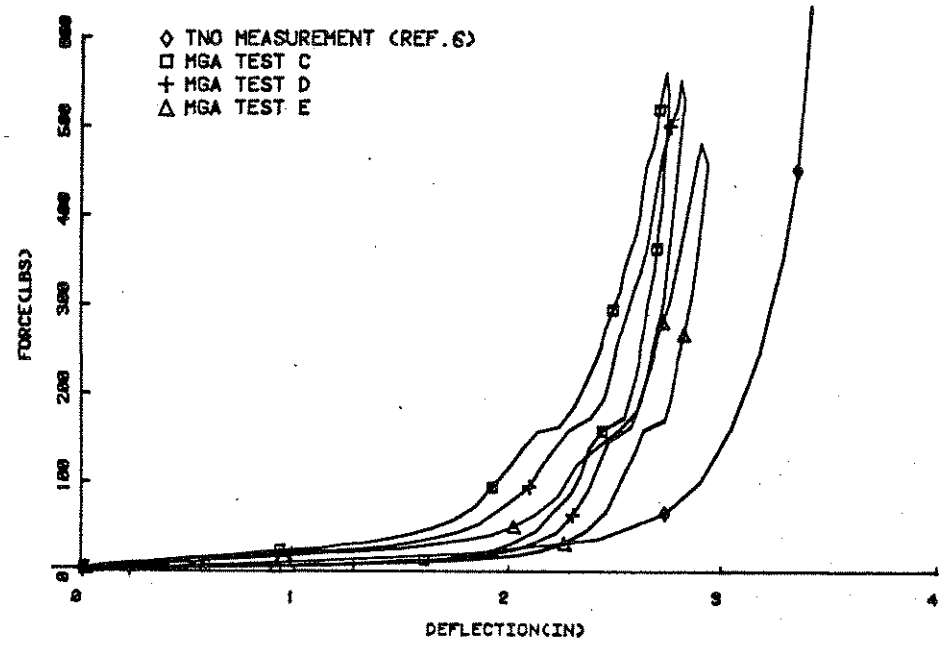

a) Ribcage Measurements

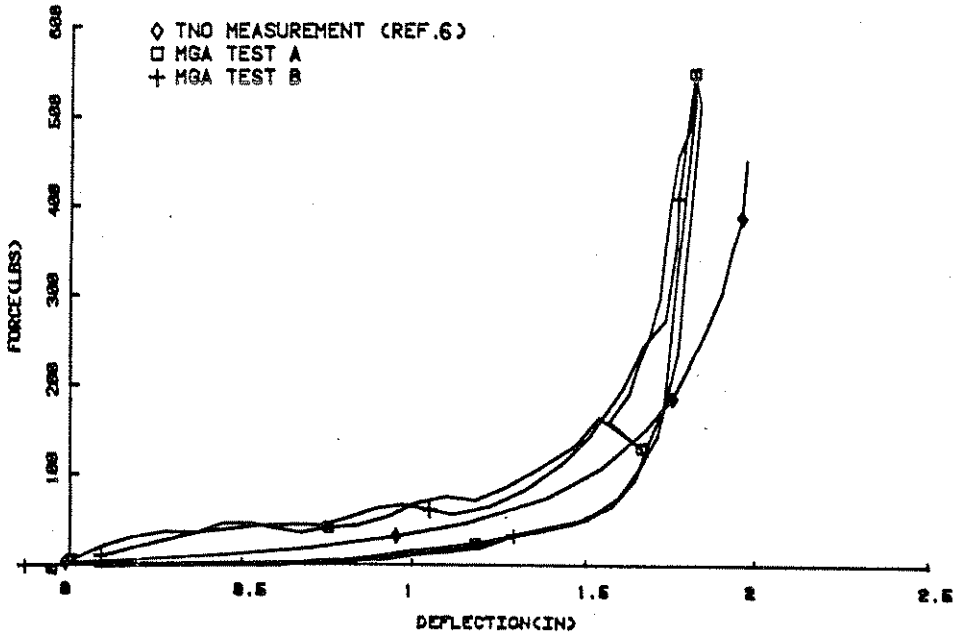

b) Jacket and Skin Measurements

Figure 3-4 SID RIBCAGE AND SKIN FORCE-DEFLECTION PROPERTIES

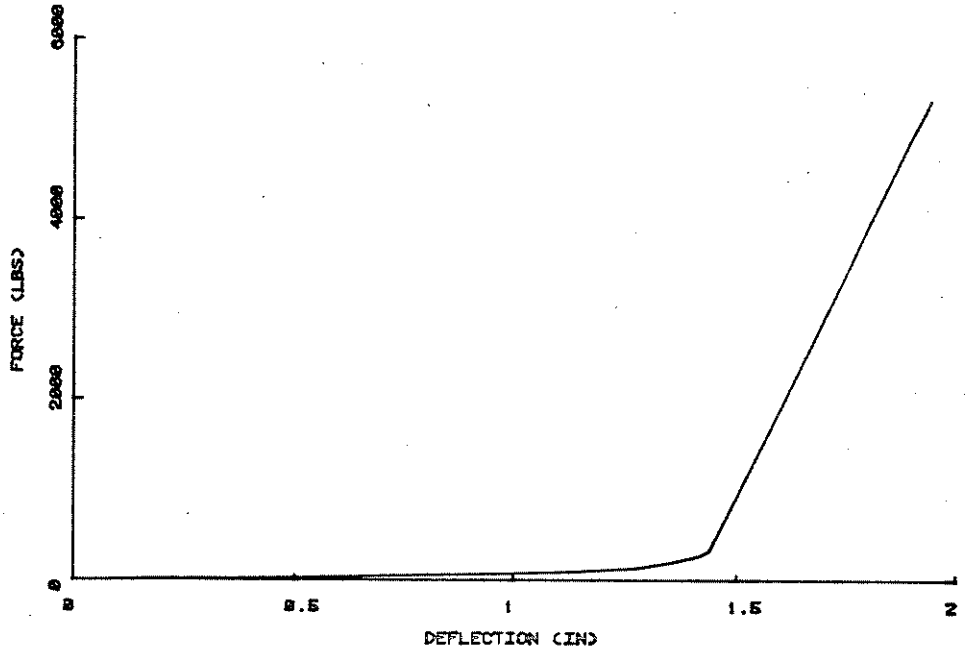

Figure 3-5 SID PELVIS PADDING PROPERTIES (FROM REF. 5)

For example, the best matching of rib and torso acceleration responses with corresponding test results for the lumped mass model was obtained with a rib weight of 20 lbs. and a spinal weight of 32 lbs.

Once data for describing a 50th percentile male side impact occupant were available based largely on SID properties, it was necessary to develop corresponding information for the other occupant sizes to be studied. These were the 95th percentile male, the 5th percentile female and the 6 year old child.

For purposes of this study, a rigorous definition of occupant anthropometry for application to the modeling activities was not warranted. That is, the general objective of the study was to show trends in injury severity over a broad range of occupant sizes, padding thicknesses and impact speeds. Indeed, rigorous definition of properties of occupants of various sizes for use in the lumped mass model was not possible since parameters for the 50th percentile male case corresponding to the SID were to some extent based on engineering judgment.

Rather than a rigorous definition of the specific occupant data sets used in the study, the approach taken, at least for adult occupants, was to develop a mathematic procedure for developing data sets for any sized adult from the baseline data set. This approach consisted of geometric and material scaling. It is recognized that the resulting extreme occupant sizes may not reflect precise anthropometric definitions, but they do, however, represent reasonable and extreme conditions of the population. Furthermore, this approach applies a consistent mathematical procedure that can be applied with consistency to all modeling activities.

It should be emphasized that scaling is normally applied to model and prototype situations where there exists large differences in size (or scale). That is, ratios of 1:3 or even 1:100 are commonly employed. On the

other hand, with this application, only small differences in scale were considered. For instance, almost the entire adult population is represented in a size range less than ± 15 percent from the 50th percentile male. This means the scaling technique is used to estimate (or approximate) incremental changes from the 50th percentile occupant size.

As mentioned, the basic scaling principles applied assumed geometric and material similarity between the occupant sizes. This results in the following scaling of variables where S is the scale factor:

	Prototype	Model
Length	L	LS
Displacement	X	XS
Strain	ε	ε
Stress	σ	σ
Time	t	tS
Velocity	V	V
Strain rate	$\dot{\varepsilon}$	$\dot{\varepsilon}/S$
Gravity	g	g/s
Density	ρ	ρ

From these variables, other significant parameters can be determined.

From a modeling viewpoint, occupant percentile size is determined by weight. This means that from the two known weights, a scale factor can be determined. Thus, if W_{50} is the weight of the 50th percentile and W_i is the weight of the other occupant, then:

$$\frac{W_i}{W_{50}} = S^3$$

where S is the scale factor between the two occupants. Or conversely,

$$S = \sqrt[3]{\frac{W_i}{W_{50}}}$$

defining the scaling relation which relates model length to prototype length:

$$\frac{L_i}{L_{50}} = S$$

Because the stresses remain constant (see listing above) forces and moments can be scaled:

$$\frac{\text{Force}}{\text{Length}^2} = \text{Stress}$$

$$\text{Moment} = \text{Force} \times \text{length}$$

which results in:

$$\frac{F_i}{F_{50}} = S^2$$

$$\frac{M_i}{M_{50}} = S^3$$

Hence, data changes can now be estimated for the occupant size variations.

It should be noted that in the mathematical models, only the occupant is changed. That is, the vehicle related parameters remain unchanged. Based on these scaling relationships scale factors for the 95th percentile male and 5th percentile female occupant (relative to the 50th percentile) and established as follows:

$$S_{95} = \sqrt[3]{\frac{W_{95}}{W_{50}}} = 1.0977$$

$$S_{5} = \sqrt[3]{\frac{W_{5}}{W_{50}}} = 0.8583$$

These scale factors were then applied to modifying 50th percentile dummy parameters (masses, force-deflection properties, and damping) to represent the different adult sized occupants. A comparison of the lumped mass occupant segment weights and thorax damping resulting is given below:

Occupant Size

	5th	50th	95th
Total Weight (lbs.)	104.	161.	177.
Effective Rib weight (lbs)	12.6	20.0	26.4
Effective Spinal weight (lbs)	20.2	32.0	42.3
Effective Pelvic weight (lbs)	50.0	79.0	104.5
Thorax damping (lb-sec/in)	3.71	5.03	6.06

While it is reasonable to assume that a scaling procedure could produce acceptable adult size occupant data sets, it was recognized that geometric scaling from an adult to a child sized data set was inappropriate. Therefore, the development of modeling data for the 6 year old child was undertaken separately. The approach taken was that of ratioing existing data. That is, an existing 6 year old child data set was available on the CAL-3D User Convenience Package data library. The ratio of the rib weight to the total torso weight for the child was kept the same as for the 50th percentile male data set. This resulted in a rib and upper torso weight of 5.6 and 8.9 lbs.

For all occupants, forces acting between segments were scaled from the corresponding 50th percentile properties based on scaling relationships

discussed earlier. However, a scale factor based on total weight was not explicitly derived in developing 6 year old child data. Since a major purpose of the model related to rib dynamic response, it was assumed that a scale factor (for the purpose of scaling force-deflection properties to the child) was developed from the cube root of the ratio of the 6 year old child rib weight to the 50th percentile male rib weight. Thus, this scale factor was used to modify the thorax force-deflection and damping properties measured for the adult male to approximate a 6 year old child.

Complete data decks were available for CAL-3D representations of the standard 50th and 95th male, 5th female and 6 year old child dummies. Thus, the major effort in developing suitable data sets for side impact modeling was that of separating a rib mass element out of the total upper torso segment. This was done by comparing predicted rib responses with those measured in tests for the 50th percentile occupant. Best overall results were achieved with a rib weight of 15 lbs. and the remainder of the upper torso segment reduced to 16.75 lbs. Note that this rib weight is less than that simulated with the lumped mass model (20 lbs) and less than that measured on the SID (26 lbs). However, in the CAL-3D representation, the arms were considered as separate segments joint connected to the upper torso. Thus, the model was not intended to represent the SID dummy directly, but rather a normal dummy (with arms) that included a separate rib segment that responded in a manner similar to that of the SID.

Initially, this 15 lb. rib weight, suitably scaled, was also applied to the other adult occupant sizes. However, because the distribution of mass between the three segments of the torso varied considerably amongst the three occupant data decks, it was found that subtracting a scaled 15 lb. rib weight from the total upper torso segment left little weight for the remainder of the upper torso segment. This appeared to be unreasonable and thus, new occupant data sets representing the 5th female and 95th male were generated from the 50th male data set by applying the scaling laws described earlier. This insured the distribution of total upper torso mass into rib and spinal

elements of approximately equal weight was uniformly applied to all adult occupant sizes.

In the case of the child, complete scaling from the 50th percentile male was inappropriate. However, it was felt that the distribution of total torso mass into a lower, center, upper torso and neck segments could be reasonably accomplished in a manner similar to the 50th male. The total torso weight from the existing 6 year old child data set on the CAL-3D User Convenience Package data library was therefore distributed accordingly to produce a new 6 year old child data set. Segmenting the upper torso into rib and spinal elements was accomplished by rationing in the same manner as existed in the 50th male data set.

3.2.3 Padding Properties

The ultimate force acting between the vehicle door and the occupant consists of three elements--the door structure, the occupant skin and padding, and padding (if any) attached to the inside of the door surface. In order to be used in either model, force-deflection properties for each element had to be available and had to be combined in series to represent a single, overall force-deflection characteristic.

Padding force-deflection characteristics were developed based on the stress-strain relationship illustrated in Figure 3-6 and geometrical properties of the occupants. This relationship, taken from Ref. 2, is based on compression tests of low density (2 lb/cubic foot) polyurethane foam and has a saturation level of approximately 20 psi. Padding thicknesses of 3 and 6 inches were simulated in the parameter study, hence, these values represent the 100% strain condition.

Stress (or pressure) was converted into a force by integrating the pressure as a function of depth of penetration over a truncated cylinder assumed to represent the occupant body segment geometry. The lengths and

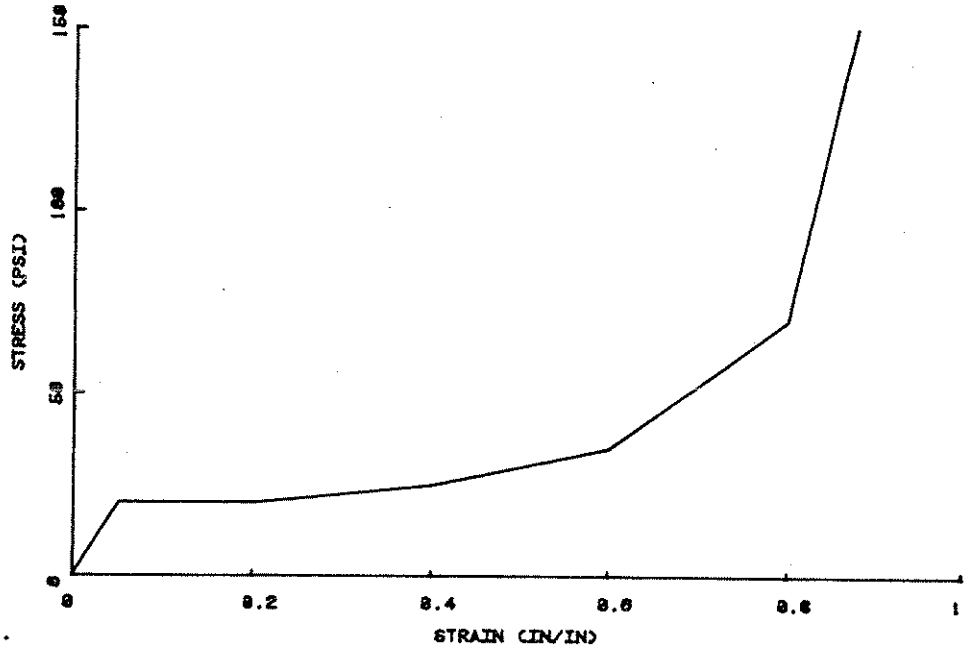

Figure 3-6 SIMULATED FOAM PROPERTIES

radii of body segments impinged into the padding for purposes of determining force-deflection characteristics for each occupant size are shown in Table 3-2.

Table 3-2
BODY DIMENSIONS ASSUMED FOR CONTACT WITH PADDING

Occupant Size	Upper Torso		Pelvis	
	Radius	Length	Radius	Length
50th % Male	4.5	7.0	5.0	13.5
95th % Male	4.9	7.7	5.5	14.8
5th % Female	3.9	6.0	4.3	22.6
6 year old child	2.9	4.6	3.3	8.8

Based on these dimensions, the complete force-deflection properties for 3 inch thick padding are shown in Figure 3-7 for each occupant size. Note that the initial rise in the curves resulted from bottoming of the dummy external skin while the final rise results from bottoming of the door padding.

In addition, the actual gap between the occupant and padded surface varied as a function of both occupant size and padding type. Based on lateral

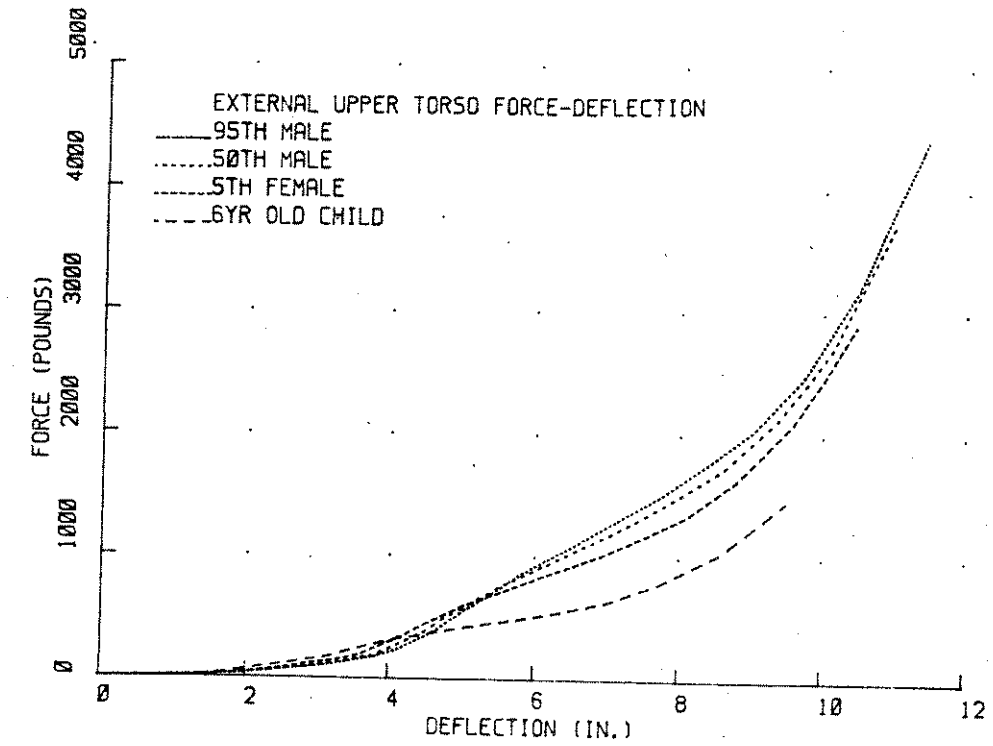

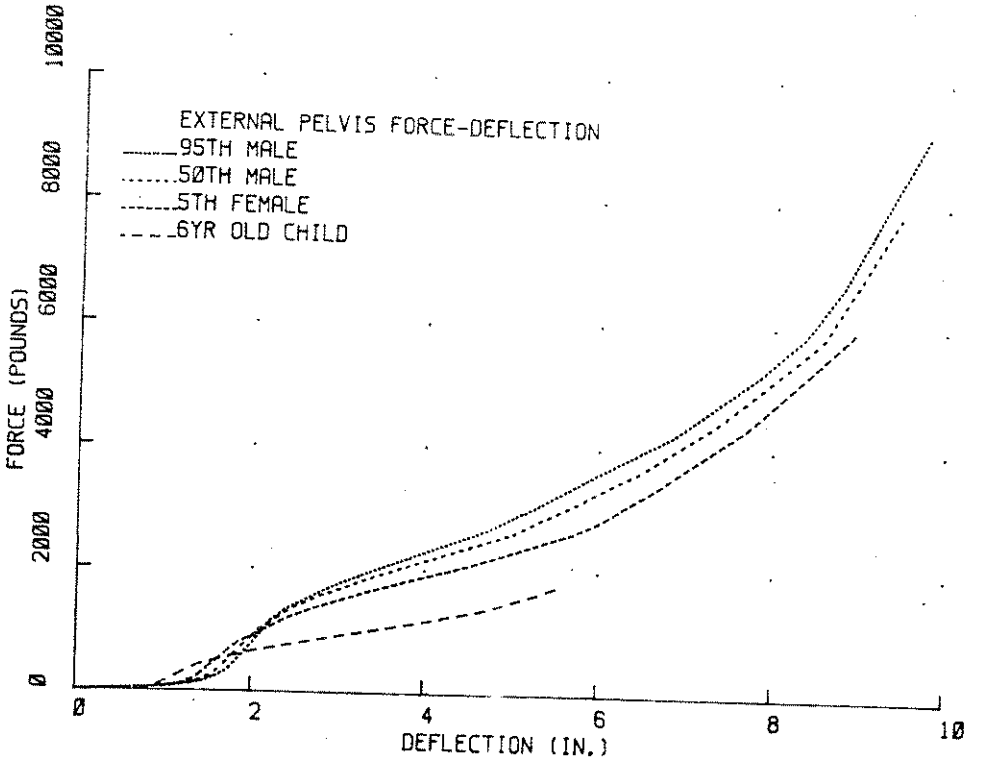

Figure 3-7 THREE INCH PADDING FORCE-DEFLECTION PROPERTIES

dimensions of the SID torso and pelvis, the gaps listed in Table 3-3 were used as a baseline condition without padding. As 3 or 6 inches of padding were simulated, these gaps were either reduced by that amount or were maintained at the initial spacings. Note that throughout the parameter study, reference is made to either 6.8, 3.8 or 0.8 inch gap conditions. This refers to the gap condition existing for the 50th percentile occupant with different paddings. Other occupants had different actual gaps based on their individual lateral dimensions.

Table 3-3

GAP VALUES FOR UNPADDED CONDITION

	Torso Gap (in.)	Pelvis Gap (in.)
50th % Male	6.83	8.33
95th % Male	6.0	7.5
5th % Female	8.03	9.53
6 Year Old Child	10.42	11.92

4. LUMPED MASS MODEL

The primary purpose of development of a simple, lumped mass model of the side impact event was to allow the use of simplified procedures in association with other modeling activities to evaluate benefits and costs of injury reduction measures. Since it is recognized that any lumped mass model representation of the side impact dummy is less than an ideal analog, some concern over the development of model parameters and the range of validity of the model results are warranted. In this section, the development of the lumped mass representation and use are described. Verification of the representation is discussed in Section 6 where comparisons with test results are presented.

4.1 Lumped Mass Model Development

To a substantial degree, the specific configuration of masses and springs used within a lumped mass model depends on the intended use of the model or its results. In the case of the side impact dummy development effort, a great deal of testing (both cadaver and dummy) has been done in which acceleration measurements at a struck rib and at a spinal location were made. The reasons for these measurements are based on the biomechanics of injury and have led to the development of an injury prediction algorithm based on the dynamics of the struck rib.

The use of this injury prediction algorithm then dictates a minimum model of the occupant's torso composed of a struck rib mass coupled to a spinal mass through a non-linear spring element. While this minimum model formed the basis for the primary injury measure, other considerations led to expansion of the model to include both a pelvic and a head mass as well as representation of the striking and struck cars. The final lumped mass model configuration is shown in Figure 4-1.

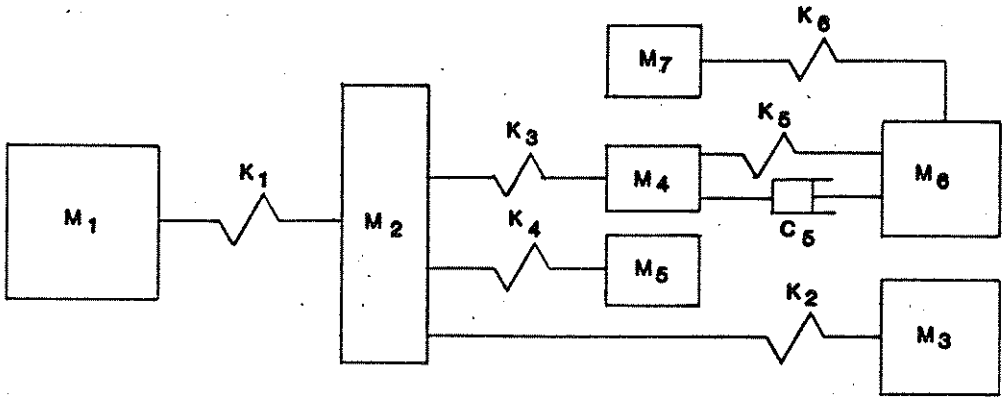

M_1 = striking car mass
M_2 = struck car door mass
M_3 = remainder of struck car mass
M_4 = struck rib mass
M_5 = pelvic and lower body effective mass
M_6 = effective upper torso mass
M_7 = head mass

K_1 = striking car frontal crush characteristics
K_2 = struck car door crush characteristics
K_3 = dummy external skin and torso padding
K_4 = dummy external skin and pelvic padding
K_5 = dummy rib compliance
K_6 = effective head to torso compliance
C_5 = dummy rib damping

Figure 4-1 LUMPED MASS SIDE IMPACT MODEL

It should be noted that the actual computer program for simulation of lumped mass dynamics was previously available at MGA. Thus, no program development was necessary. Rather, model development consisted of configuring the springs and masses to adequately represent the system and developing suitable data. The program was provided to NHTSA for subsequent use and is installed on the NHTSA VAX 11/780 computer system.

Data for the model came from a variety of sources. Information for representing the striking and struck cars including both mass values and structural force-deflection properties were obtained from data presented in Ref. 3. Note that this data is representative of the side impact sled testing device designed and fabricated to simulate actual car-to-car lateral crash tests. Emphasis was placed on simulation of tests conducted with this device because a rather large data base was available for comparison and verification of model results.

Data for describing the mass distribution and connectivity of the occupant was not as readily available. The breakout of discrete mass elements to represent various body elements from a continuous system is somewhat subjective. However, based on measurements of the SID component weights and force-deflection properties described in the previous section, and adjustments of parameter values in attempting to best match results from tests, a baseline 50th percentile occupant data set was developed. Sources for individual data elements are described below:

K_5 - Dummy rib compliance and damping. Force-deflection properties of the rib structure relative to the spine were measured at MGA. Damping value used was reported in Ref. 6.

K_3 - External skin and padding properties. Force-deflection properties of foam and skin external to

the rib structure were measured at MGA. Upper door padding properties were obtained from Ref. 3 for a standard door structure. These properties were then combined in series (with additional padding properties if appropriate) to form a single compliance.

K_4 - Pelvic external skin and padding properties. Pelvic lateral force-deflection properties were obtained from Ref. 5. These were combined in series with door structure properties (Ref. 3) and padding as appropriate.

K_6 - Head to neck compliance. A pseudo spring characteristic was developed from a CAL-3D side impact run by plotting the head acceleration times head weight against the difference between head and upper torso lateral displacement. (Note, it is recognized that this is a very restrictive representation that is likely to produce reasonable results only at a limited set of conditions.)

M_5 - Pelvic Mass. Effective mass reflected in the pelvis to lower door contact. Value previously used (Ref. 2) was also used in this study.

M_4,M6 - Effective rib mass and remainder of upper torso mass. The values of these two masses were based on the total weight of the upper torso as measured at MGA (52 lbs.) and an adjusted distribution of mass between the two that resulted in the best compromise of responses as compared to test results.

Note, no coupling is included between the torso and pelvis (M_6 and M_5). The head is assumed to make no contact although in some car-to-car impacts, it is seen to make contact with the hood of the penetrating (bullet) car (Ref. 2).

Table 4-1 summarizes the lumped mass weights and torso damping values used for the baseline 50th percentile occupant. Note that vehicle weights were obtained from Ref. 2 as representative of actual side impact sled component values. Masses for the occupant, in conjunction with force-deflection properties, represented the best compromise between physical measurements and predicted responses. The force-deflection characteristic acting between the rib and spinal mass used in the model is shown in Figure 4-2. The intial portion of this curve was developed from measurements of a SID with most up-to-date modifications. The linear bottoming portion of the curve was assumed.

As noted in the previous section, geometric scaling was assumed as a basis for modifying this 50th percentile data to reflect other adult occupant sizes. This approach was believed to be reasonable for estimating properties of a 95th male and 5th female since the actual differences are quite small relative to traditional scale factor usage. However, this approach was not directly used for the 6 year old child data set in which significant changes in weight distribution amongst body segments was expected. In this case, lumped mass parameters were actually developed based on an existing CAL-3D 6 year old child dummy data set. The weights of the individual torso segments were then ratioed in a manner identical to that of the 50th percentile occupant. Damping and thorax force-deflection data were then scaled based on a geometric scale factor developed from rib weights.

A compilation of weight and damping data used in the lumped mass model for all occupant sizes is provided in Table 4-2.

Table 4-1

BASELINE 50TH PERCENTILE OCCUPANT DATA VALUES

M_1	-	Striking Car Weight	=	2357 lbs.
M_2	-	Struck Door Weight	=	165 lbs.
M_3	-	Struck Car Weight	=	2248 lbs.
M_4	-	Struck Rib Weight	=	20 lbs.
M_5	-	Effective Pelvic Weight	=	79 lbs.
M_6	-	Effective Upper Torso Weight	=	32 lbs.
M_7	-	Head Weight	=	10.2 lbs.
C_5	-	Torso Damper	=	5.03 lb/(in/sec)

Table 4-2

EFFECTIVE WEIGHT AND DAMPING DATA SUMMARY FOR ALL OCCUPANTS

	50th	5th Female	95th Male	6 Yr Old
Rib weight	20	12.6	26.4	5.6
Spinal weight	32	20.2	42.3	8.9
Pelvic weight	79	50.0	104.5	21.0
Head weight	10.2	7.4	12.4	7.2
Thorax Damping	5.03	3.71	6.06	2.15

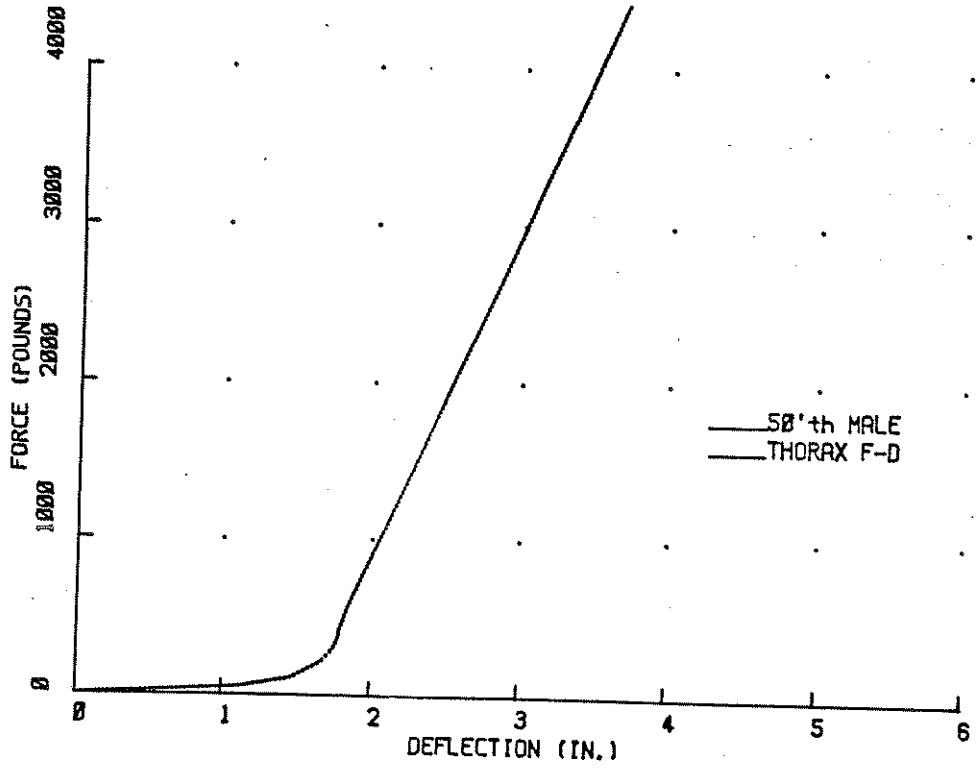

Figure 4-2 FIFTIETH PERCENTILE MALE RIB TO SPINE FORCE-DEFLECTION CHARACTERISTIC

Comparisons between lumped mass model predictions and corresponding test results were made in order to attempt to validate or verify the results of this occupant representation. A detailed discussion of these comparisons is contained in Section 6. Next, the parameter study conducted with this model is described.

4.2 Lumped Mass Parameter Study

The parameter study conducted with the lumped mass model consisted of 123 runs investigating the effects of changes to four parameters. These were:

- Occupant size
- Striking vehicle speed
- Padding characteristics
- Striking vehicle weight

As indicated previously, four occupant sizes were studied representing a 50th percentile male, 95th percentile male, 5th percentile female and 6 year old child. Striking vehicle speeds studied were 10, 20, 30 and 40 MPH. Striking vehicle weight variations included vehicles of 1650, 2350 and 3250 lbs.

Five different padding configurations were simulated. The first condition was that of a standard interior door structure with no padding. That is, the forces acting between the occupant and door resulted from crush of the interior door structure and the simulated occupant skin. In conjunction with this pading condition, an initial gap between the 50th percentile pelvis and door surface of 8.3 inches was simulated. The corresponding upper body gap was 6.8 inches. The remaining four padding conditions simulated either 3 or 6 inches of light weight (20 psi) polyurethane foam placed between the occupant and door (thus reducing the gap

by a corresponding amount) or installed in an effectively widened car permitting the initial nominal 6.8 inch gap irrespective of padding thickness.

The actual padding representation was that of a pressure vs. deflection characteristic as mentioned in the previous section. An approximation of the geometric interface between the occupant and padding, which varied with occupant size, was used to develop a force vs. deflection characteristic from pressure vs. deflection. The complete force-deflection characteristic acting between the occupant and door consisted of a series combination of this padding characteristic, an appropriate occupant skin and padding characteristic, and a door structure characteristic.

Given the basic parameters to be varied, a parameter study consisting of 123 runs was structured. The complete run matrix is listed in Table 4-3. Note from the table that emphasis has been placed on variations in occupant size, padding thickness and striking car speed.

Figure 4-3 illustrates typical time history responses resulting from the parameter study runs. This example, Run 3 in the parameter study, is a 30 MPH impact speed with a 50th percenitle male occupant and an unpadded door structure. The nominal impact vehicle weight of 2350 lbs. was used. As is seen in the figure, the struck vehicle experiences a velocity change of abour one-half the striking vehicle velocity. The struck vehicle door achieves a maximum velocity relative to the occupant compartment in excess of 25 MPH early in the event. Accelerations of the struck rib and pelvis result directly from interactions with the door. Accelerations of the upper torso and head masses lag the rib response as a result of the force-deflection coupling. The rib and upper torso exhibit an out-of-phase oscillation after the initial impact.

Similar results (i.e., time history plots) were available for each of the 123 runs made in the study. However, in view of the large amount of data resulting from the study, emphasis was instead placed on quantifying run

Table 4-3

LUMPED MASS PARAMETER STUDY

(SEE APPENDIX B FOR RESULTS SUMMARY)

RUN No.	OCCUPANT	PADDING/GAP	STRIKING SPEED	VEHICLE WEIGHT
1	50th Male	0"/6.8"	10 mph	2350 lbs.
2	50th Male	0"/6.8"	20 mph	2350 lbs.
3	50th Male	0"/6.8"	30 mph	2350 lbs.
4	50th Male	0"/6.8"	40 mph	2350 lbs.
5	95th Male	0"/6.8"	10 mph	2350 lbs.
6	95th Male	0"/6.8"	20 mph	2350 lbs.
7	95th Male	0"/6.8"	30 mph	2350 lbs.
8	95th Male	0"/6.8"	40 mph	2350 lbs.
9	5th Female	0"/6.8"	10 mph	2350 lbs.
10	5th Female	0"/6.8"	20 mph	2350 lbs.
11	5th Female	0"/6.8"	30 mph	2350 lbs.
12	5th Female	0"/6.8"	40 mph	2350 lbs.
13	50th Male	3"/3.8"	10 mph	2350 lbs.
14	50th Male	3"/3.8"	20 mph	2350 lbs.
15	50th Male	3"/3.8"	30 mph	2350 lbs.
16	50th Male	3"/3.8"	40 mph	2350 lbs.
17	95th Male	3"/3.8"	10 mph	2350 lbs.
18	95th Male	3"/3.8"	20 mph	2350 lbs.
19	95th Male	3"/3.8"	30 mph	2350 lbs.
20	95th Male	3"/3.8"	40 mph	2350 lbs.
21	5th Female	3"/3.8"	10 mph	2350 lbs.
22	5th Female	3"/3.8"	20 mph	2350 lbs.
23	5th Female	3"/3.8"	30 mph	2350 lbs.
24	5th Female	3"/3.8"	40 mph	2350 lbs.
25	50th Male	6"/0.8"	10 mph	2350 lbs.
26	50th Male	6"/0.8"	20 mph	2350 lbs.
27	50th Male	6"/0.8"	30 mph	2350 lbs.
28	50th Male	6"/0.8"	40 mph	2350 lbs.
29	95th Male	6"/0.8"	10 mph	2350 lbs.
30	95th Male	6"/0.8"	20 mph	2350 lbs.
31	95th Male	6"/0.8"	30 mph	2350 lbs.
32	95th Male	6"/0.8"	40 mph	2350 lbs.
33	5th Female	6"/0.8"	10 mph	2350 lbs.
34	5th Female	6"/0.8"	20 mph	2350 lbs.
35	5th Female	6"/0.8"	30 mph	2350 lbs.
36	5th Female	6"/0.8"	40 mph	2350 lbs.
37	50th Male	3"/6.8"	20 mph	2350 lbs.
38	50th Male	3"/6.8"	30 mph	2350 lbs.
39	95th Male	3"/6.8"	20 mph	2350 lbs.
40	95th Male	3"/6.8"	30 mph	2350 lbs.
41	5th Female	3"/6.8"	20 mph	2350 lbs.
42	5th Female	3"/6.8"	30 mph	2350 lbs.
43	50th Male	6"/6.8"	20 mph	2350 lbs.
44	50th Male	6"/6.8"	30 mph	2350 lbs.
45	95th Male	6"/6.8"	20 mph	2350 lbs.
46	95th Male	6"/6.8"	30 mph	2350 lbs.
47	5th Female	6"/6.8"	20 mph	2350 lbs.
48	5th Female	6"/6.8"	30 mph	2350 lbs.
49	6Yr old	0"/6.8"	20 mph	2350 lbs.
50	6Yr old	0"/6.8"	30 mph	2350 lbs.
51	6Yr old	3"/3.8"	20 mph	2350 lbs.
52	6Yr old	3"/3.8"	30 mph	2350 lbs.
53	6Yr old	6"/0.8"	20 mph	2350 lbs.
54	6Yr old	6"/0.8"	30 mph	2350 lbs.
55	6Yr old	3"/6.8"	20 mph	2350 lbs.
56	6Yr old	3"/6.8"	30 mph	2350 lbs.
57	6Yr old	6"/6.8"	20 mph	2350 lbs.
58	6Yr old	6"/6.8"	30 mph	2350 lbs.
59	50th Male	0"/6.8"	20 mph	1650 lbs.
60	50th Male	0"/6.8"	30 mph	1650 lbs.
61	50th Male	0"/6.8"	40 mph	1650 lbs.
62	50th Male	0"/6.8"	10 mph	3250 lbs.
63	50th Male	0"/6.8"	20 mph	3250 lbs.
64	50th Male	0"/6.8"	30 mph	3250 lbs.
65	50th Male	3"/3.8"	20 mph	1650 lbs.
66	50th Male	3"/3.8"	30 mph	1650 lbs.
67	50th Male	3"/3.8"	40 mph	1650 lbs.
68	50th Male	3"/3.8"	10 mph	3250 lbs.
69	50th Male	3"/3.8"	20 mph	3250 lbs.
70	50th Male	3"/3.8"	30 mph	3250 lbs.
71	50th Male	6"/0.8"	20 mph	1650 lbs.
72	50th Male	6"/0.8"	30 mph	1650 lbs.
73	50th Male	6"/0.8"	40 mph	1650 lbs.
74	50th Male	6"/0.8"	10 mph	3250 lbs.
75	50th Male	6"/0.8"	20 mph	3250 lbs.
76	50th Male	6"/0.8"	30 mph	3250 lbs.
77	95th Male	0"/6.8"	20 mph	1650 lbs.
78	95th Male	0"/6.8"	30 mph	1650 lbs.
79	95th Male	0"/6.8"	40 mph	1650 lbs.
80	95th Male	0"/6.8"	10 mph	3250 lbs.
81	95th Male	0"/6.8"	20 mph	3250 lbs.
82	95th Male	0"/6.8"	30 mph	3250 lbs.
83	95th Male	3"/3.8"	20 mph	1650 lbs.
84	95th Male	3"/3.8"	30 mph	1650 lbs.
85	95th Male	3"/3.8"	40 mph	1650 lbs.
86	95th Male	3"/3.8"	10 mph	3250 lbs.
87	95th Male	3"/3.8"	20 mph	3250 lbs.
88	95th Male	3"/3.8"	30 mph	3250 lbs.
89	95th Male	6"/0.8"	20 mph	1650 lbs.
90	95th Male	6"/0.8"	30 mph	1650 lbs.
91	95th Male	6"/0.8"	40 mph	1650 lbs.
92	95th Male	6"/0.8"	10 mph	3250 lbs.
93	95th Male	6"/0.8"	20 mph	3250 lbs.
94	95th Male	6"/0.8"	30 mph	3250 lbs.
95	5th Female	0"/6.8"	20 mph	1650 lbs.
96	5th Female	0"/6.8"	30 mph	1650 lbs.
97	5th Female	0"/6.8"	40 mph	1650 lbs.
98	5th Female	0"/6.8"	10 mph	3250 lbs.
99	5th Female	0"/6.8"	20 mph	3250 lbs.
100	5th Female	0"/6.8"	30 mph	3250 lbs.
101	5th Female	3"/3.8"	20 mph	1650 lbs.
102	5th Female	3"/3.8"	30 mph	1650 lbs.
103	5th Female	3"/3.8"	40 mph	1650 lbs.
104	5th Female	3"/3.8"	10 mph	3250 lbs.
105	5th Female	3"/3.8"	20 mph	3250 lbs.
106	5th Female	3"/3.8"	30 mph	3250 lbs.
107	5th Female	6"/0.8"	20 mph	1650 lbs.
108	5th Female	6"/0.8"	30 mph	1650 lbs.
109	5th Female	6"/0.8"	40 mph	1650 lbs.
110	5th Female	6"/0.8"	10 mph	3250 lbs.
111	5th Female	6"/0.8"	20 mph	3250 lbs.
112	5th Female	6"/0.8"	30 mph	3250 lbs.
113	6Yr old	6"/6.8"	40 mph	2350 lbs.
114	5th Female	6"/6.8"	40 mph	2350 lbs.
115	50th Male	6"/6.8"	40 mph	2350 lbs.
116	95th Male	6"/6.8"	40 mph	2350 lbs.
117	6Yr old	3"/6.8"	40 mph	2350 lbs.
118	5th Female	3"/6.8"	40 mph	2350 lbs.
119	50th Male	3"/6.8"	40 mph	2350 lbs.
120	95th Male	3"/6.8"	40 mph	2350 lbs.
121	6Yr old	0"/6.8"	40 mph	2350 lbs.
122	6Yr old	3"/3.8"	40 mph	2350 lbs.
123	6Yr old	6"/0.8"	40 mph	2350 lbs.

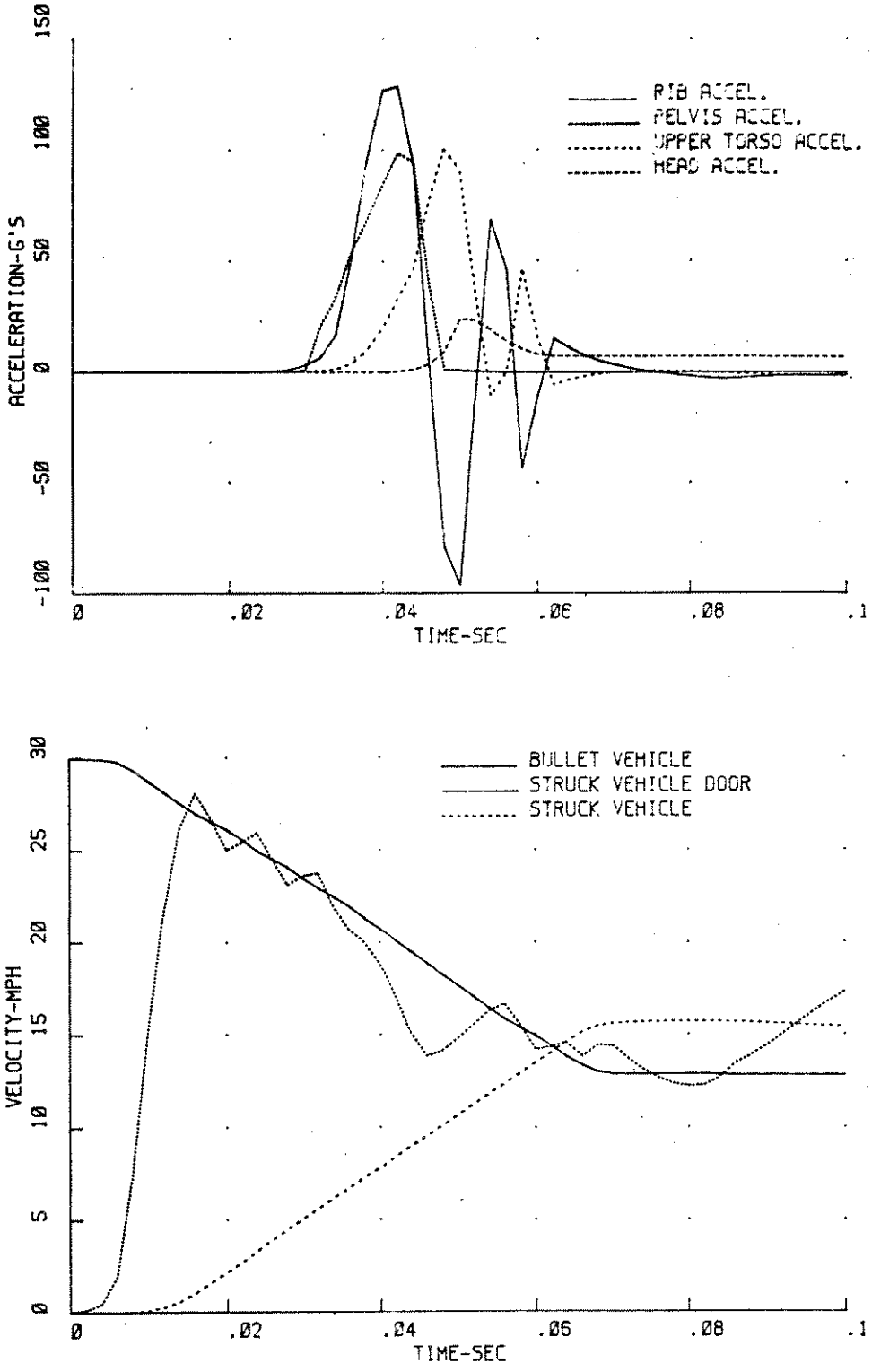

Figure 4-3 TYPICAL LUMPED MASS TIME-HISTORY RESPONSES

results by a number of single valued metrics. These included:

- Peak rib Gy
- Peak torso Gy
- Peak pelvis Gy
- AIS
- CSI
- Maximum rib delta - V
- Maximum torso delta - V
- Door velocity at contact with rib

Each of these metrics is tabulated for all runs made in Appendix B. For purposes of the subsequent discussion, emphasis was placed on three values - AIS, CSI and peak torso Gy - as representing commonly used severity indices for lateral impacts. However, all values are listed in the appendix and are installed on a data base management system at MGA Research for subsequent analysis.

It should also be noted that for calculation of an AIS, a common age of 30 years was assumed. This assumption is obviously not correct for children. Indeed the application of an AIS equation developed by regression of adult cadaver test results to the child may be less than ideal. However, at a minimum, a consistent measure of injury potential based on struck rib response relative to the far side rib is obtained by this means.

Unpadded Door Results

Figure 4-4 illustrates three different severity measures as a function of bullet car impact speed for each of the occupants simulated. The results shown in this figure are for the no-padding condition with the nominal 6.8 inch gap between the occupant and interior door surface. As expected, all severity measures increase with increasing impact velocity. Note, however,

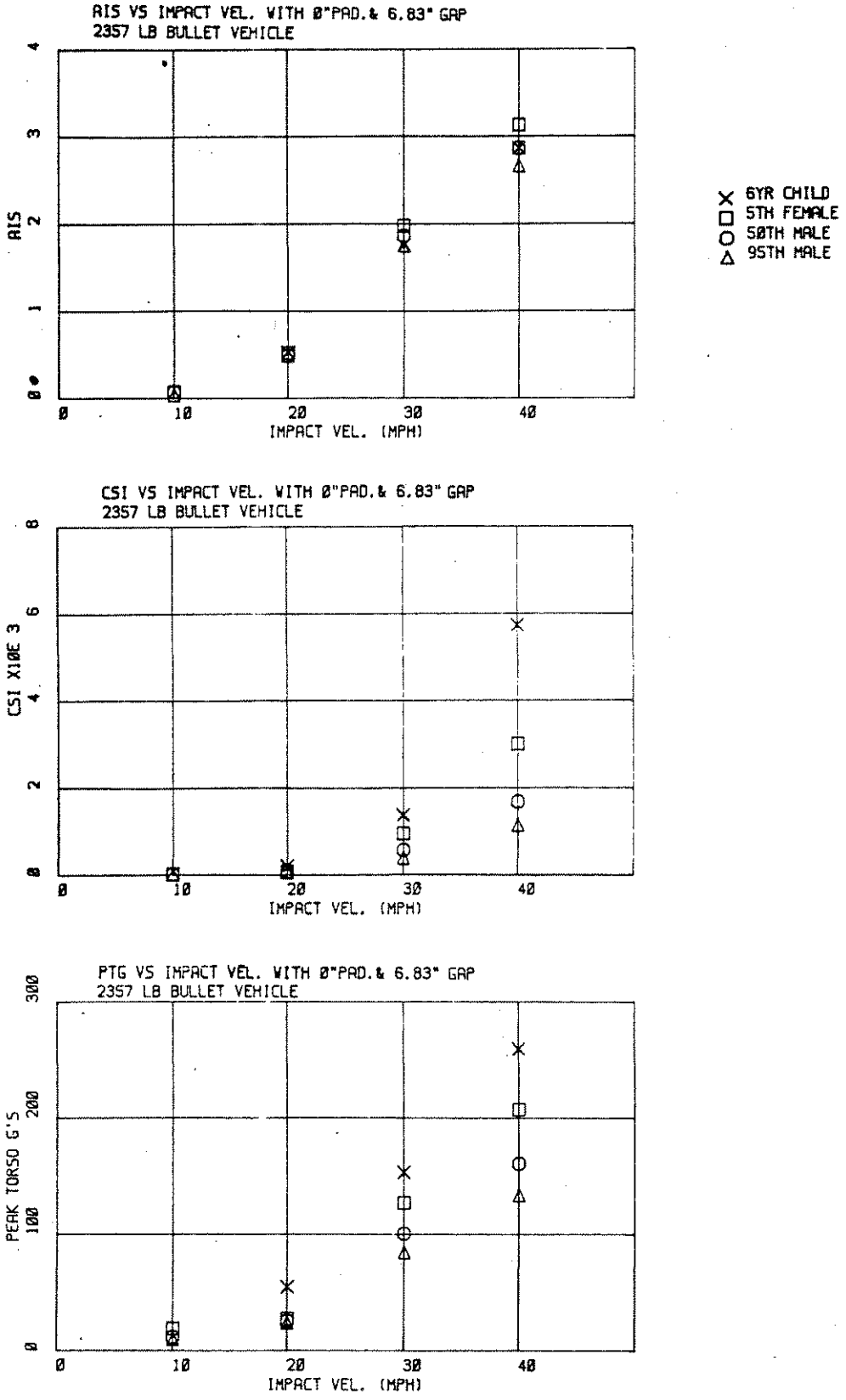

Figure 4-4 SIMULATED INJURY MEASURES FOR UNPADDED DOOR SURFACE

that the range of values across occupant size for a given impact speed is much less for the AIS severity measure than for the CSI or peak torso acceleration measures. Also note that, unlike the other measures, the AIS values for the 6 year old child are less than those seen for the 5th percentile female.

As mentioned earlier, for purposes of this study, the AIS severity measure was actually used as an indication of maximum velocity change of the struck rib relative to the far rib. This was done to allow direct comparison of severity measures irrespective of occupant age which is an important factor in the AIS algorithm. Figure 4-5 illustrates the struck rib and upper torso responses for the four occupants at a striking vehicle speed of 30 MPH and no interior door padding. In the rib responses, two peaks are evident. The first results from direct contact with the intruding door surface. The second results from a coupled dynamic response between the rib and upper torso masses. It should be noted that a number of effects are present in the first response peak which duplicate real world situations. First, the total force-deflection property acting between the door mass and rib mass represents a scaled and unscaled component. That is, the door structure properties remain the same, irrespective of the occupant while the occupant external skin and padding properties were scaled to account for size differences. Second, and in this case perhaps more significant, each occupant was assumed to be seated at the centerline of the seat. Thus, the initial gap between the occupant and door varied with occupant size. The nominal condition referred to in this study as a 6.8" gap is based on the 50th percentile seating geometry. This gap varied as follows for the other sizes.

95th male	- 6.0" gap
5th female	- 8.0" gap
6 year old child	- 10.4" gap

Thus, the response differences in the first peak reflect differing force-deflection properties and different spacings between the occupant and door surface.

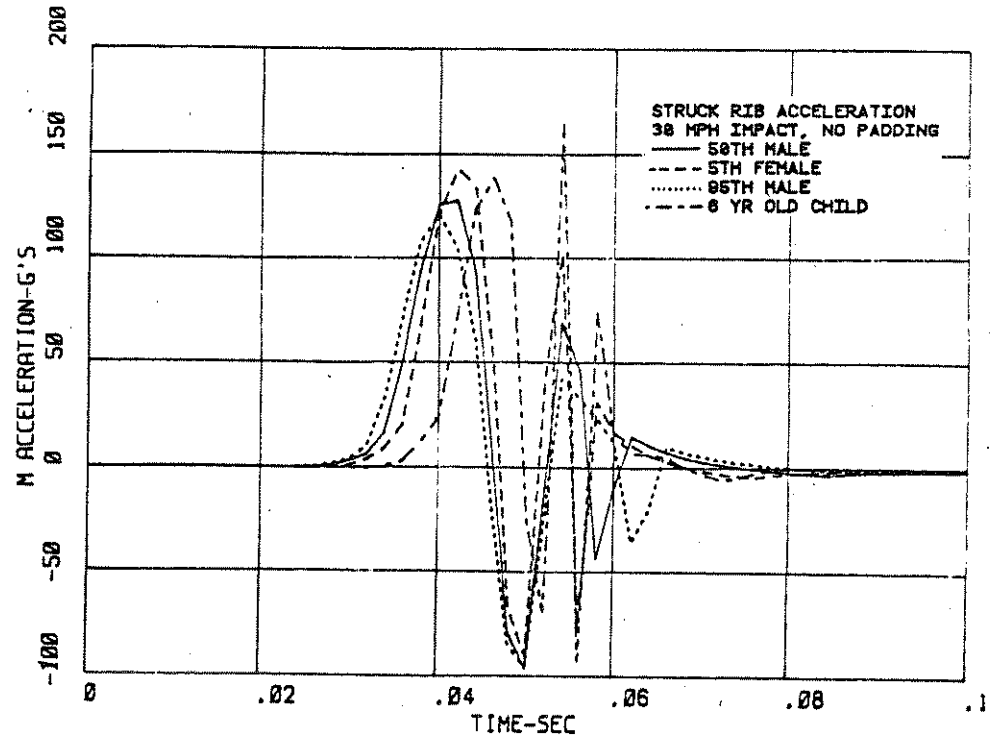

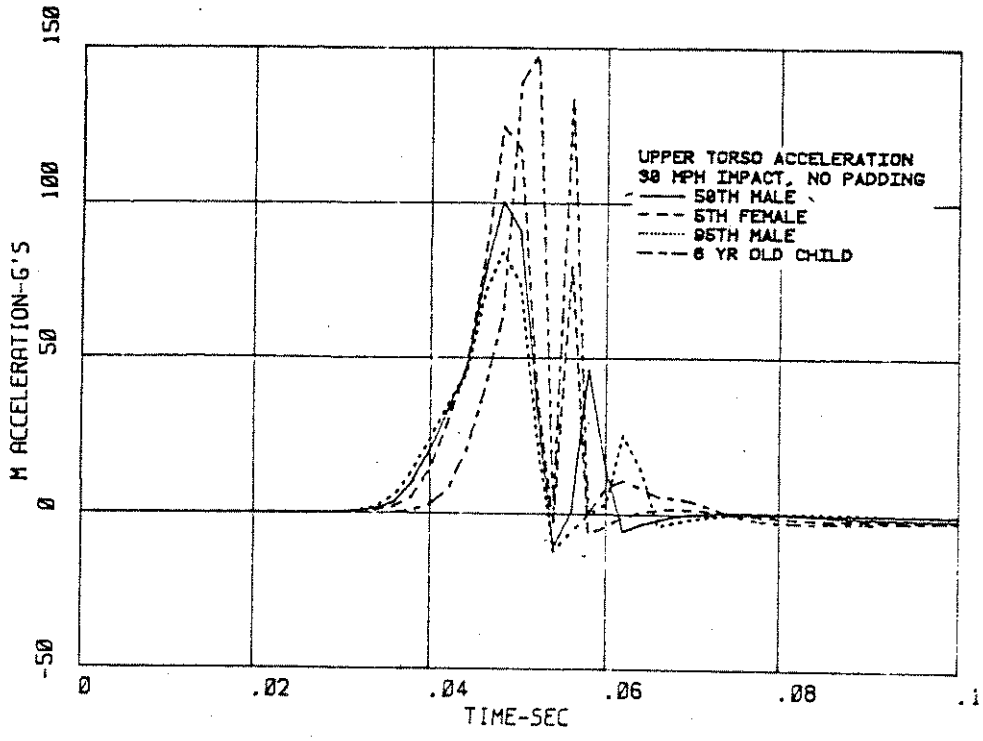

Figure 4-5 COMPARISON OF OCCUPANT RIB AND TORSO RESPONSES WITH UNPADDED DOOR

Differences in the second positive peak are quite large and maximum values increase as occupant size decreases. This clearly results from dynamic coupling between the rib and torso masses, however, the degree of reasonableness of this response pattern is uncertain. As is indicated in Section 6, the 50th percentile representation does a reasonable job of matching experimental results. Since corresponding experimental results with side impact dummies are not avialable for other occupant sizes, it cannot be ascertained at this point whether data scaling procedures cause this behavior or whether it is reasonable.

A significant point should be made with respect to the 6 year old child injury severity measures. That is, as is seen in Figure 4-5, the peak rib acceleration occurs at the second, or coupled response peak. On all other occupants, the peak occurs at the time of door contact. Similarly, the torso response for the 6 year old child shows a significantly higher second peak. This may have a substantial effect on the calculated CSI. Thus, single valued measures of severity may be biased due to this post-impact coupled dynamic behavior of the torso and rib masses.

Padded Door Results

As padding is added between the door and occupant, severity measures decrease. Figure 4-6 illustrates the AIS severity measure with 0, 3 and 6 inches of 20 psi polyurethane padding for each occupant as a function of impact speed. Figure 4-7 shows CSI results for the same padding conditions. Note that in all of these runs, the initial gap between the door and occupant was the same as for the baseline unpadded cases shown in Figure 4-4. Consistent with the unpadded case, AIS shows much less scatter across occupant size than does CSI.

In studying these figures, it is apparent that introduction of even 3 inches of padding between the occupant and door structure can offer a

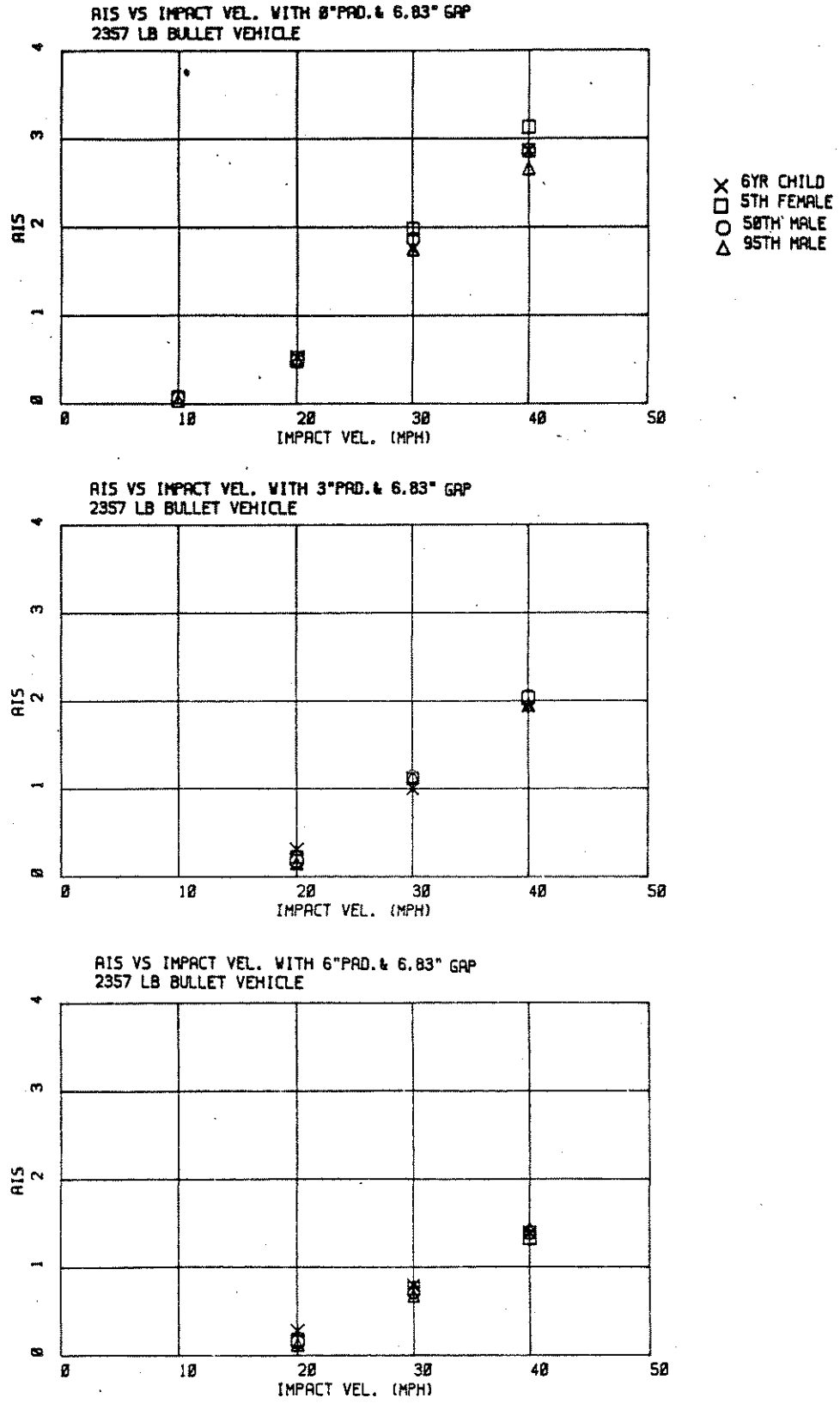

Figure 4-6 REDUCTIONS IN AIS WITH THE ADDITION OF PADDING

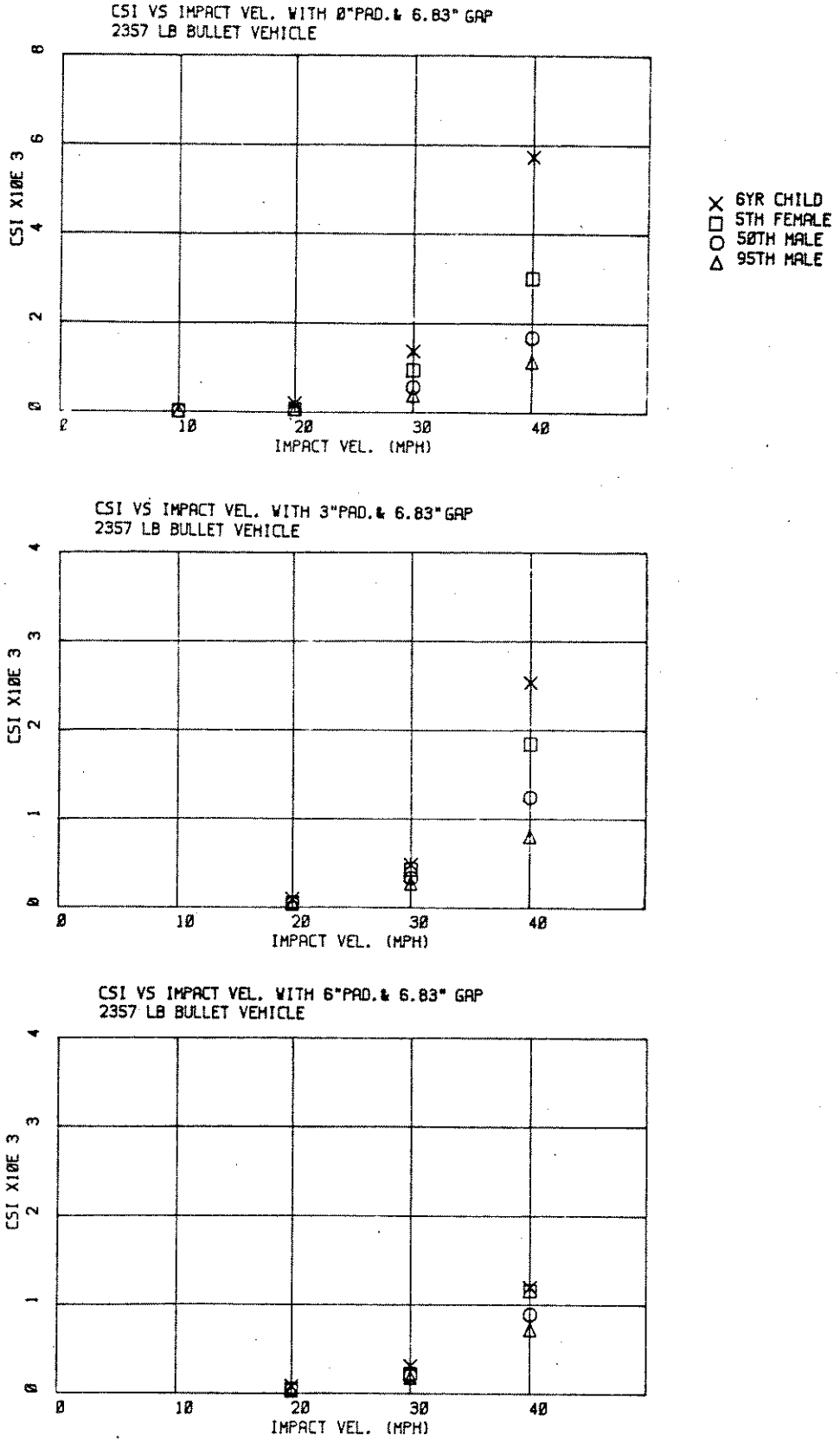

Figure 4-7 REDUCTIONS IN CSI WITH THE ADDITION OF PADDING

substantial benefit. With an unpadded door, the average AIS for all occupants at 40 MPH impact speed was 2.88 while with 3 inches of padding it was 1.99 and 6 inches of padding it was 1.39. Corresponding average CSI values were 2887, 1604 and 915, respectively. It can also be noted from these figures that the introduction of padding reduces the differences in severity measures across different occupant sizes.

Time history plots of rib and torso accelerations illustrating the reductions in acceleration obtained with different padding thicknesses are shown in Figure 4-8. These results are for a 50th percentile male at an impact speed of 30 MPH. Compared with the no padding condition, padding of 3" and 6" thicknesses were interposed between the door and occupant with the initial gap was maintained as the same in all cases. As can be seen, significant reductions in both rib and torso accelerations are achieved. Note, however, that secondary peaks resulting from dynamic interactions between rib and torso masses are not substantially reduced by padding and are, in fact, higher than the primary peaks when 6 inches of padding was simulated.

Effects of Padding and Gap

As noted previously, five padding conditions were simulated during the study. In addition to the no padding condition, two conditions of 3 and 6 inches of padding were simulated. In the first case, the padding was assumed to be interposed between the occupant and door resulting in a reduction of the nominal gap by either 3 or 6 inches. The second case assumed that the vehicle was widened by either 3 or 6 inches in order to accommodate the padding while maintaining the original gap between the occupant and door.

Results of simulations for all padding conditions with the 50th percentile male occupant are shown in Figure 4-9. As is seen there, padding does not make a large different at impact speeds of 20 MPH or below. However, at impact speeds of 30 and 40 MPH (velocity changes of approximately 15 and 20

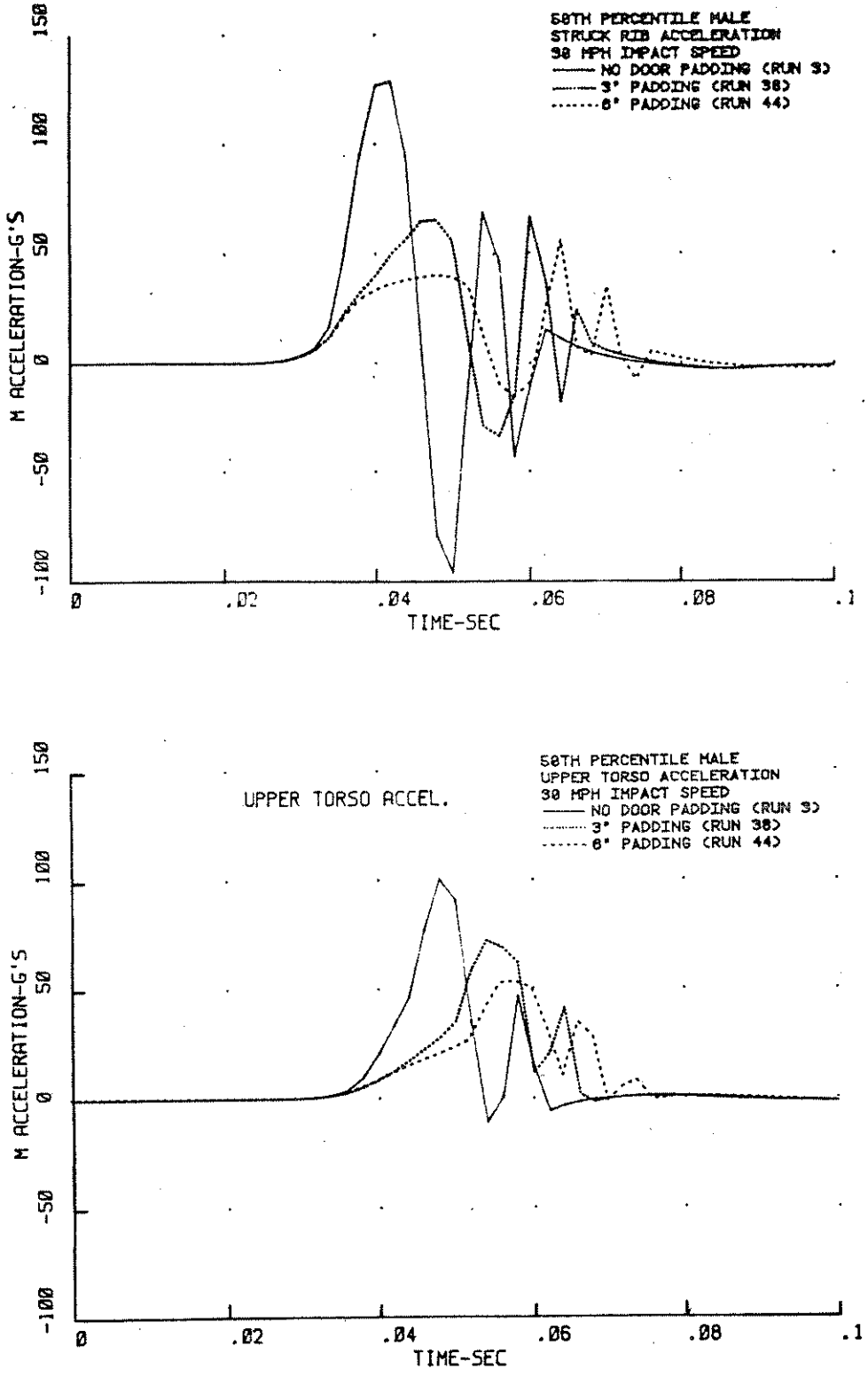

Figure 4-8 EFFECTS OF PADDING THICKNESS ON RIB AND TORSO ACCELERATIONS

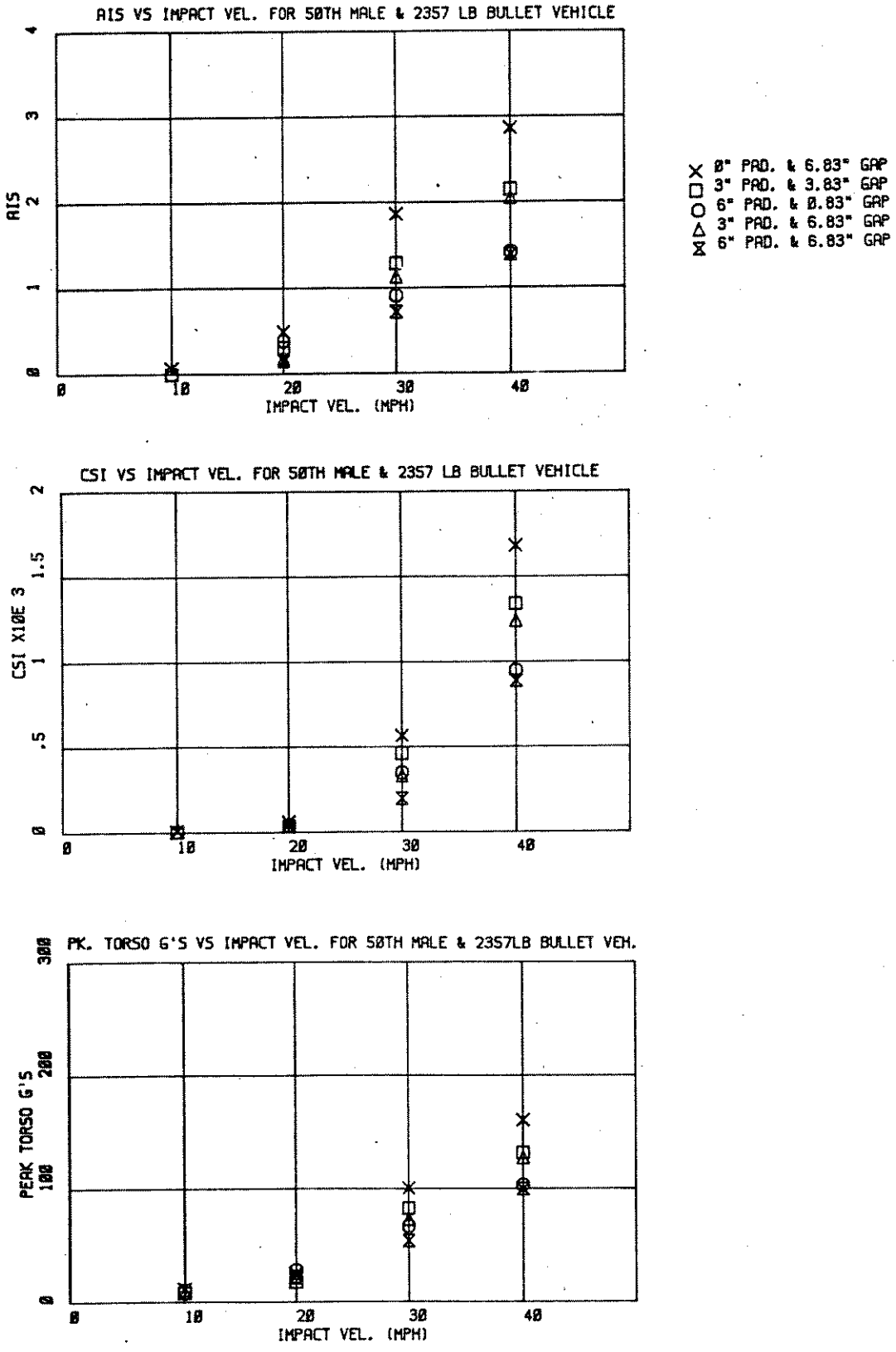

Figure 4-9 EFFECTS OF PADDING AND IMPACT SPEED ON 50TH PERCENTILE MALE

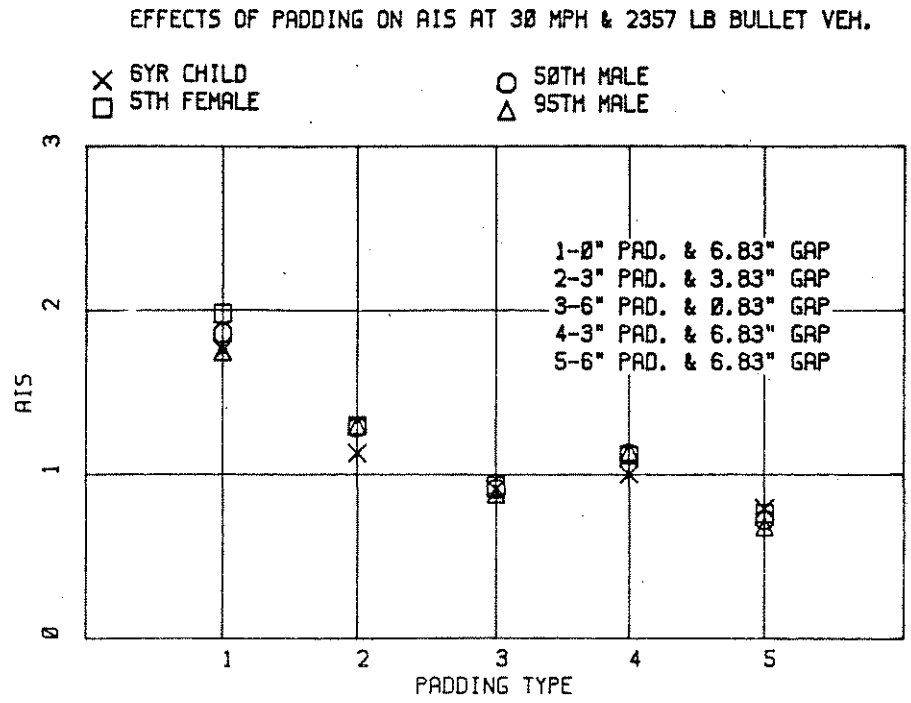

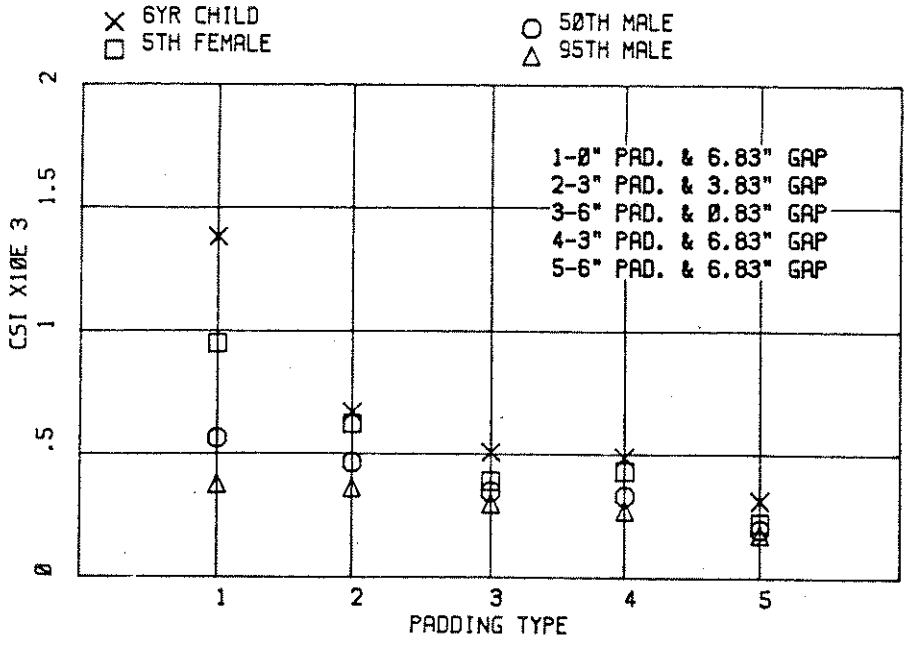

Figure 4-10 EFFECTS OF PADDING TYPE ON OCCUPANT INJURY MEASURES

MPH) padding is shown to offer a significant reduction in severity measures. It is also noted that the influence of spacing or gap between the occupant and padding is much less significant than the presence or absence of padding at the 40 MPH impact speed. That is, increasing the gap from 3.8 to 6.8 inches with 3 inches of padding reduces the severity measures somewhat but the reduction is much less than the difference between no padding and three inches of padding. This effect is further illustrated in Figure 4-10 which presents severity measures as a function of padding type parametric in occupant size. As is seen there, increase the gap from 3.8 to 6.8 inches (padding type 2 and 4 for 3" and types 3 and 5 for 6" thick padding, respectively) does provide some additional benefit, but much less of an increment than the presence of even 3 inches of padding.

Changes in responses with gap changes are further illustrated in Figure 4-11 which presents time history responses for 3 inches of padding with the two different gaps for a 50th percenitle occupant at 30 MPH impact speed. As is seen, both the rib and upper torso responses are shifted in time reflecting the different gaps. A reduction in primary peak acceleration values is also apparent with the increased gap.

Effect of Occupant Size

Figure 4-12 summarizes injury severity measures for all occupant and padding combinations at a 30 MPH impact speed. The CSI injury severity measure shows a clear trend toward an increase in severity as occupant size decreases. The amount of the severity increase, however, decreases as padding effectiveness increases. Thus, padding appears to offer the potential for more incremental benefit to smaller occupants based on the CSI injury measure.

When AIS is used as the severity measure,the same trends hold for the adult occupants, however, the rate of severity change with occupant size is much less. The trend does not continue when considering the child

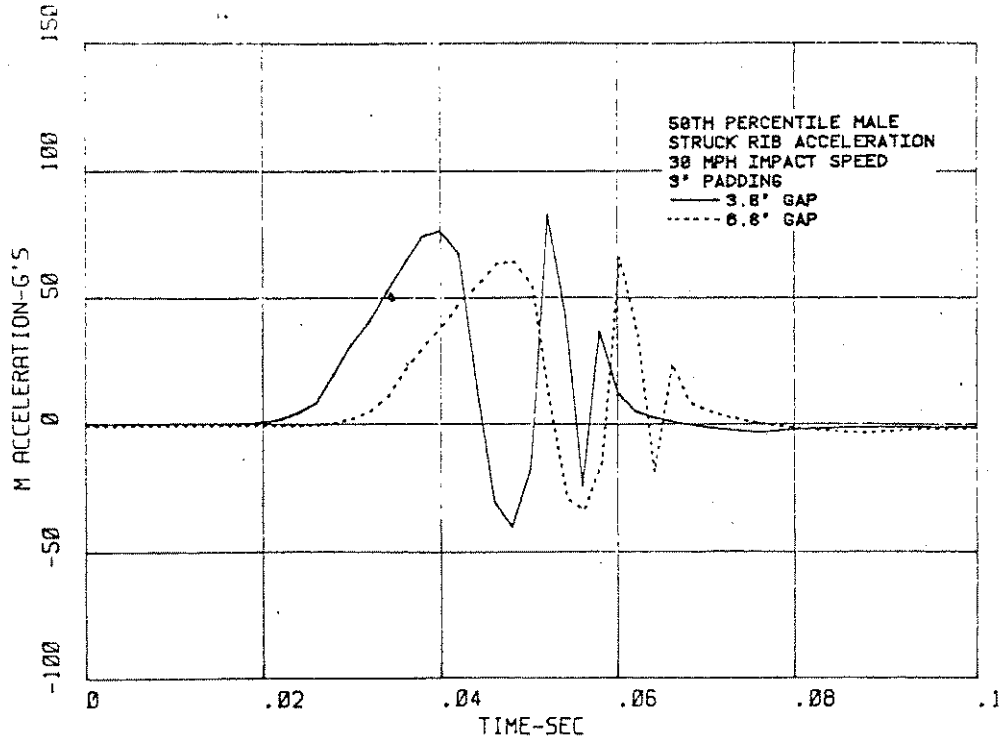

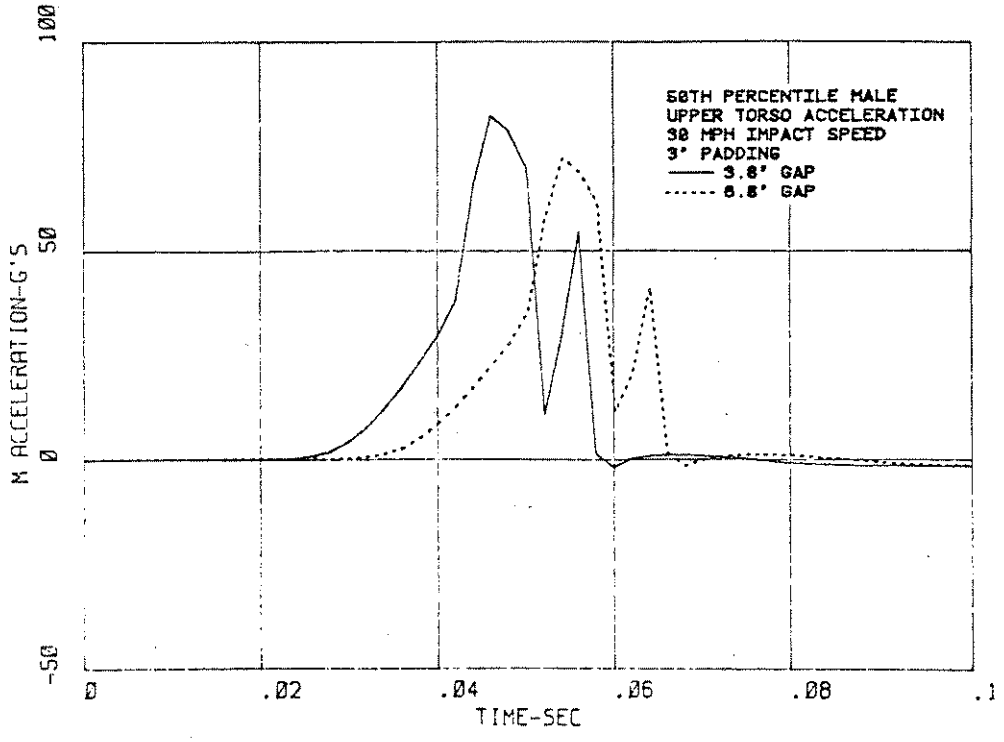

Figure 4-11 EFFECTS OF GAP DIFFERENCES ON RIB AND TORSO ACCELERATIONS

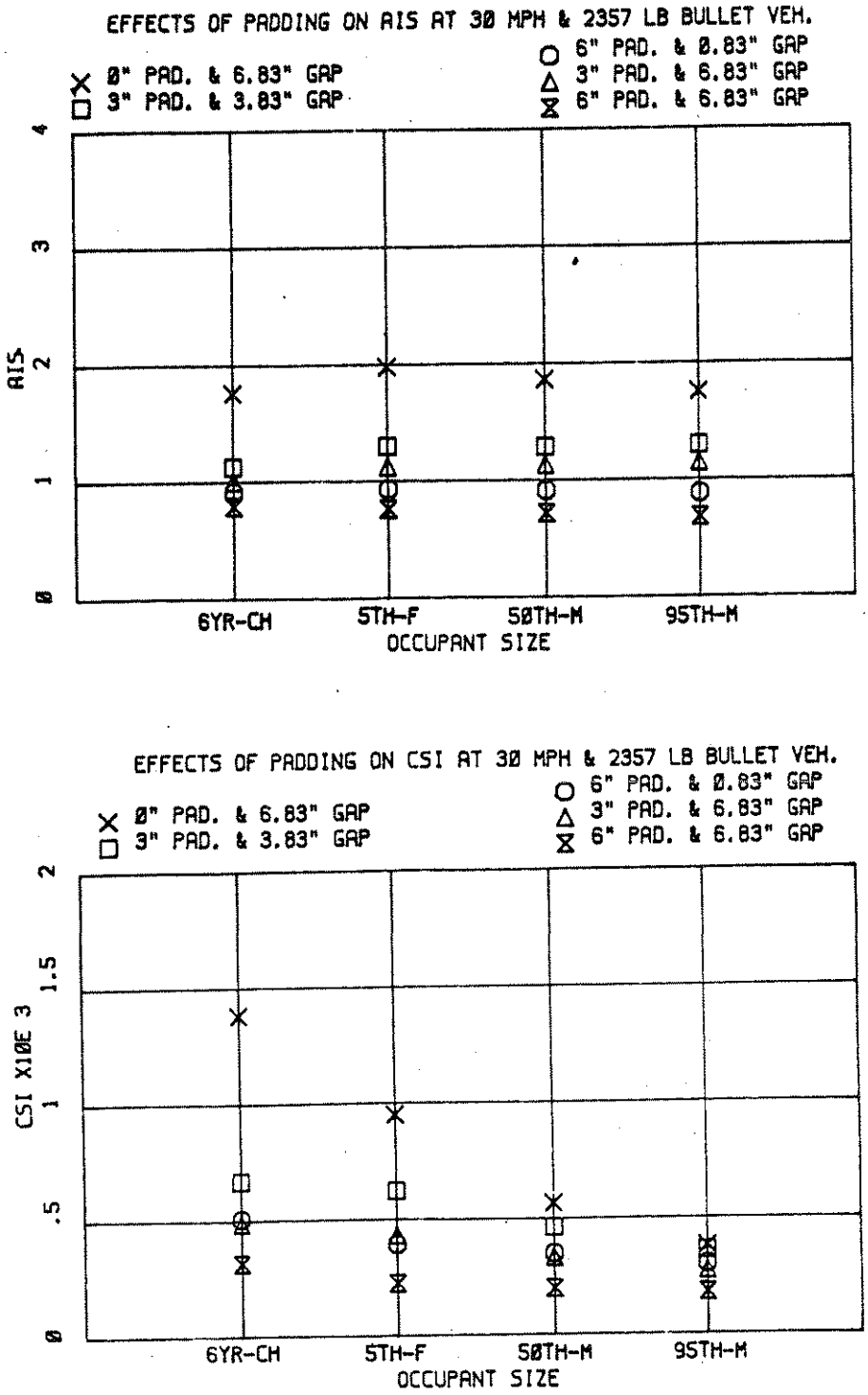

Figure 4-12 EFFECTS OF OCCUPANT SIZE ON INJURY MEASURES

occupant. The reasons for this behavior are not fully understood but may be related to the post-door contact coupled dynamic oscillations of the rib and spinal masses.

Effects of Striking Vehicle Weight

The effects of varying striking vehicle weight are illustrated in the rib acceleration time histories shown in Figure 4-13. In each of these three runs, the striking car was initially traveling at 30 MPH. As would be expected, the heaviest striking car produces the most severe acceleration response to the struck rib as a result of inducing the largest velocity change to the struck car. This is further demonstrated in the plot of CSI vs. struck car velocity change shown in Figure 4-14. Shown on this plot are the CSI values for 50th percentile males in an unpadded vehicle as functions of impact speed and impact vehicle weight.

The interesting fact to note from this plot is that struck car ΔV, in and of itself, is not a good indicator of occupant severity even given identical occupants, padding, gap, etc. The CSI values are also related to striking car speed as well. For example, if we consider the nominal striking vehicle (2350 lbs.) CSI vs. ΔV curve, one would expect an CSI value of about 1000 given a struck car ΔV of 17.5 MPH. However, the heavy striking vehicle (3250 lbs.) at 30 MPH impact speed also produces a ΔV to the struck car of about 17.5 MPH but the occupant CSI is about 750. This lower than expected value is believed to result from a correspondingly lower struck door velocity produced by the different striking weight and speed combinations. As can be seen on the figure, the opposite is true in the case of the light striking vehicle.

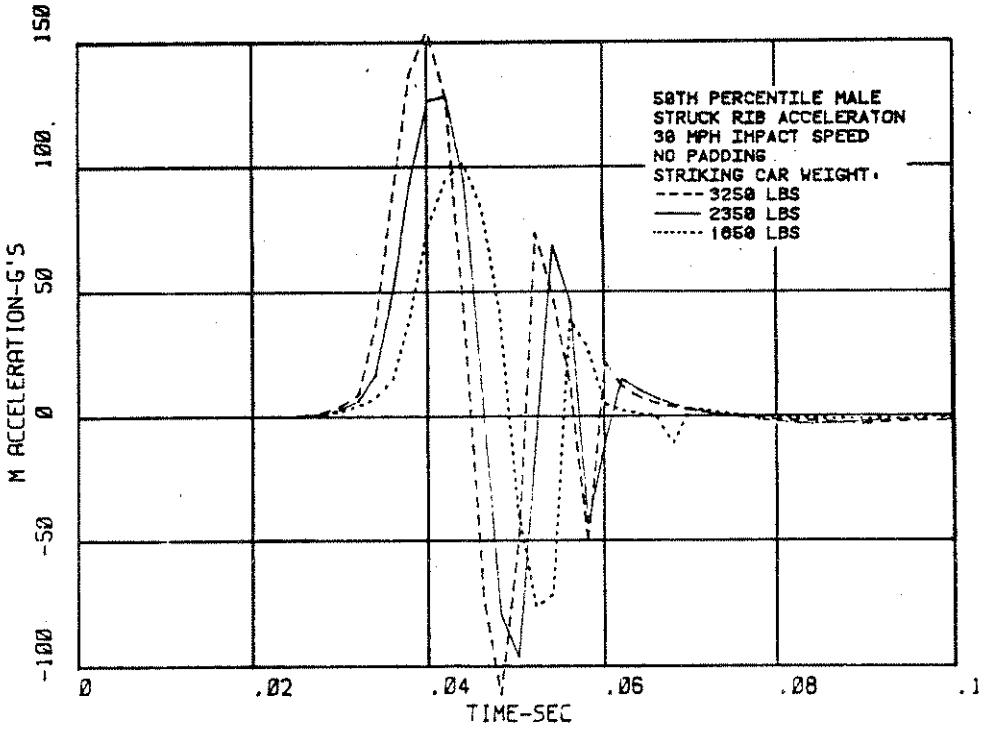

Figure 4-13 RIB ACCELERATION DIFFERENCES RESULTING FROM DIFFERENT STRIKING CAR WEIGHTS

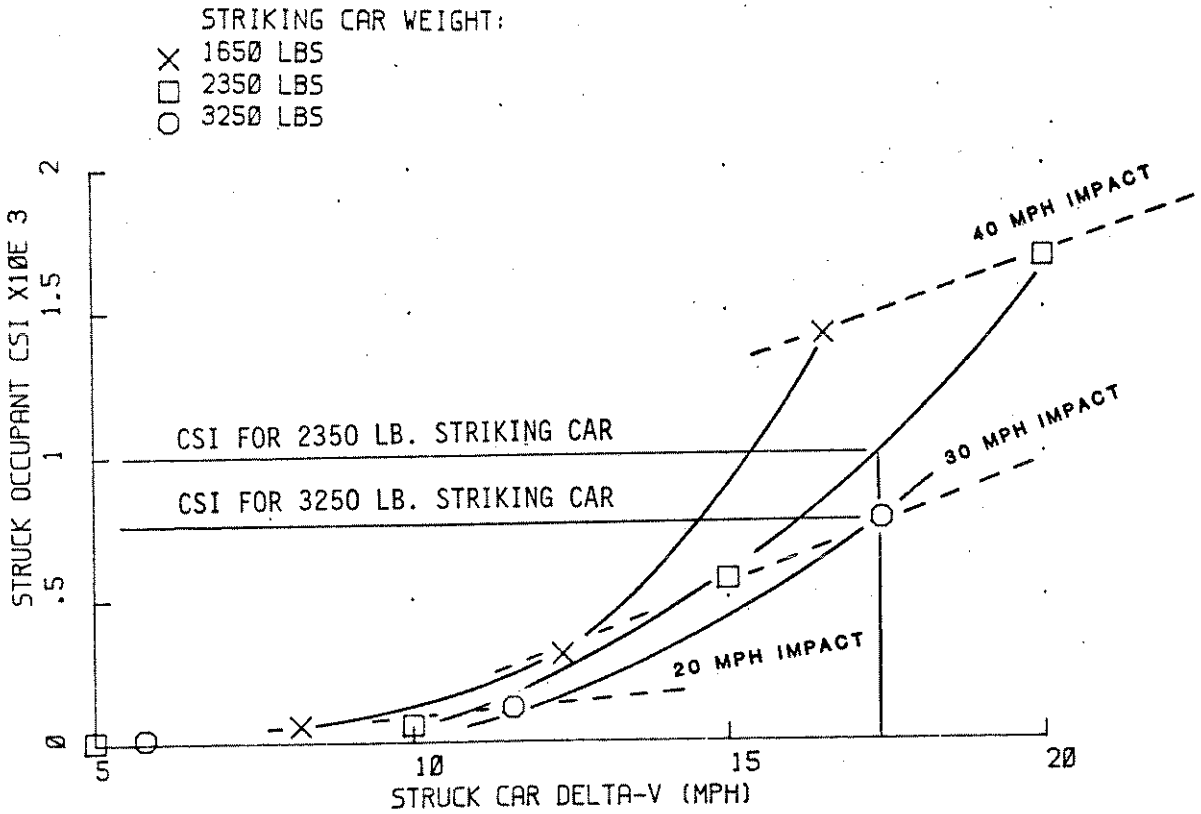

Figure 4-14 INFLUENCE OF STRIKING CAR SPEED AND WEIGHT ON OCCUPANT INJURY

5. CAL-3D CVS MODEL

While the simplicity and ease of use of a lumped mass model are definite advantages under some conditions, the attempt at modeling a multi-dimensional side impact event with a one-dimensional representation leads to concern over the general applicability of the results. The use of a more complex model, like the CAL-3D Crash Victim Simulation, allows a much more realistic representation of the occupant and largely avoids the problem of developing artificial coupling between body segments in order to achieve a good match with test results. Furthermore, recent advances in the ease of use of the CAL-3D as evidenced by the User Convenience Package (Ref. 4) have greatly increased the ability to make and analyze CAL-3D runs. Consequently, the CAL-3D model was also configured to simulate side impacts with the intent of investigating the ranges of applicability of the lumped mass modeling procedure. It should be emphasized that both simple and complex modeling approaches are recognized as being valuable for specific purposes and should not be viewed as being competitive. Rather, they should be thought of as augmenting and supporting each other.

5.1 CAL-3D Model Representation

The traditional representation of the automobile occupant with the CAL-3D model has consisted of fifteen body segments connected by fourteen joints. The automobile is also treated as a separate rigid body segment undergoing prescribed motion within the program. There are two difficulties with this representation in modeling side impacts. First, substantial intrusion of the struck side door panel occurs which has a strong influence on the dynamics of the occupant. Second, much of the recent biomechanics research suggests that the dynamic response of the struck rib is strongly related to injury.

With the traditional representation of the vehicle as a single segment to which contact planes are attached, modeling of an intruding door

panel is not possible. However, this apparent restriction can be readily overcome through use of available CAL-3D features. Thus, in order to model an intruding door panel within a passenger compartment, two segments are used. The first represents the vehicle and all planes that move with the vehicle (floor, seat, etc.) are attached to this segment. The motion of the vehicle is prescribed with an input acceleration, velocity or displacement time history. A second segment has a contact plane representing the intrusion door surface attached to it and is assigned a motion time history that reflects the motion of the vehicle itself with the door motion relative to the vehicle (intrusion) superimposed over it. Thus, separate motion of the door is allowed in a straightforward and easily implemented manner through appropriate specification of standard CAL-3D inputs. Program modifications are not required.

Modeling the dynamics of the struck rib, necessary for injury prediction, also requires the use of an additional segment. This segment must, however, be physically connected to the spine and must interact with the torso in a manner similar to that of the Side Impact Dummy. Thus, the occupant is composed of sixteen segments. The rib segment is connected to the upper torso segment by a vertical axis pin joint located at the spine. Interaction between the rib and upper torso segments is accomplished with an ellipsoid-to-ellipsoid contact. That is, each segment has an ellipsoid attached to it and an appropriate force-deflection characteristic generates interacting forces when the ellipsoids come into contact. Note that a rate sensitive (damping) characteristic is also used in this contact. This CAL-3D configuration is illustrated in Figure 5-1.

This approach towards modeling the occupant in side impact situations requires only minimal additional information over and above the standard fifteen segment occupant representation. That is, physical properties of the rib element and upper torso element (mass, moments of inertia, etc.), the rib joint (location, pivot axis, torques, etc.) and the interaction between the rib element and torso (contact ellipsoid locations, sizes and force-deflection properties) must be specified.

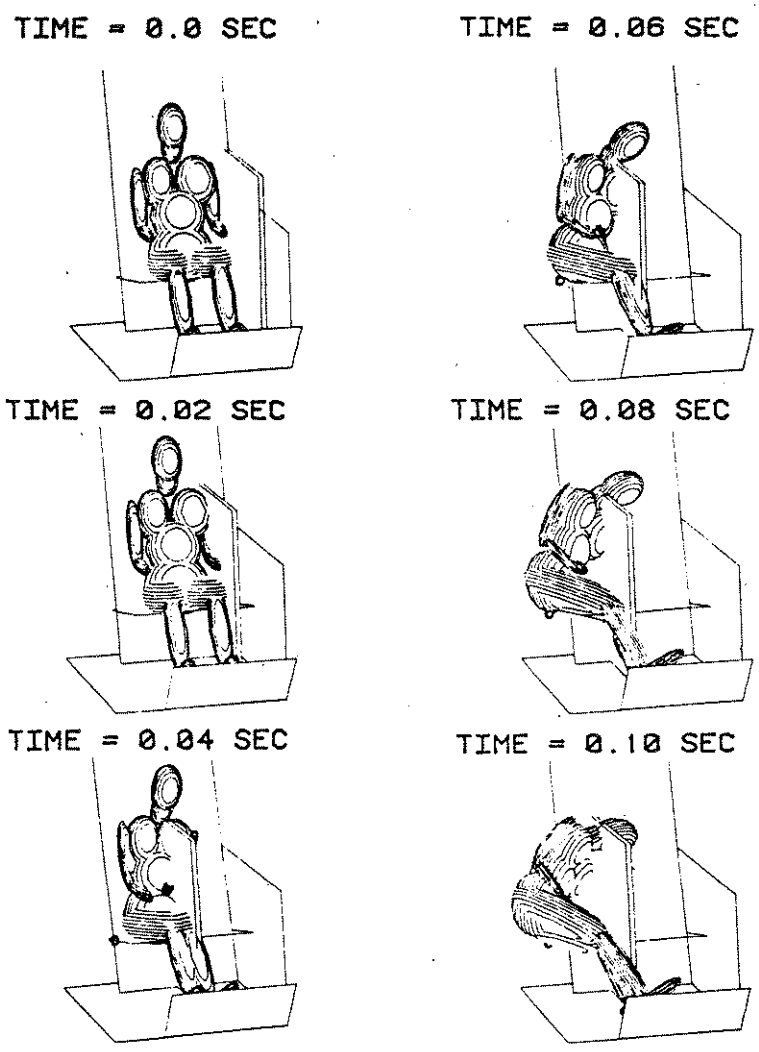

Figure 5-1 CAL-3D SIDE IMPACT SIMULATION

Developing the side impact dummy data deck consisted of primarily splitting the existing upper torso segment properties of estimated (Alderson) Part 572 data deck contained on the CAL-3D User Convenience Library (Ref. 4) into two segments, one representing the rib. It should be noted that the mass distribution of the SID is substantially different than that of the Part 572 dummy. That is, the SID upper torso weighs approximately 52 lbs. while other 50th percentile male upper torsos weigh between 32 and 37 lbs. This is, in part, due to the attempt to include the arm mass within the rib/upper torso segment of the physical dummy. In developing a mathematical model, we did not attempt to model the SID, per se. Separate arm segments were simulated. Thus, the total upper torso weight in the starting dummy data set was about 32 lbs. From this, 15 lbs. was allocated to a separate rib segment. This rib weight was based partially on trial and error matching of test cases and partially on engineering judgment. Mass, inertial and dimensional properties of the resulting 50th percentile male side impact occupant are shown in Table 5-1.

The connection between the rib and upper torso was modeled as a simple pin joint located at and aligned with the spine. Thus, the rib element was allowed to rotate about the spine in a manner similar to that observed in the SID dummy. Interaction between the upper torso and rib segments was obtained through contact ellipsoids attached to each. Note from Figure 5-1 that the rib ellipsoid was somewhat larger than the torso ellipsoid in order to approximate the actual lateral dimension of the SID (i.e., the false arm molded into the torso jacket).

The force-deflection characteristic acting between these ellipsoids was shown in Figure 4-2 and was based on static compression tests conducted at MGA. Note that this same loading curve was used in both lumped mass and CAL-3D models. Damping acting between the segments for the CAL-3D representation was also the same as used in the lumped mass model. It should, however, be

Table 5-1

CAL-3D 50TH PERCENTILE MALE INPUTS

CRASH VICTIM EST. PART 572 DUMMY 17 SEGMENTS 16 JOINTS CARD P.1

CARDS P.2

T	SEGMENT SYM	PLOT	WEIGHT (LBS)	PRINCIPAL MOMENTS OF INERTIA (LBS-SEC**2-INCH) X	Y	Z	SEGMENT CONTACT ELLIPSOID SEMIAXES (INCH) X	Y	Z	CENTER (INCH) X	Y	Z	PRINCIPAL AXES (DEG) YAW	PITCH	ROLL
1	LT	5	35.750	1.7100	1.1400	1.7100	4.340	6.940	6.000	-.400	0.000	-.900	0.00	0.00	0.00
2	CT	4	9.339	.3250	.3140	.1450	4.650	5.200	6.000	2.130	0.000	-3.550	0.00	0.00	0.00
3	UT	3	16.750	1.1400	.8250	.6650	4.650	5.479	5.700	.500	0.000	1.250	0.00	0.00	0.00
4	N	2	1.500	.0400	.0400	.0044	2.570	2.760	3.280	-.570	0.000	0.000	0.00	0.00	0.00
5	H	1	10.200	.2500	.3110	.2000	4.000	3.100	4.700	.400	0.000	0.000	0.00	0.00	0.00
6	PHL	6	19.600	.7273	.7030	.1540	3.350	3.740	11.000	0.000	0.000	-1.700	0.00	0.00	0.00
7	PLL	7	6.900	.4400	.4420	.0190	2.100	2.230	9.500	0.000	0.000	-.500	0.00	0.00	0.00
8	RF	8	2.200	.0253	.0434	.0132	1.500	1.800	5.200	0.000	0.000	.850	0.00	0.00	0.00
9	LHL	9	19.600	.7270	.7030	.1540	3.350	3.740	11.000	0.000	0.000	-1.700	0.00	0.00	0.00
10	LLL	A	9.900	.6400	.6400	.0150	2.100	2.230	9.300	0.000	0.000	-.500	0.00	0.00	0.00
11	LF	B	2.300	.0383	.0434	.0132	1.500	1.800	5.200	0.000	0.000	.850	0.00	0.00	0.00
12	RUA	C	4.300	.1640	.1440	.0141	2.070	1.640	7.050	0.000	0.000	.550	0.00	0.00	0.00
13	RLA	D	4.300	.2550	.2500	.0115	1.300	1.110	6.000	0.000	0.000	-1.650	0.00	0.00	0.00
14	LUA	E	4.300	.1640	.1440	.0141	2.070	1.640	7.050	0.000	0.000	.550	0.00	0.00	0.00
15	LLA	F	4.300	.2550	.2500	.0115	1.300	1.110	6.000	0.000	0.000	-1.650	0.00	0.00	0.00
16	RHA	G	15.300	1.1600	.9250	.6650	4.550	4.270	5.200	0.000	-4.270	0.000	0.00	0.00	0.00
17	PHL	G	1.000	1.0000	1.0000	1.0000	1.000	1.000	1.000	0.000	0.000	0.000	0.00	0.00	0.00

CARDS P.3

J	JOINT SYM	PLOT	JNT	RTN	LOCATION(INCH) - SEG(J,N) X	Y	Z	LOCATION(INCH) - SEG(J+1) X	Y	Z	PRIN. AXIS(DEG) - SEG(J,N) YAW	PITCH	ROLL	PRIN. AXIS(DEG) - SEG(J+1) YAW	PITCH	ROLL
1	P	9	1	-2	-2.200	0.000	-3.750	0.000	0.000	1.050	0.00	0.00	0.00	0.00	0.00	0.00
2	N	0	2	-2	0.000	0.000	-1.050	-1.400	0.000	10.420	0.00	0.00	0.00	0.00	0.00	0.00
3	NP	0	3	-2	1.250	0.000	-1.780	0.000	0.000	1.770	0.00	0.00	0.00	0.00	15.00	0.00
4	UB	0	4	-2	0.000	0.000	-1.790	.100	0.000	2.350	0.00	0.00	0.00	0.00	0.00	0.00
5	PH	0	1	0	-.100	4.450	.900	0.000	0.000	-8.810	0.00	0.00	0.00	0.00	-84.00	5.72
6	PK	0	6	1	0.000	0.000	4.790	0.000	0.000	-8.000	0.00	0.00	0.00	0.00	75.00	0.00
7	PA	0	7	-2	0.000	2.000	8.200	1.700	0.000	-2.200	0.00	0.00	0.00	0.00	-80.00	0.00
8	EL	T	1	0	-.100	-4.450	.900	0.000	0.000	-8.810	0.00	0.00	0.00	0.00	-84.00	-5.72
9	EK	U	6	1	0.000	0.000	4.790	0.000	0.000	-8.000	0.00	0.00	0.00	0.00	75.00	0.00
10	EA	V	10	-2	0.000	0.000	8.200	1.700	0.000	-2.200	0.00	0.00	0.00	0.00	-80.00	0.00
11	RC	A	3	-2	-.150	7.600	-.930	0.000	0.000	-5.000	0.00	0.00	0.00	0.00	-55.00	10.19
12	RE	X	12	-1	0.000	0.000	6.100	0.000	0.000	-6.650	0.00	0.00	0.00	0.00	-72.50	0.00
13	LC	Y	3	-2	-.150	-7.600	-.930	0.000	0.000	-5.000	0.00	0.00	0.00	0.00	-55.00	-10.19
14	LE	Z	14	-1	0.000	0.000	6.100	0.000	0.000	-6.650	0.00	0.00	0.00	0.00	-72.50	0.00
15	RTHH	H	3	1	-4.150	0.000	1.570	-4.650	0.000	0.000	0.00	0.00	90.00	0.00	0.00	90.00
16	NN		0	0	0.000	0.000	0.000	0.000	0.000	0.000	0.00	0.00	0.00	0.00	0.00	0.00

pointed out that the option within the CAL-3D that allows the use of rate dependent forces (i.e., damping) also precludes the use of hysterisis in static force functions. Thus, loading and unloading occur on the same curve and all energy absorption occurs due to damping. This is different than the lumped mass representation in which both hysterisis and damping were modeled.

Rather than develop side impact representations of other adult occupant sizes from existing data decks, other occupant sizes were based directly on this 50th percentile occupant data set. Scaling procedures described in Section 3 were applied to the 50th percentile data deck to produce 95th male and 5th female data decks. The six year old child data was not scaled directly from this 50th percentile data. Rather, the total torso weight as obtained from an existing 6 year old child data set, was distributed to segments in the same manner as existed in the 50th percentile data. Complete occupant data sets for each occupant are given in Appendix C.

The side impact occupant model was verified by comparison with test results as is described in Section 6, prior to use in the parameter study. The structure of the parameter study runs is described next followed by a detailed discussion of the parameter study results.

5.2 CAL-3D CVS Parameter Study

The parameter study conducted with the CAL-3D was intended to supplement that done with the lumped mass model. Since it was expected that the CAL-3D results would be more realistic over a greater range of conditions than the lumped mass model, the CAL-3D results were intended to spot check or corraborate results from the simplified model.

The runs made with this model are listed in Table 5-2. Note that the run numbers given in the table correspond to parallel run numbers in the lumped mass model parameter study. As can be seen from the table, the CAL-3D

Table 5-2

CAL-3D PARAMETER STUDY RUNS

RUN	OCCUPANT	IMPACT SPEED (MPH)	PADDING
3	50th Male	30	No padding
7	95th Male	30	No padding
11	5th Female	30	No padding
50	6 Year Old Child	30	No padding
15	50th Male	30	3" padding
19	95th Male	30	3" padding
23	5th Female	30	3" padding
52	6 Year Old Child	30	3" padding
27	50th Male	30	6" padding
31	95th Male	30	6" padding
35	5th Female	30	6" padding
54	6 Year Old Child	30	6" padding
38	50th Male	30	3" padding, reduced gap
44	50th Male	30	6" padding, reduced gap
14	50th Male	20	3" padding
16	50th Male	40	3" padding

parameter study concentrated on a nominal impact speed condition of 30 MPH and focused on differences in padding properties and occupant size.

A tabulation of important single valued injury measures resulting from these CAL-3D run conditions is provided in Table 5-3.

Rib and torso acceleration responses for the 30 MPH baseline (no padding) condition for all four occupants are shown in Figure 5-2. As would generally be expected, the peak acceleration of the rib increases as occupant size decreases. Differences in the time of acceleration onset reflect different physical sizes of the occupants. That is, each occupant was assumed to be seated at the centerline of the seat; thus smaller occupants had larger gaps to the door than did larger occupants (see Table 3-3).

Also noted on the figure is the difference between the three adult sized occupant upper torso acceleration responses and that of the child. On the child response an initial peak is followed by a fall off and a second, larger acceleration peak which is about the same level as that seen with the 50th male occupant. This different behavior apparently results from differences in dynamic coupling between the rib, upper torso and the rest of the occupant in the child run.

The effect of including 3 and 6 inches of padding between the occupant and door (with a corresponding reduction in gap) is shown in Figure 5-3. Note that the rib response again follows expected trends with the smaller occupants sustaining higher peak rib accelerations. The discontinuity in the child accelerations near the peak value results from a reversal in joint torque sign at rib joint. Although small rib joint torque values were used in the simulations, this reversal was still enough to cause about a 10 percent change in level. Overall, the effect of interposing padding between the occupant and door is to reduce peak acceleration levels but also to decrease the differences amongst the various occupant sizes. That is, padding appears to increase the consistency of the responses for different occupant sizes.

Table 5-3

CAL-3D PARAMETER STUDY RESULTS SUMMARY

RUN NO.	AIS	CSI	MAX TORSO ACCEL. G'S	MAX RIB ACCEL. G'S	MAX HEAD ACCEL.G'S
3	1.633	683.74	104.14	113.2	29.7
7	1.46	473.76	89.73	104.1	22.6
11	1.86	979.47	121.6	129.9	30.85
50	1.609	661.53	103.1	146.1	26.5
15	1.412	501.5	81.8	82.1	26.3
19	1.355	429.96	73.95	77.9	22.2
23	1.579	653.8	90.4	89.7	27.9
52	1.426	385.94	76.95	91.7	27.3
27	1.178	398.03	63.3	60.2	25.96
31	1.060	299.48	53.9	55.4	22.1
35	1.266	456.45	67.7	64.8	26.6
54	1.346	368.90	67.51	79.21	32.69
38	1.214	389.96	72.9	70.4	22.8
44	.896	242.68	52.85	48.2	20.4
14	.299	53.48	27.8	24.4	8.2
16	2.59	1687.57	134.3	142.0	52.9

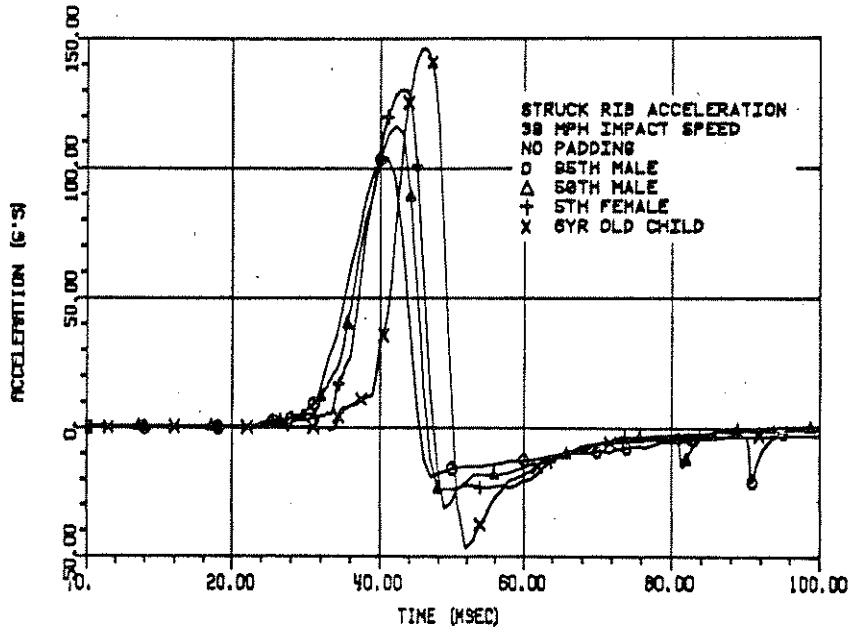

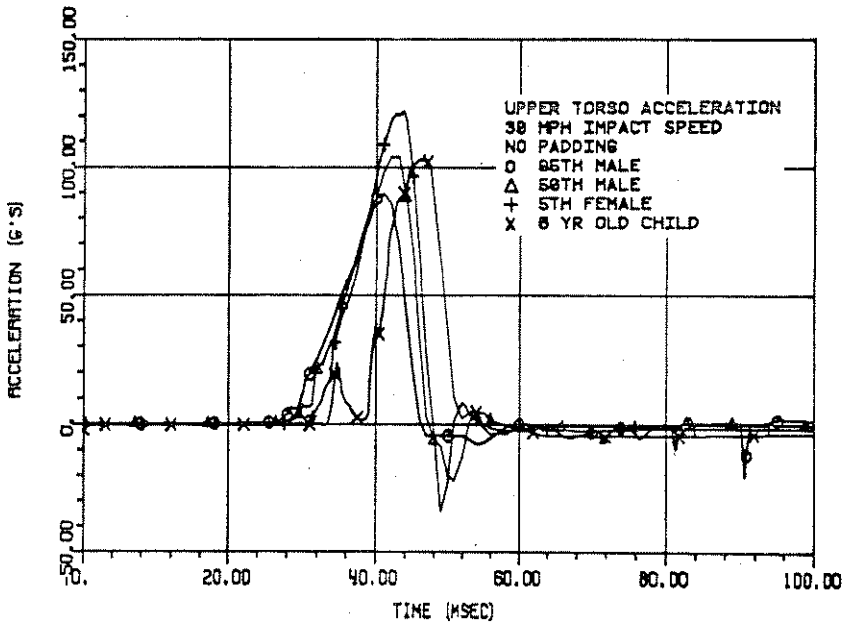

Figure 5-2 DIFFERENCES IN RIB AND TORSO ACCELERATIONS FOR ALL OCCUPANT SIZES

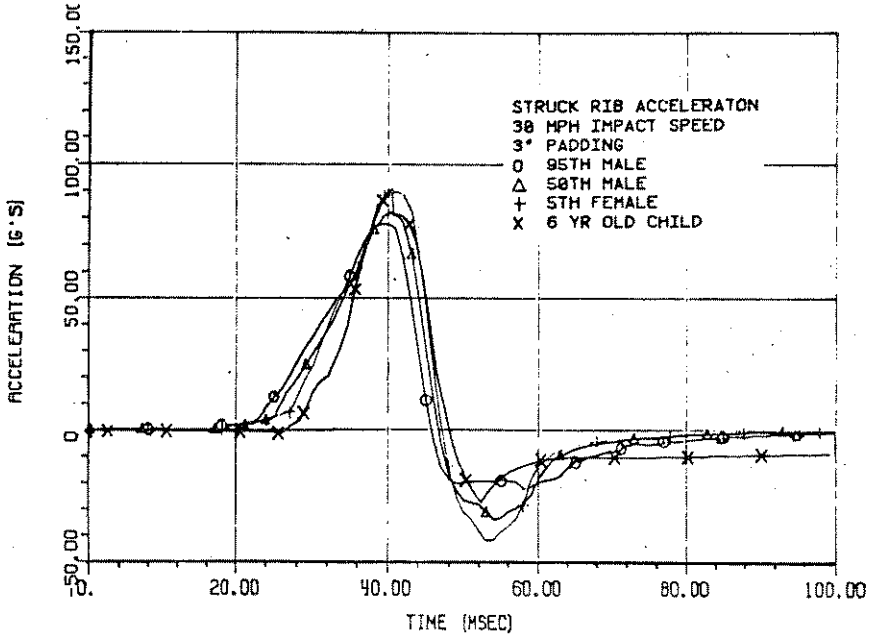

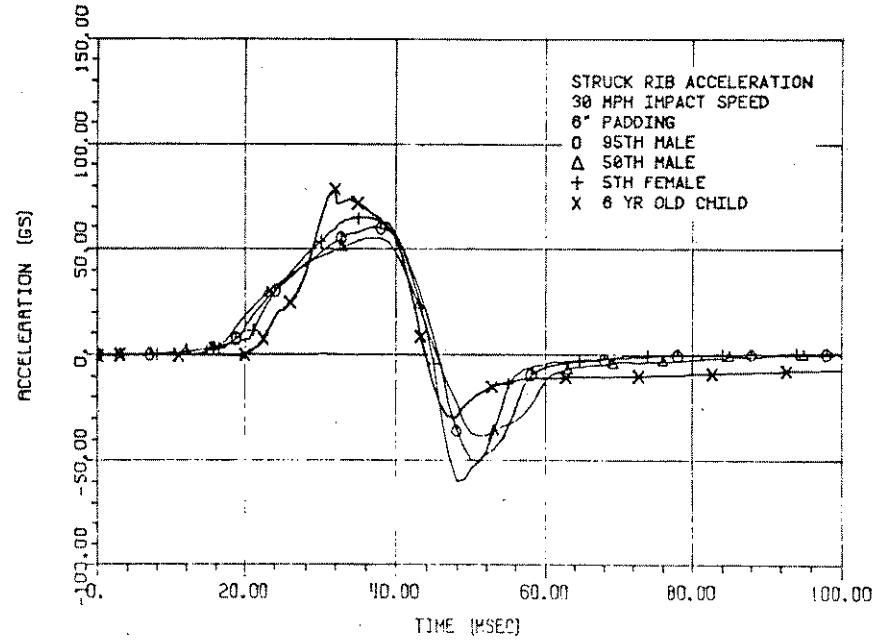

Figure 5-3 EFFECTS OF PADDING ON RIB ACCELERATION

Single point injury indicies for all 30 MPH runs are summarized in Figure 5-4. As was mentioned previously, the general effect of padding is to reduce both levels of and spread across occupants of peak rib accelerations. The average injury indicies for all occupants for 0, 3, and 6, inches of padding are summarized below:

Padding	AIS	CSI	Peak Torso Accel
0"	1.64	699	104.25
3"	1.445	492.5	80.5
6"	1.215	376.25	63.25
Difference 0" to 3"	0.195	206.5	23.75
Difference 3" to 6"	0.230	116.25	17.25

It can be seen that substantial reductions in injury indicies are achieved in adding 3 inches of padding to a baseline door structure. Both CSI and Peak Torso Acceleration show a lesser decrease in absolute value when adding an additional 3 inches of padding. The calculated AIS, however, shows an increase in reduction for the second 3 inches of padding.

Recalling that the above discussed padding types reduced the gap between the occupant and door by the padding thickness, the effect of gap can be seen in Table 5-4 by a comparison with padding types 4 and 5 where the original (no padding) gap was maintained with the 50th percentile male occupant.

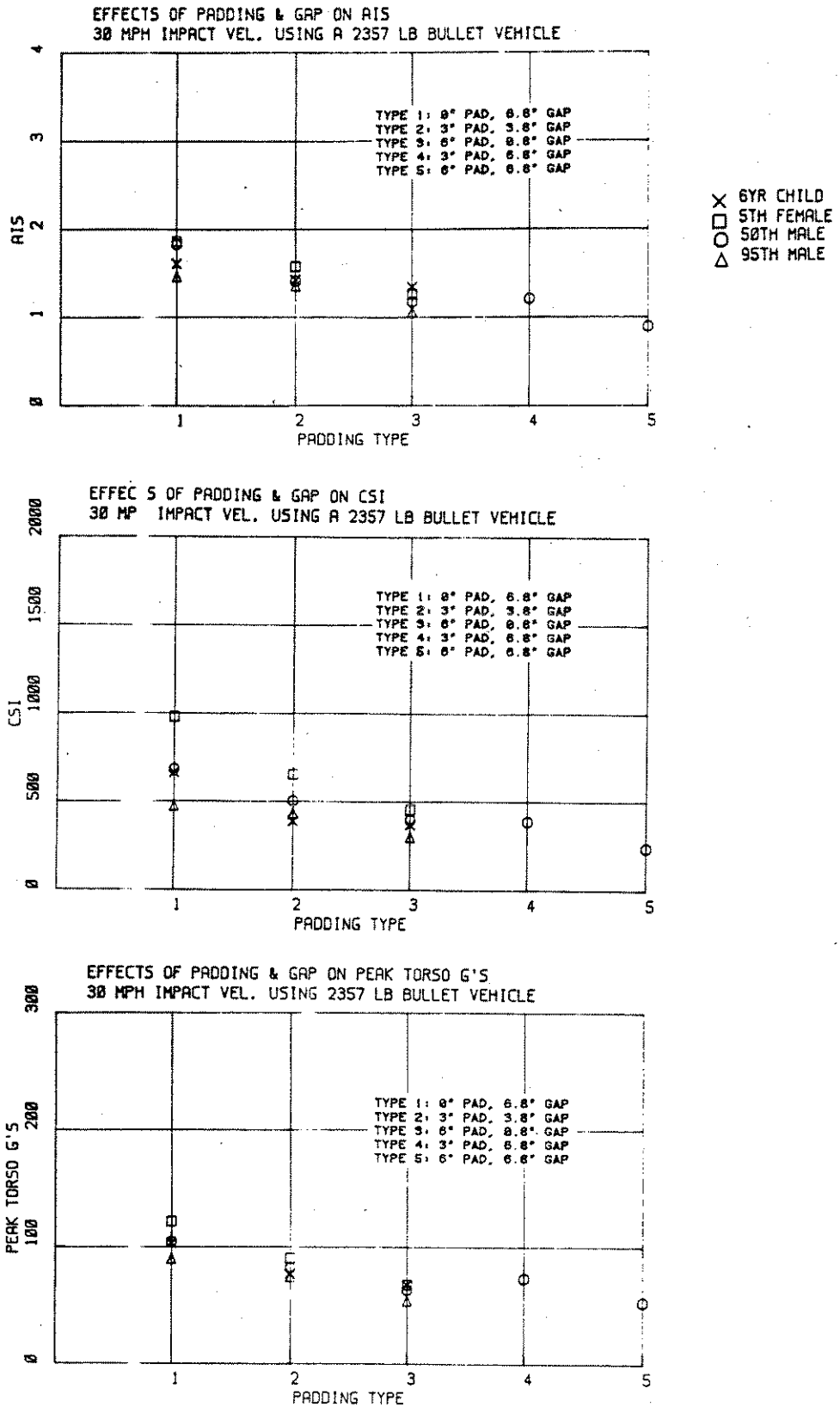

Figure 5-4 EFFECTS OF PADDING ON INJURY MEASURES

Table 5-4

EFFECTS OF GAP ON 50TH PERCENTILE MALE RESPONSE

Padding	Gap	AIS	CSI	Peak Torso Accel
0"	6.8"	1.63"	683	104
3"	3.8"	1.41"	501	82
6"	0.8"	1.18"	398	63
3"	6.8"	1.21"	398	72
6"	6.8"	0.90"	244	53

It is apparent from this table that maintaining a gap between the occupant and intruding door can be of benefit. That is, 3 inches of padding with a 6.8 inch gap is approximately as effective as 6 inches of padding with a small (0.8 inch) gap in reducing injury measures.

Table 5-5 summarizes results for the 50th percentile male occupant with 3 inches of padding and 3.8 inch gap as striking car impact speed is varied. As is seen, all torso severity indicies increase strongly with impact speed as is expected.

Although a head mass was added to the lumped mass representation of the side impact occupant, the general connectivity of what is, at a minimum, a two-dimensional system by a one-dimensional model is not reasonably achievable. An "effective" spring acting between the head and upper torso was developed for the head acceleration and lateral displacement of the head relative to the torso from a CAL-3D run. This spring was used between the head and torso masses in the lumped mass simulations performed. However, in

Table 5-5

EFFECTS OF IMPACT SPEED ON 50TH PERCENTILE MALE RESPONSES

Impact Speed (MPH)	AIS	CSI	Torso Accel (G's)
20	0.299	53.5	27.8
30	1.412	501.5	81.8
40	2.59	1687.6	134.3

general, the results obtained were obvsiously unreaslistic and, therefore, analyses was not attempted.

On the other hand, the CAL-3D results, by the nature of the model, produce a reasonable representation of head dynamics. It is therefore of interest to document the results obtained in this study. Figure 5-5 illustrates the peak head resultant acceleration obtained in all parameter study runs made. Note that the head response results from dynamic coupling with the remainder of the body only. No head contacts were simulated. While these results do indicate that padding may reduce head acceleration in adult occupants, the results from the higher and lower impact speed runs shown on the figure suggest that impact speed is a dominant factor. The child head acceleration results suggest that as more padding is added, higher head accelerations result. However, the observed behavior is believed to result from reductions in gap as 3 and 6 inches of padding were simulated with the child occupant. Since variations in gap were not made with the child, this could not be confirmed with available results.

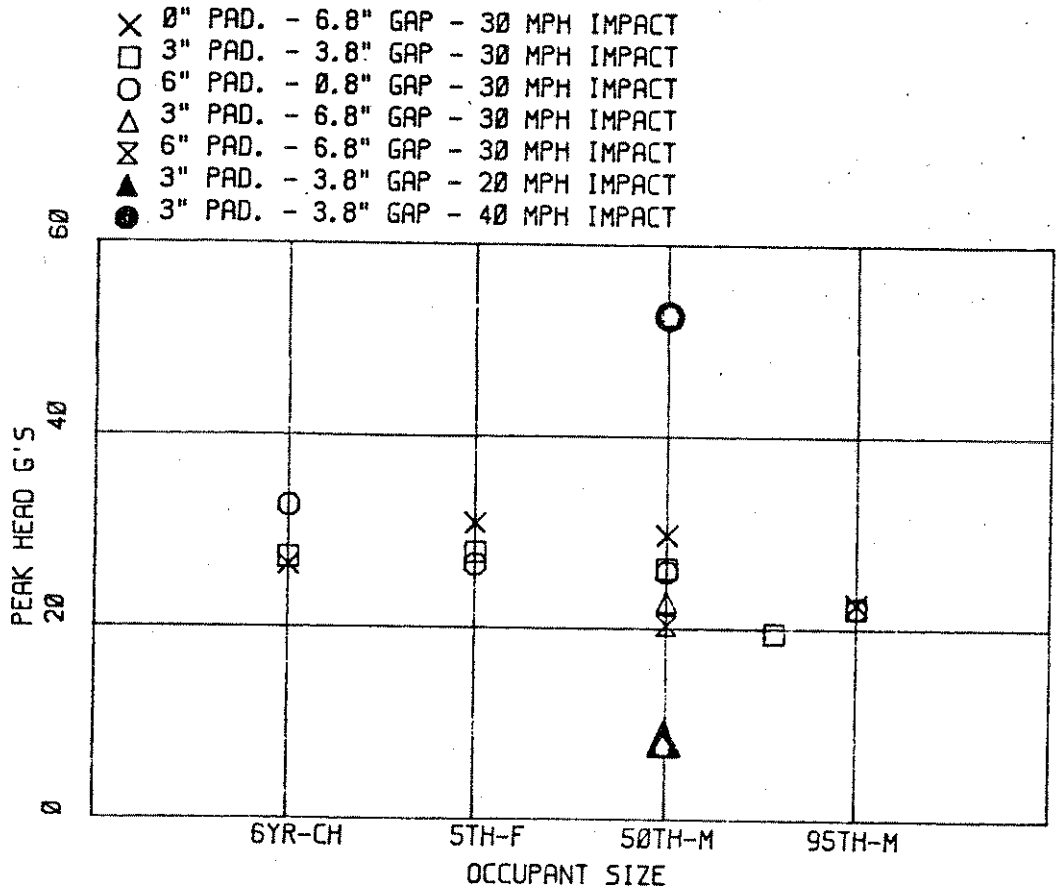

Figure 5-5 PEAK HEAD ACCELERATION FOR ALL CAL-3D RUNS

6. MODEL COMPARISONS

This section presents comparisons made with results of the models used in the study. First, comparisons are made between the results from fifteen side impact sled tests reported in Ref. 2 and model results from corresponding simulations. The intent of these comparisons was to verify that the models were adequately predicting side impact phenomena. It should be emphasized that a rigorous validation of models was not undertaken and was, in fact, outside the scope of the effort. Existing test results were not used for validation purposes as adequate documentation of significant parameters (e.g., door force-deflection properties) was not available. Thus, estimates of important parameters were developed from other sources and the general results of the models were verified as being reasonable as compared with test results.

The second subsection contains a comparison of corresponding parameter study runs made with the lumped mass and CAL-3D models. The intent of this comparison is to identify where the models result in agreement or disagreement.

6.1 Model Verification

Initial model verification (and to a limited extent, parameter adjustment) was accomplished by comparing model results with three replicate side impact sled tests conducted under Contract No. DOT-HS-9-02177, "Countermeasures for Side Impact," (Ref. 2). These tests were designed as T3-24, T3-26 and T3-27 in Ref. 2 and involved bullet sled impact speeds of 27.8 to 28.2 MPH with a standard VW Rabbit inner door structure. The initial gap between the SID dummy and the inner door at hip level was nominally 6 inches. In the three tests, two different SID dummies were used.

Data input to the lumped mass model to simulate these tests are summarized in Section 3. Comparisons of lumped mass simulation and test responses are provided in Figures 6-1 through 6-6. Predicted velocity time histories of both the striking and struck vehicles (Figures 6-1 and 6-2) compared favorably with test results. The velocity time history of the struck door (Figure 6-3) follows the experimental pattern and generally falls within the experimental band.

A comparison of the struck rib acceleration response is shown in Figure 6-4. Although the initial peak is somewhat lower than the experimental results, overall the prediction represents a good compromise in terms of modeling the ribcage structure as a single mass element. Upper thorax lateral responses are compared in Figure 6-5. The predicted peak acceleration is higher than seen in the experiments and the overall wave shape is shorter in duration. This difference is attributed to a difference between the physical system and the idealized model. That is, in the actual side impact dummy, the nature of the rib to spine connection allows a direct mechanical force path through the leather hinge in addition to a compliant force path representing hinge rotation and rubber pad bottoming. This direct force path would allow earlier buildup of upper thorax lateral acceleration and likely a reduction in peak levels. This dual force path cannot be modeled with the simplified lumped mass procedure. Thus,the results shown represent the best compromise modeling results achieved.

The pelvis lateral acceleration comparison is shown in Figure 6-6. The predicted peak level is lower than seen in the experiments. In the current representation, the pelvis is treated as an independent mass with an effective weight assigned to it. The peak acceleration is therefore influenced by the effective mass or the force-deflection properties of the door panel only. Since force-deflection data on the specific door configurations used in the test program were not available, these results were accepted as reasonable based on estimates of those properties.

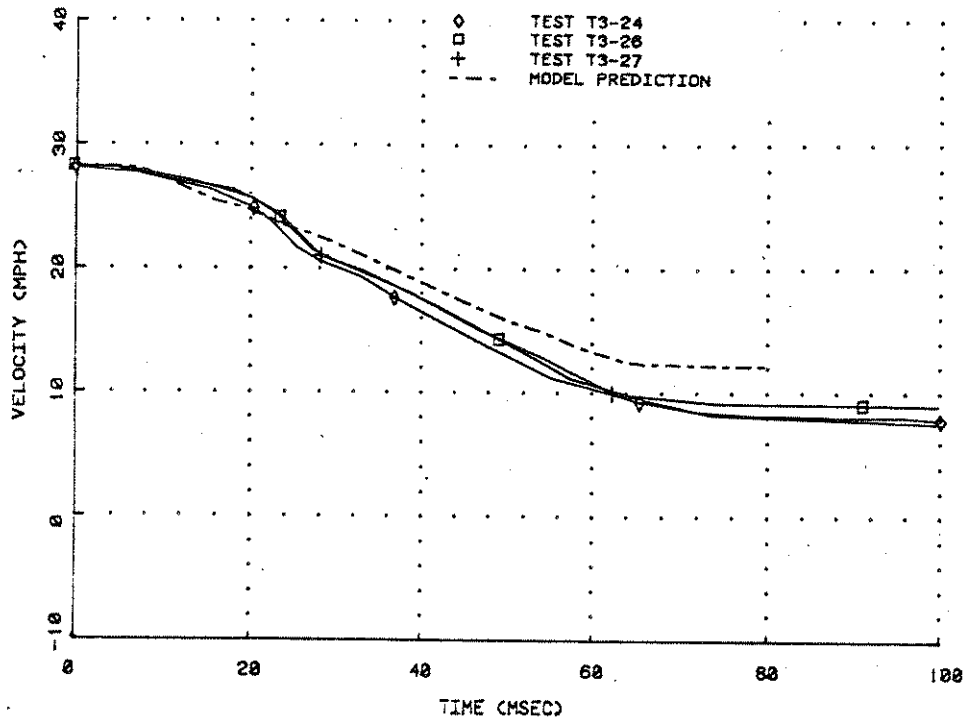

Figure 6-1 LUMPED MASS PREDICTED AND EXPERIMENTAL STRIKING CAR SPEED

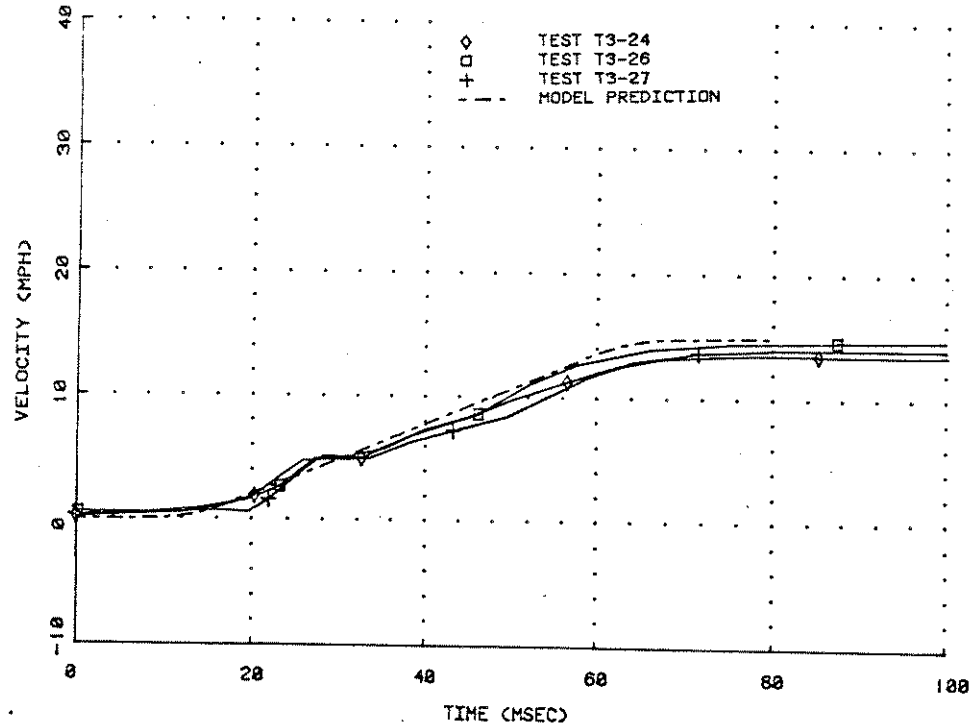

Figure 6-2 LUMPED MASS PREDICTED AND EXPERIMENTAL STRUCK CAR SPEED

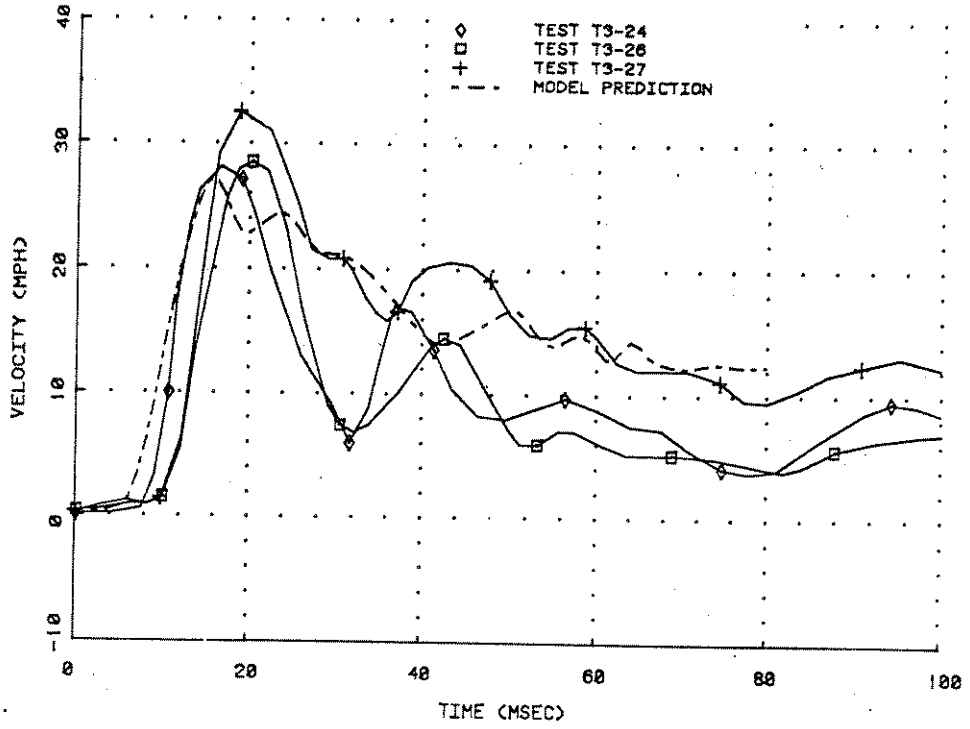

Figure 6-3 LUMPED MASS PREDICTED AND EXPERIMENTAL DOOR VELOCITY

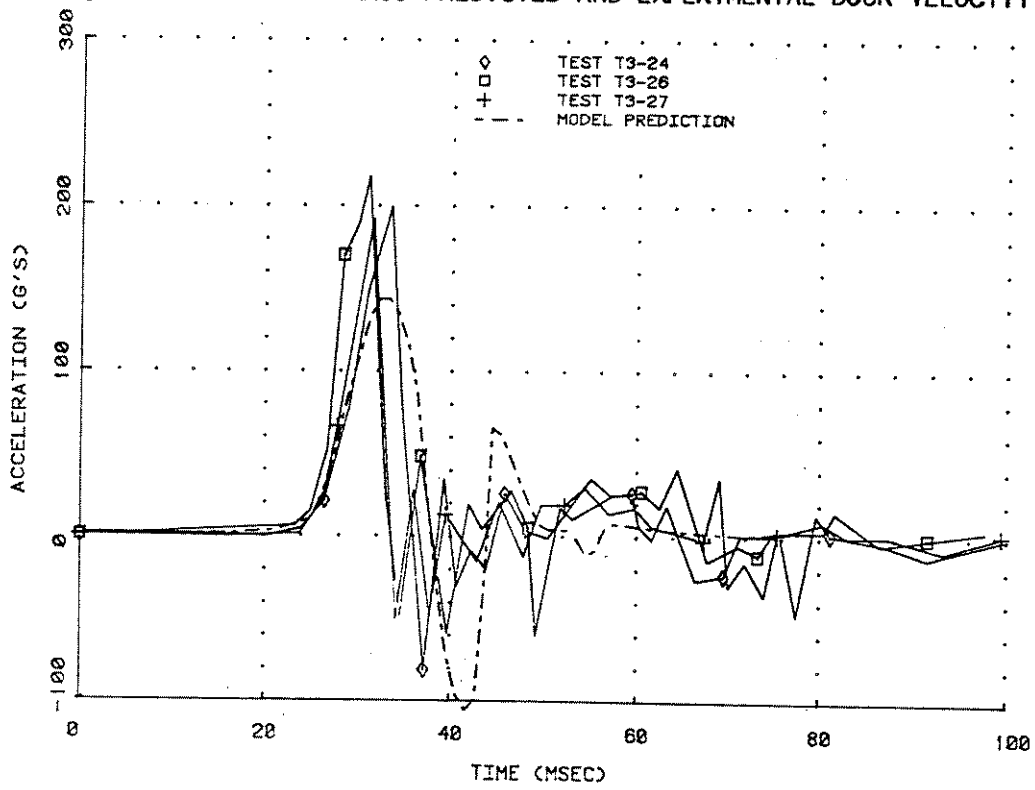

Figure 6-4 LUMPED MASS PREDICTED AND EXPERIMENTAL RIB RESPONSE

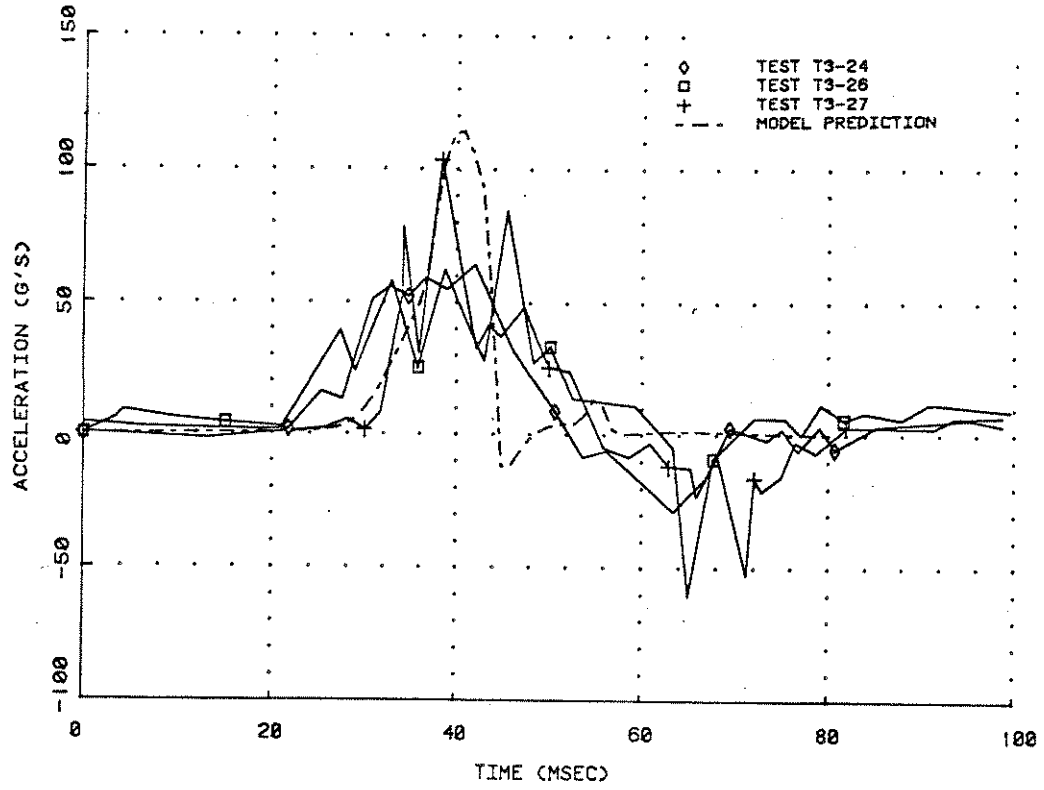

Figure 6-5 LUMPED MASS PREDICTED AND EXPERIMENT UPPER TORSO RESPONSE

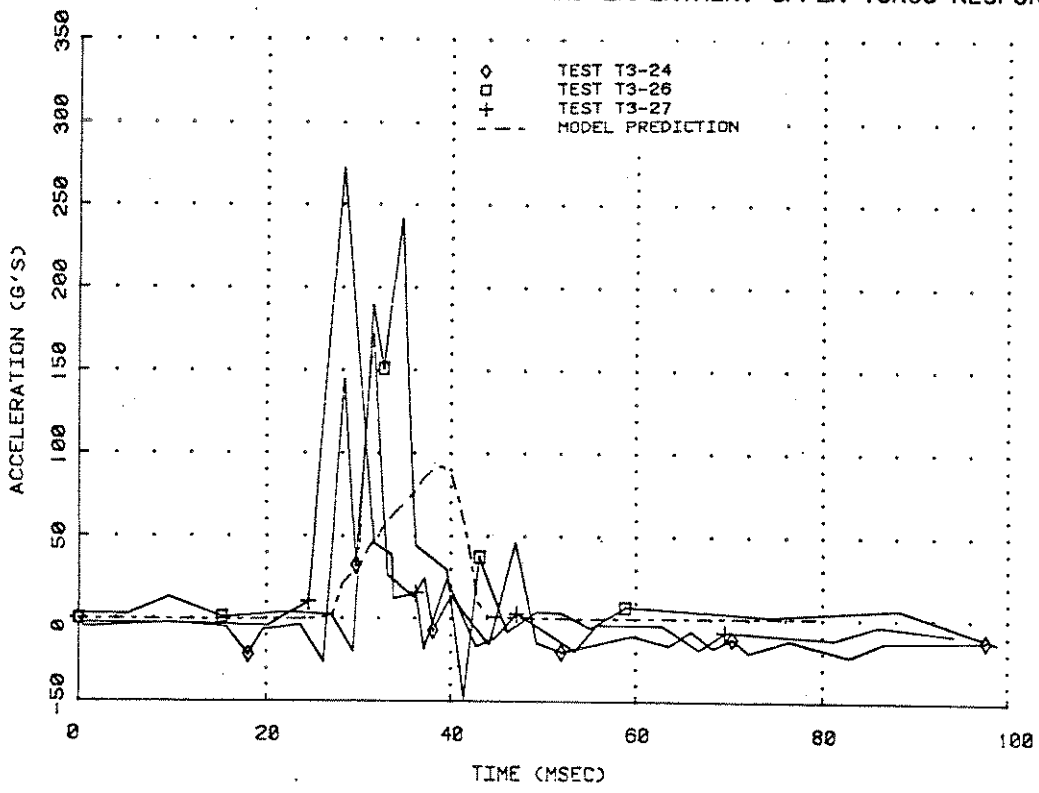

Figure 6-6 LUMPED MASS PREDICTED AND EXPERIMENTAL PELVIS RESPONSE

These tests were also simulated with the CAL-3D model. Force-deflection data used was the same as that used in the lumped mass model. Thus, this comparison provides not only a means of verifying the CAL-3D but a means of evaluating response differences resulting from the two modeling approaches. CAL-3D results are shown plotted over corresponding test results in Figures 6-7 through 6-10. The peak acceleration of the struck rib is considerably lower than the test results. It is also lower than that seen in the corresponding lumped mass results. Note, however, that in comparison with the lumped mass results, the shape of the CAL-3D rib response curve appears to better match the experimental curve shape. In particular, the oscillatory response of the lumped mass model is not present after the initial impact.

The response of the upper torso, Figure 6-8, is in much better agreement with test results than was seen with the lumped mass model. The peak value is in good agreement with test results and the curve shape tends to follow the experiments better. This results from the more realistic coupling between the rib and torso in the CAL-3D representation. The lower torso response (Figure 6-9) is again considerably lower than the test results. The head acceleration (Figure 6-10) tends to lead the experimental results somewhat but generally exhibits a similar wave shape and peak value. It should be noted that a force-deflection curve derived from this CAL-3D head acceleration response was subsequently employed in the lumped mass model to attempt to approximate the coupling between the head and upper torso.

These three tests represent approximately the middle of a range of impact speeds investigated in the experimental study (Ref. 2). Four additional tests with a standard VW Rabbit door structure, two each at higher and lower impact speeds, were also available and were utilized to check model predictions. A summary of peak values from these, and the previously discussed tests, are shown in Table 6-1 as compared to simulation results. A visual comparison of peak values as a function of impact speed is shown in Figure 6-11. From the figure, it can be seen that the models tend to underpredict peak thorax and rib accelerations. Note, however, that when 3

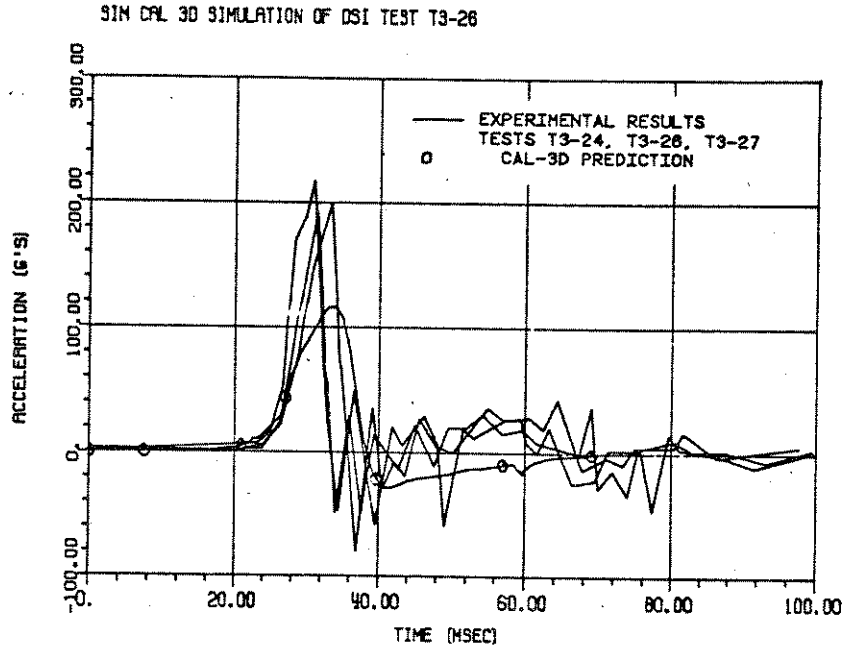

Figure 6-7 CAL-3D PREDICTED AND EXPERIMENTAL RIB RESPONSE

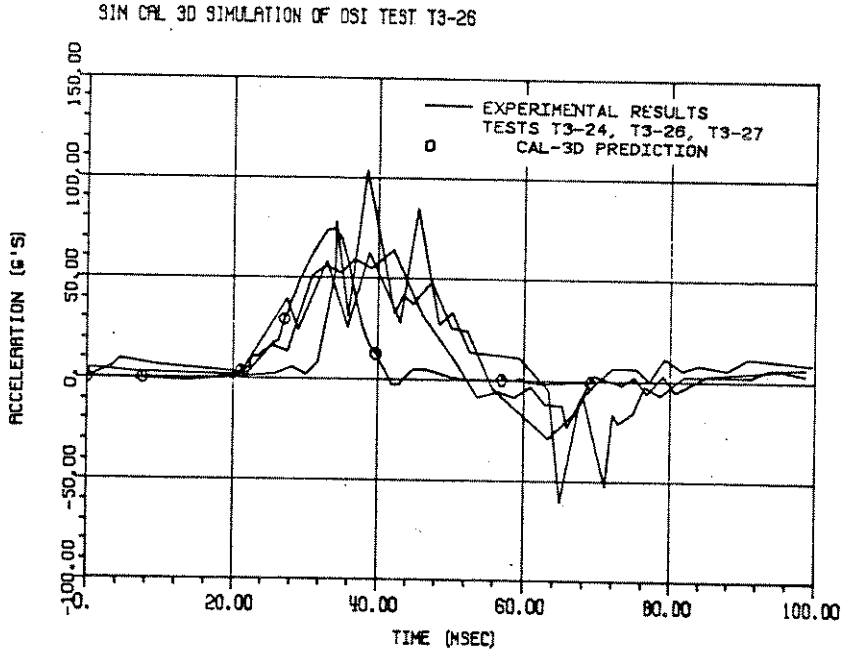

Figure 6-8 CAL-3D PREDICTED AND EXPERIMENTAL TORSO RESPONSE

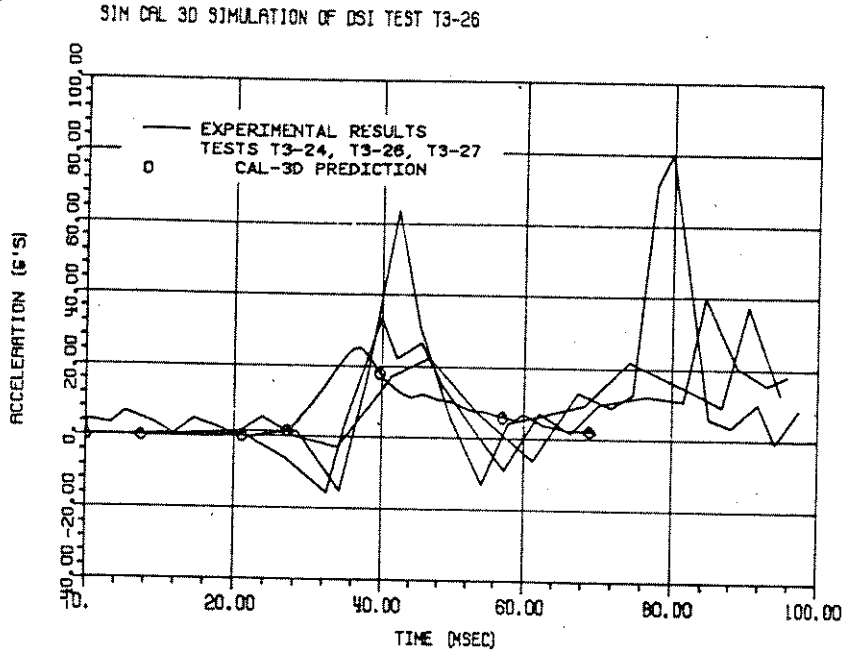

Figure 6-9 CAL-3D PREDICTED AND EPXERIMENTAL PELVIS RESPONSES

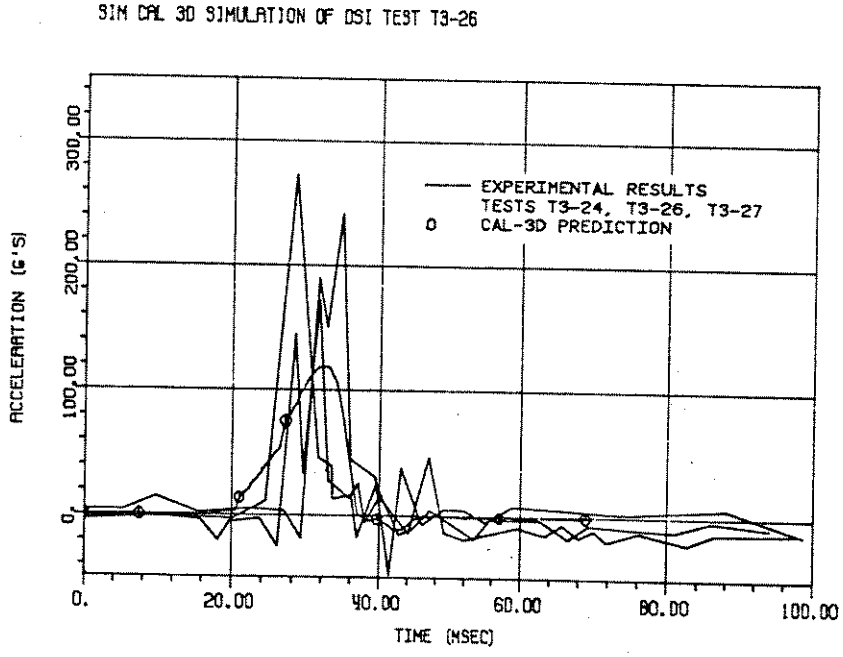

Figure 6-10 CAL-3D PREDICTED AND EXPERIMENTAL HEAD RESPONSES

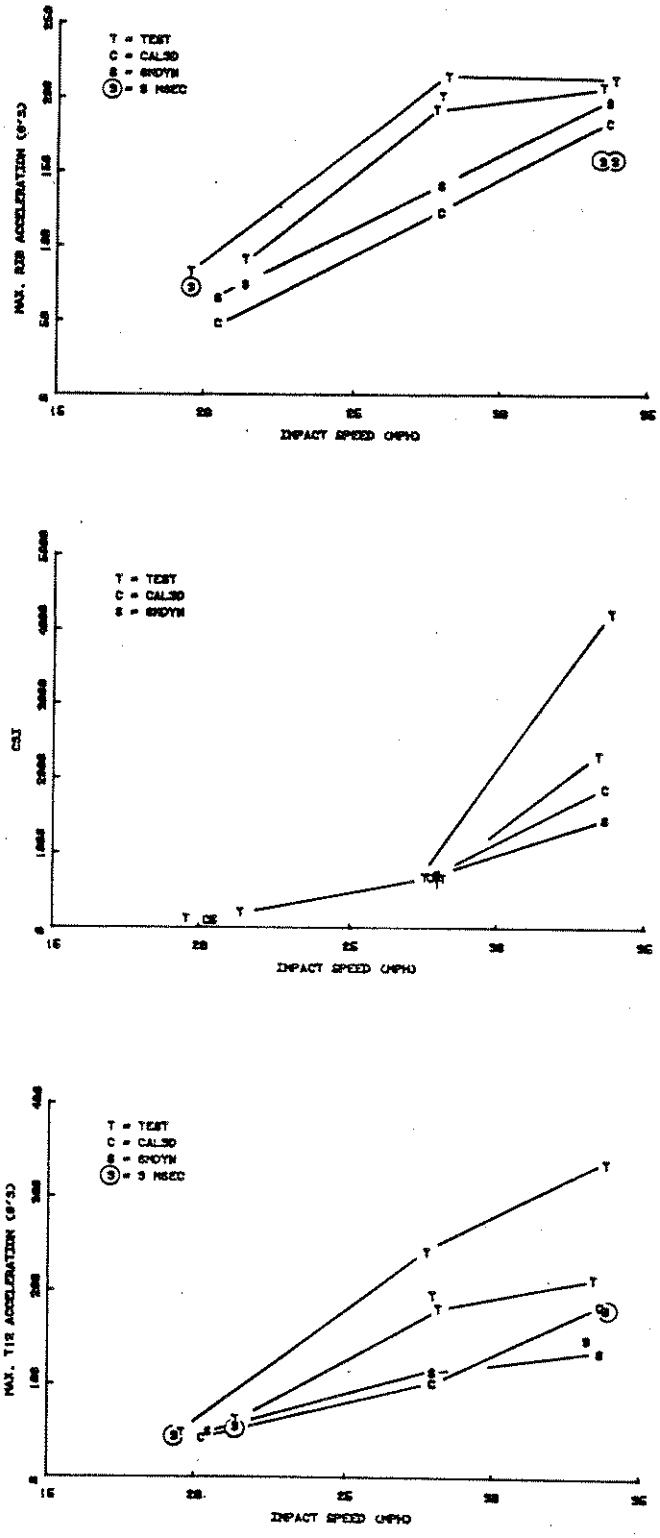

Figure 6-11 COMPARISON OF PREDICTED AND MEASURED PEAK ACCELERATIONS

Table 6-1

SUMMARY OF MODEL VERIFICATION COMPARISONS (UNPADDED DOOR)

Test/Simulation	Impact Speed	Lower Thorax (T12) Lateral Acceleration SI	Max.	3 msec Clip	Struck Rib Lateral Acceleration Max.	3 msec Clip
T3-13	21.4	209	62	54	91	74
T3-14	19.6	121	48	44	83	72
Test Average	20.5	165	55	49	87	73
Lumped Mass	20.5	103	49	--	65	--
CAL-3D	20.5	101	42	--	48	--
T3-24	28.0	602	195	--	201	--
T3-26	28.2	670	181	--	214	--
T3-27	27.8	683	241	--	192	--
Test Average	28.0	652	206	--	202	--
Lumped Mass	28.0	724	113	--	141	--
CAL-3D	28.0	685	101	--	123	--
T3-8	33.5	2307	212	148	207	158
T3-9	33.9	4216	336	180	212	158
Test Average	33.7	3262	274	164	210	158
Lumped Mass	33.7	1454	134	--	197	--
CAL-3D	33.7	1870	184	--	183	--

msec. clip accelerations are available, the model predictions are considerably closer or are in between these and the peak values.

In an effort to further verify model predictions, eight additional comparisons with test results were made. These tests (Ref. 2) all included low denisty polyurethane foam of varying thickness as a padding material. Variations in the initial gap between the occupant and padding were also made and tests were done with a standard 6 year old child and a 95th percentile male dummy. A summary of these tests is provided below.

Test No.	Occupant	Padding Thickness	Impact Speed	Gap
T4-4	SID	5"	27.3	1.5
T4-5	SID	5"	27.3	1.5
T4-14	SID	4"	27.9	2.0
T4-18	SID	4"	25.4	2.0
T4-20	6yrchild	10"	26.9	0
T4-21	95thmale	10"	27.0	0
T4-27	SID	7"	27.1	1.0
T4-30	SID	3.5"	27.2	2.5

Lumped mass and CAL-3D runs were made corresponding to the above test conditions. Comparisons between test results and model predictions are summarized according to variations in impact speed and initial pelvis to door spacing (Gap) on Figures 6-12 through 6-14.

Figure 6-12 summarizes four comparison measures (CSI, maximum T12, rib and pelvis lateral acceleration) for test condition T4-18 and T4-14. These test conditions were essentially identical except for impact speed of the bullet vehicle. As is seen in the figure, both models appear to predict maximum T12 accelerations and CSI values that are in reasonable agreement with

test results. The peak rib acceleration measured in the lower speed test is a suspect data point as it does not follow expected trends. Both models do predict an increase in peak rib acceleration with increasing impact speed and are quite close to the higher speed test result. The models both tend to underpredict peak pelvis acceleration with the CAL-3D closer to the test results than the lumped mass model.

Figure 6-13 presents similar comparisons as a function of gap. Different padding thicknesses were used in the tests with the appropriate padding thickness simulated. In only one case, that of the 1 inch gap, did the simulated padding fail to bottom. Generally, the CAL-3D does a better job of predicting CSI and maximum torso acceleration than does the lumped mass model. The CAL-3D predicted peak pelvis acceleration is also closer to test results.

An additional set of comparisons is shown in Figure 6-14. This presents data for a 95th percentile male and 6 year old child test and predictions. As is seen, the CAL-3D is clearly superior for predicting responses of the child while both models appear to do a good job for the 95th percentile male occupant.

In summary, over the speed range considered, both models appear to do a reasonable job of predicting responses for the 50th percentile male. As gap (or occupant spacing) is varied, the CAL-3D appears to be more realistic. The CAL-3D also is clearly superior when considering small occupants.

6.2 Parameter Study Comparisons

The primary emphasis of the CAL-3D runs were to provide a comparison base for variations in occupant size and padding properties. Thus, twelve of the sixteen runs conducted involved four different occupants with three different padding conditions. For each of these, a corresponding lumped mass run was also made.

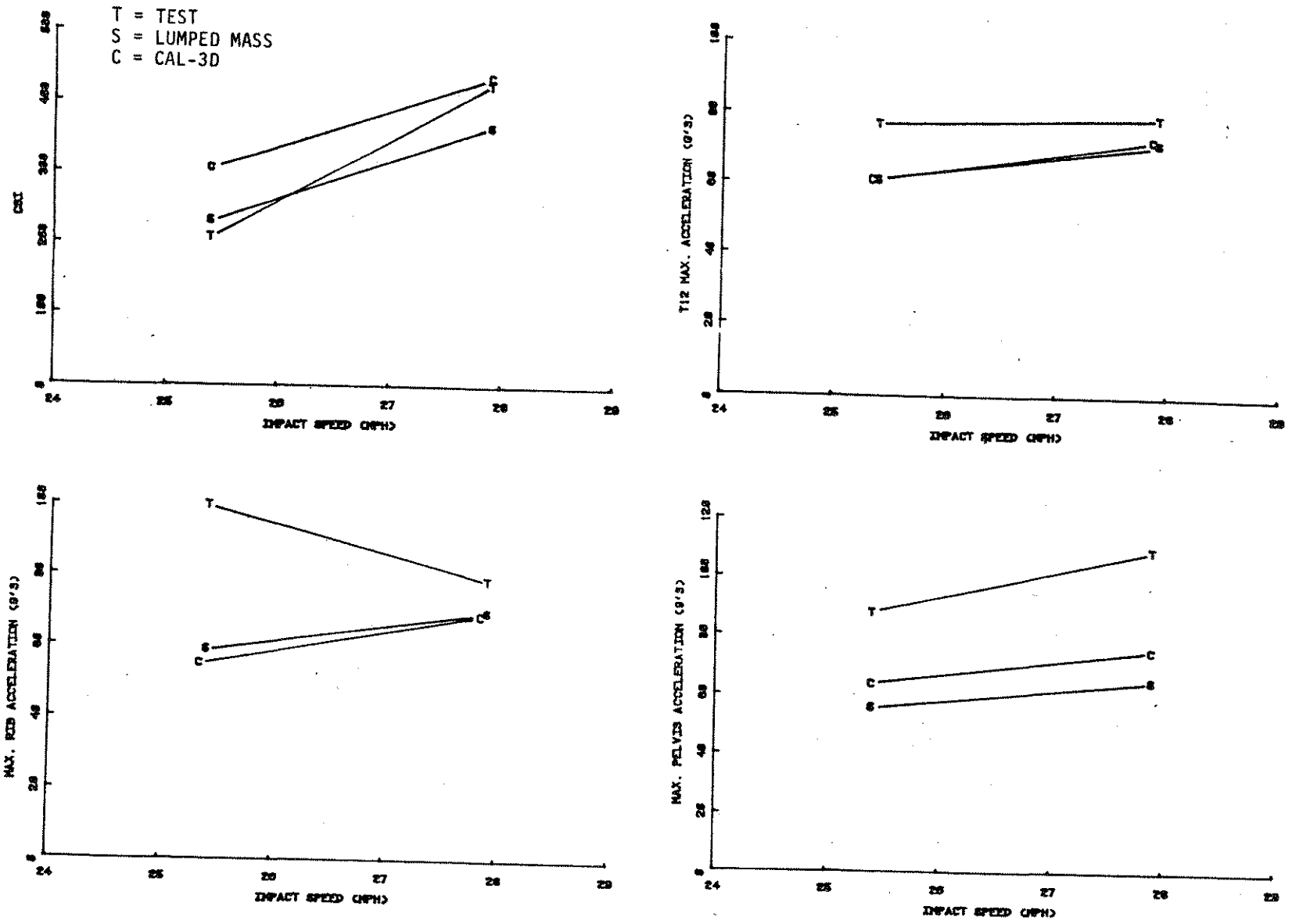

Figure 6-12 COMPARISON OF ANALYTICAL VS. TEST RESULTS AS FUNCTION OF IMPACT SPEED

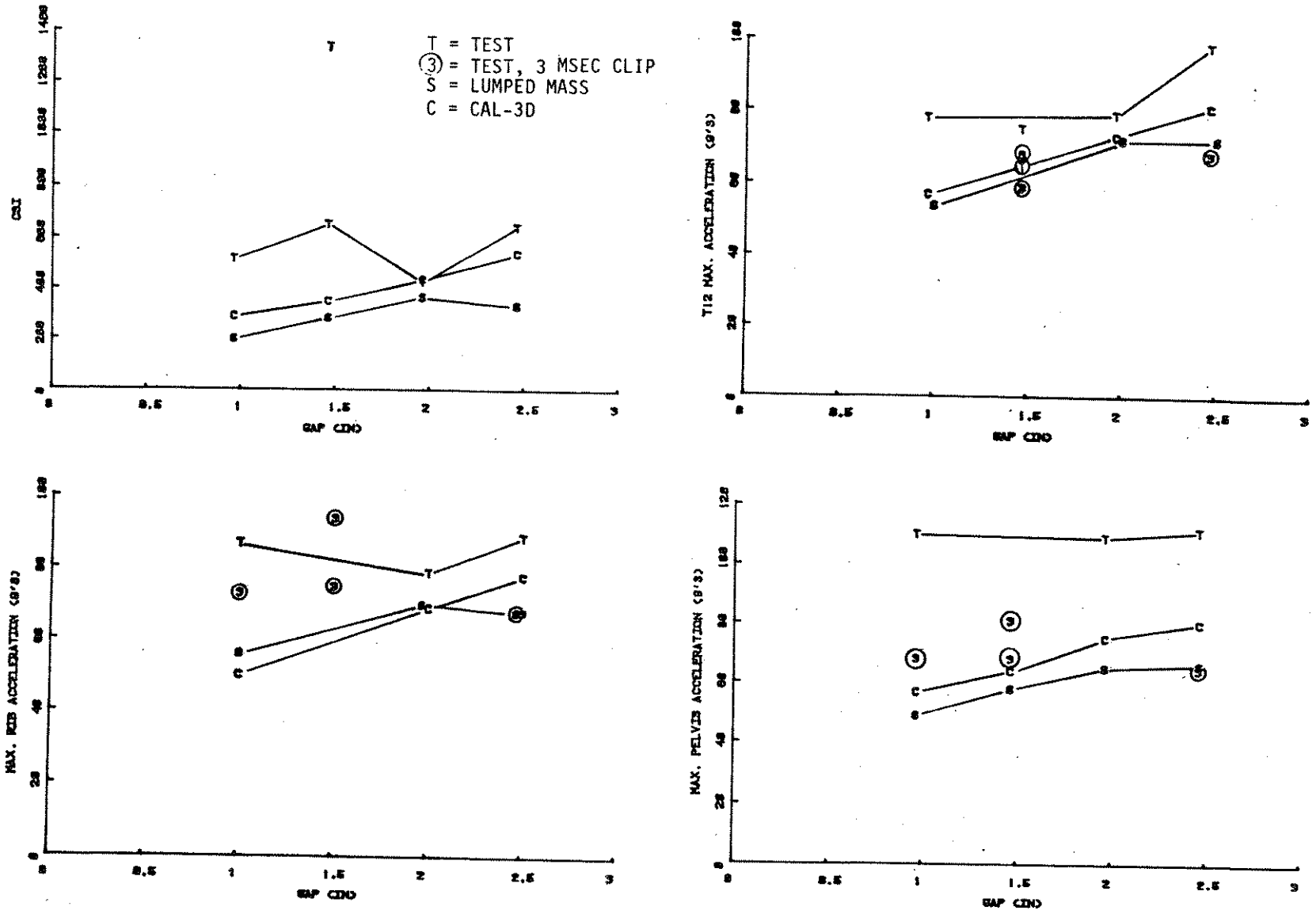

Figure 6-13 COMPARISON OF ANALYTICAL VS. TEST RESULTS AS A FUNCTION OF GAP

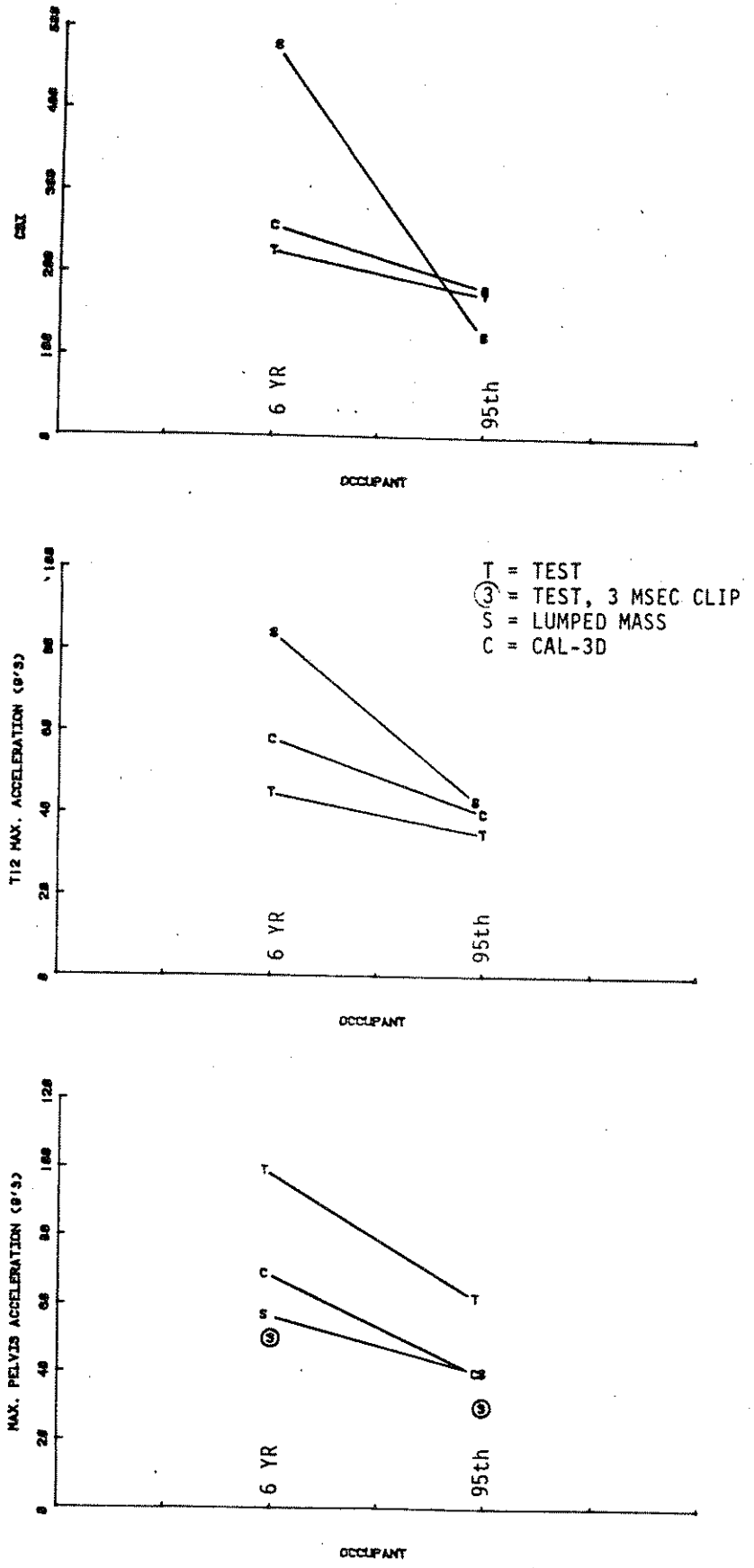

Figure 6-14 COMPARISON OF ANALYTICAL VS. TEST RESULTS AS FUNCTION OF OCCUPANT SIZE

Comparisons between the two modeling approaches for the first set of runs are presented in Figure 6-15. The conditions represented there include all occupant sizes striking the baseline or unpadded door with an impacting vehicle speed of 30 MPH. As can be seen, a definite trend is evident in all three severity measures for the three adult occupants. That is, all measures increase as occupant size decreases. However, when the 6 year old child is simulated, this trend is no longer consistent. The CAL-3D shows a decrease in all severity measures for the child from the expected trend. The lumped mass results are mixed. The AIS shows a decrease while the CSI and peak torso acceleration show an increase or a continuation of the expected trend.

Similar results also exist for the 3 inch padding condition shown in Figure 6-16. That is, the largest discrepancy between the modeling approaches occurs with the child occupant. As padding thickness is increased, Figure 6-17, similar trends exist. Note that in comparing the three padding conditions, generally the largest differences between model predictions is in the AIS severity measure. Across all severity measures, closest percentage agreement between the two modeling approaches is seen with 3 inches of padding and worst for the 6 inch padding case for the adult occupants. The actual percentage differences of the lumped mass results from the CAL-3D results are summarized for these runs in Table 6-2. The average, absolute difference for the adult occupants is largest for the AIS measure and smallest for the peak torso acceleration.

Two CAL-3D runs were also made at impact speeds above and below the nominal 30 MPH condition. These runs used only the 50th percentile male occupant and the 3 inch padding with 3.8 inches of gap. A comparison of severity indicators with corresponding lumped mass results is made in Figure 6-18. As can be seen there, both models agree quite favorably, particularly at the 20 MPH and 30 MPH impact velocities. At 40 MPH, all lumped mass model injury indicators are below those resulting from the CAL-3D by up to 20%.

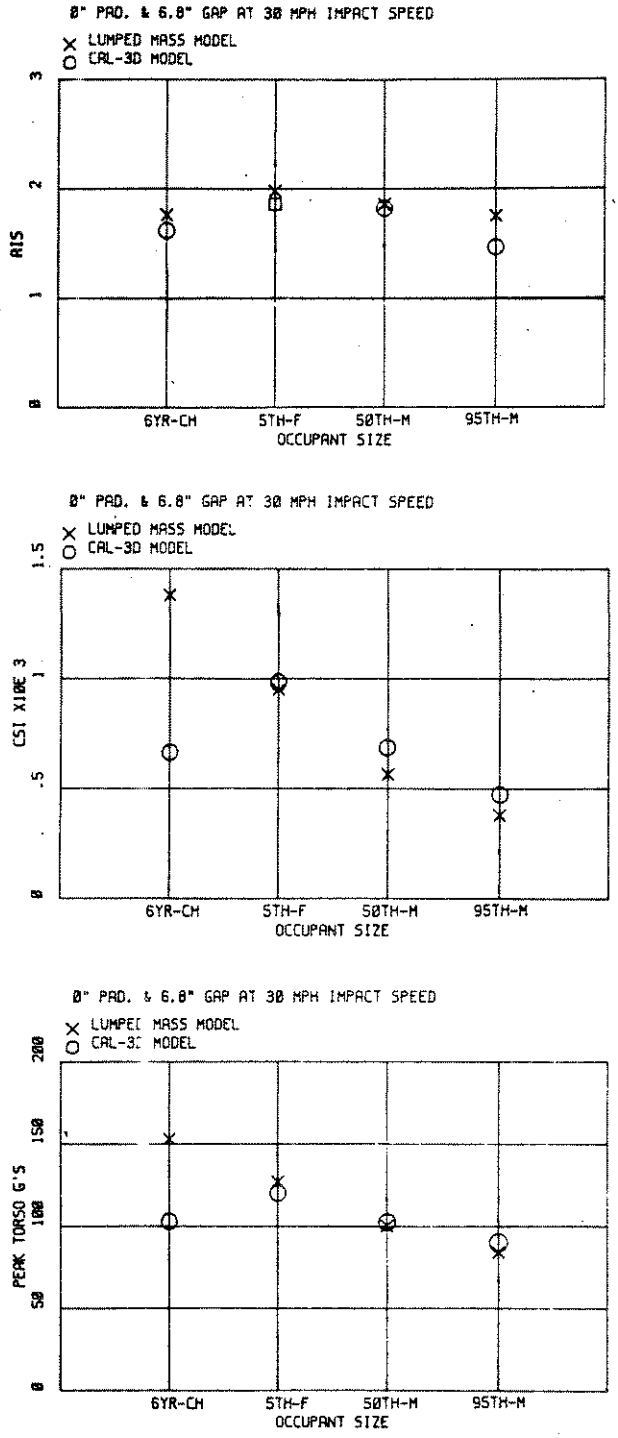

Figure 6-15 COMPARISON OF CAL-3D AND LUMPED MASS RESPONSES FOR UNPADDED DOOR

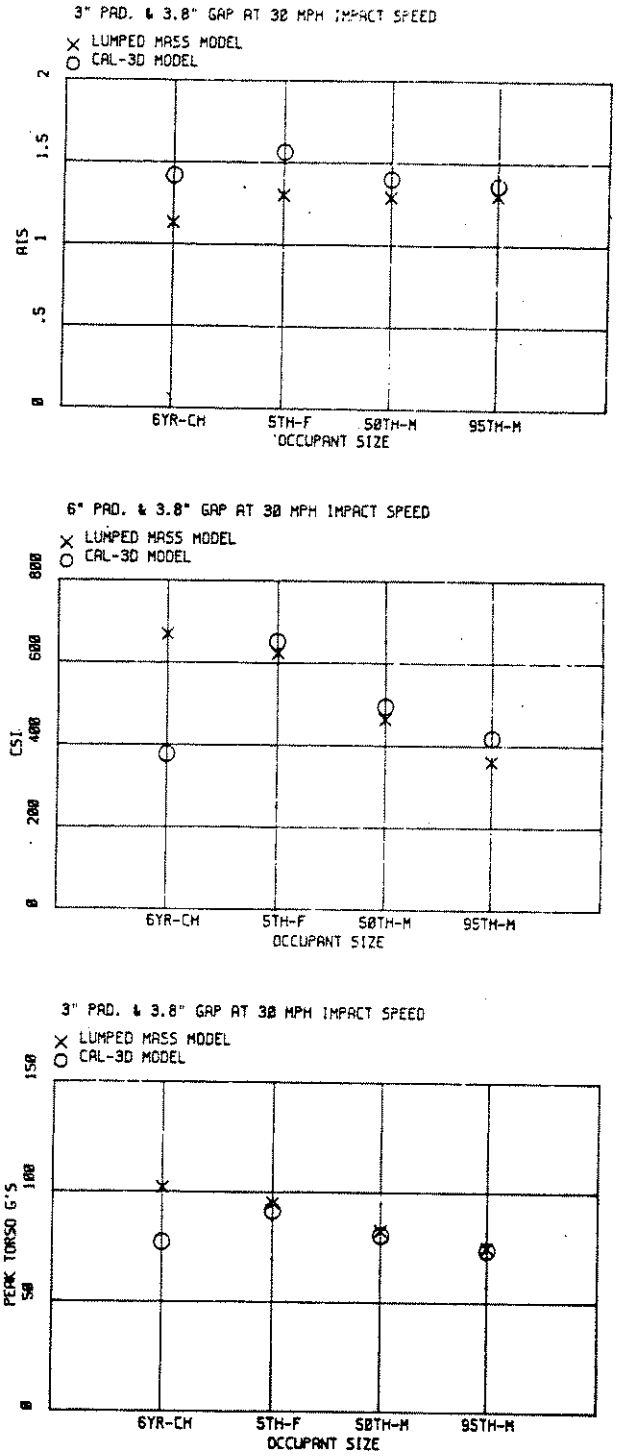

Figure 6-16 COMPARISON OF CAL-3D AND LUMPED MASS RESPONSES FOR 3 INCH PADDING

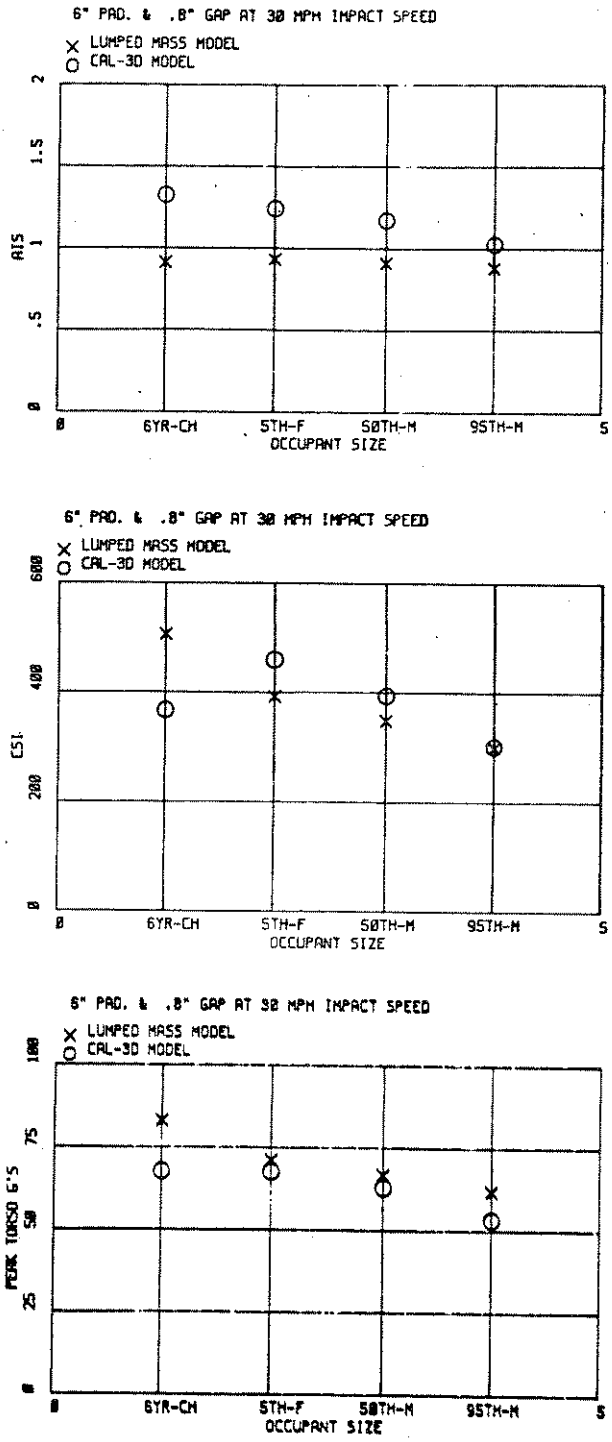

Figure 6-17 COMPARISON OF CAL-3D AND LUMPED MASS RESPONSES FOR 6 INCH PADDING

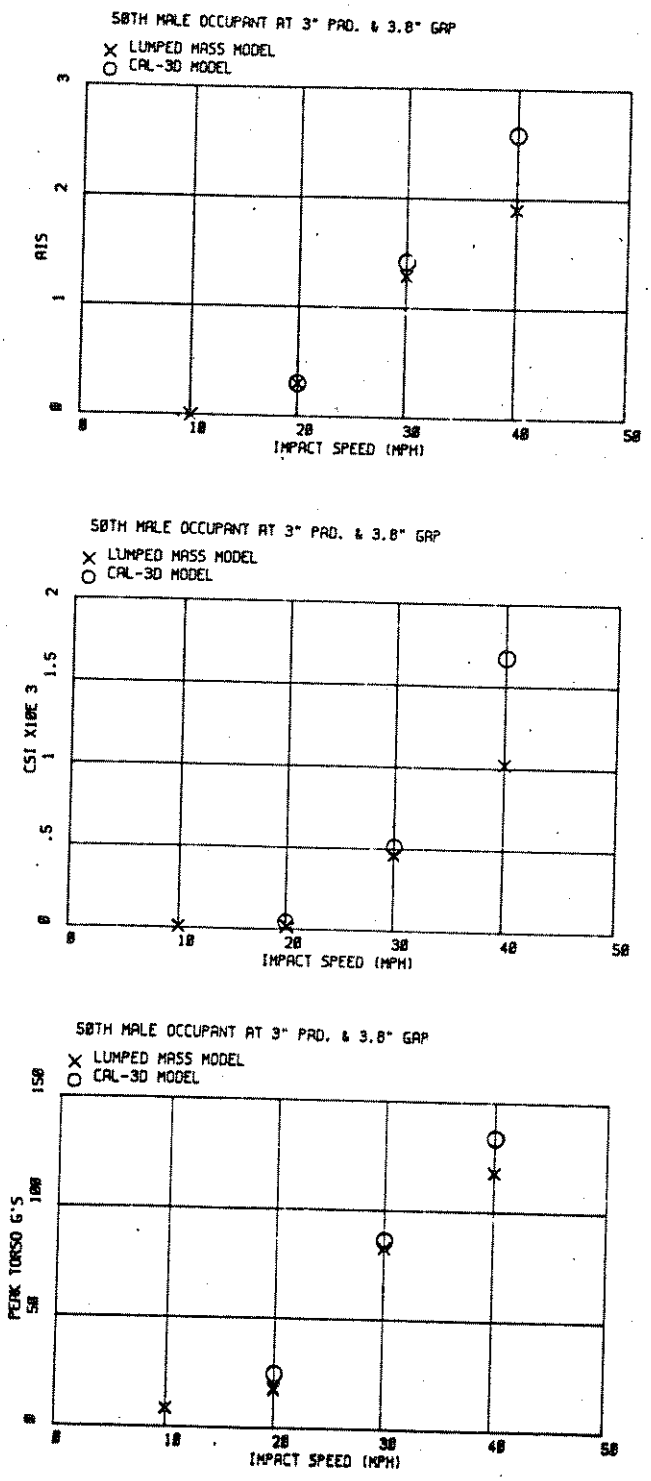

Figure 6-18 COMPARISON OF CAL-3D AND LUMPED MASS RESPONSES VERSUS IMPACT SPEED

Table 6-2
PERCENTAGE DIFFERENCES IN SEVERITY MEASURES BETWEEN MODELING APPROACHES

Run No.	Occupant	Padding (IN)	Nominal GAP (IN)	LUMPED MASS DIFFERENCE FROMCAL-3D (%) AIS	CSI	Peak Torso Accel
3	50th	0	6.8	14.1	-17.5	-3.6
7	95th	0	6.8	20.0	-20.2	-6.2
11	5th	0	6.8	6.5	-3.1	-4.4
50	6yr	0	6.8	9.3	108.6	48.4
15	50th	3	3.8	-8.5	-7.8	0.8
19	95th	3	3.8	-4.4	-16.3	0.9
23	5th	3	3.8	-17.7	-4.7	5.1
52	6yr	3	3.8	-38.6	54.0	32.4
27	50th	6	0.8	-22.9	-12.6	3.4
31	95th	6	0.8	-17.0	0.3	14.7
35	5th	6	0.8	-26.8	-14.0	5.0
54	6yr	6	0.8	-50.3	39.4	23.0

7. DISCUSSION

This section constitutes a discussion of some of the significant results uncovered as a result of the study. In the interest of clarity, this section is divided into discussion of model verification and of parameter study results.

7.1 Model Verification

The ultimate objective of this, and most other highway safety analytical or modeling efforts, is to predict injury severity occurring to humans exposed to automotive accidents. Due to the diverse nature of the human population and the limited availability of experimental results, it is generally necessary to construct a model representation of a mechanical analog of the human being, that is, an anthropometric dummy. Thus, modeling activities frequently attempt to represent the mechanical analog rather than the human directly, in the interest of being able to define the system mathematically and in having comparison test results available for verifying model predictions.

The thrust of this project followed this general approach. That is, modeling efforts were directed at representing the 50th percentile male Side Impact Dummy (SID) which, in turn, is expected to be a reasonable analog of a correspondingly sized human.

Although initial model development activities used pendulum test data as an aid in guiding the assignment of certain modeling parameters, the actual verification effort consisted of comparisons with side impact sled test results taken from Ref. 2. Thus, verification was based on performance in an environment that closely duplicates actual lateral collisions rather than a component test environment.

It should be noted here that the model/test comparisons made in this study have been termed verification rather than validation. The interpretation of a validation effort implies the conduct of tests with extensive effort to fully document test parameters and conditions with the objective of providing data for modeling comparisons. In this case, existing test results, which were not conducted for that purpose nor documented to the extent necessary for rigorous validation purposes, were used to compare model results. Much data supplied to the model in order to simulate test conditions were obtained from the test documentation, but other information was obtained from various sources and applied with some degree of engineering judgment. Consequently, comparisons between model and experiment are expected only to indicate that the models reasonably agree with test results and exhibit the same trends as are discovered in experiments.

Verification comparisons were presented and discussed in the previous section and will not be repeated here. Rather, a number of points will be presented.

Rib Responses

Rib responses generally were better predicted by the CAL-3D model over the entire impact event. This resulted from the more realistic and complete coupling with the remainder of the occupant. In contrast, the lumped mass rib is coupled only with the upper torso mass. Secondary oscillations (subsequent to door contact) coupled to the upper torso mass were evident only with the lumped mass model. Where substantial padding limited the primary rib response peak, this second, coupled peak sometimes exceeded the primary. Since the algorithm used to calculate an AIS level is directly dependent upon the response of the struck rib, the extent to which the second peak influences the calculated AIS is of concern.

Upper Torso Response

Because the lumped mass model induces upper torso responses only through compression of the spring acting between it and the rib, the rib and upper torso responses are closely associated. As a result, the period of the primary rib response is predicted quite well within the model, however, the predicted upper torso response is a much shorter duration than is seen in the test results. The CAL-3D, on the other hand, has additional load paths which cause upper torso responses. These include joint connections to the center torso and neck segments and to the rib segment. In particular, as the rib is modeled as a pin jointed segment rotating around a vertical axis, some load is transmitted directly through this joint. Predicted results from the CAL-3D do, in fact, show a longer duration response of the upper torso more closely agreeing with the experimental results. It is believed that refinements to this rib model can be made which would likely improve agreement further.

Head Response

Although an attempt was made to include a head mass in the lumped mass representation, reasonable predictions of head responses were not obtained. The head/neck/torso connectivity implies at least a two-dimensional representation in order to model head motions which in side impacts typically involve substantial rotations. Attempts to represent this connectivity with a one-dimensional force-deflection characteristic was in general not successful. Such a characteristic can be determined from test or CAL-3D results for one condition, but the application of such a characteristic to other impact conditions frequently resulted in unrealistically large extensions between the head and torso. As a result, lumped mass predictions of head responses were not reviewed in any detail.

The appropriate connectivity is, however, inherent in the CAL-3D model. Thus, predicted head responses were expected to be in reasonable

agreement with test results. This, indeed, was the case when direct contacts with the vehicle interior did not occur. In general, it appears that if head responses are of interest or if contacts with the vehicle may occur, a one-dimensional lumped mass model is not sufficient for side impact studies. In these cases, use of the CAL-3D is recommended.

Pelvis Response

The response of the pelvis is directly influenced by the force acting between it and the door. Coupling with other parts of the occupant may add effective mass to the pelvis and in the CAL-3D may have an influence of upper torso responses. Accurate simulation of pelvis responses will, however, be highly dependent on the force-deflection properties used.

7.2 Parameter Study

This section summarizes significant findings resulting from the parameter study runs made with both models.

Parameter Study Comparisons

The principal comparisons between the lumped mass and CAL-3D models in the parameter study consisted of variations in padding interposed between the door and occupants at a constant impacting vehicle speed of 30 MPH. Twelve direct comparisons were made, consisting of three levels of padding with four occupants simulated with each. Differences in single point severity measures between the lumped mass and CAL-3D runs were summarized by run in Section 6. Generally, the average absolute difference between the models was less than 20% for the adult occupants. Differences for the simulated child occupant were much larger, averaging about 45%. This is illustrated in Table 7-1 where the average adult and child injury indicies are listed for each model. Closer agreement from model to model is more evident for the adult occupants than for the child.

Table 7-1

COMPARISON OF PREDICTED SEVERITY MEASURES FOR DIFFERENT MODELS

	CAL-3D MODEL PADDING			LUMPED MASS MODEL PADDING		
	0"	3"	6"	0"	3"	6"
Ave. Adult AIS	1.65	1.45	1.27	1.86	1.20	0.91
Child AIS	1.61	1.43	1.35	1.76	1.13	0.91
Ave. Adult CSI	721.	528.	384.	630	482	346
Child AIS	662.	386.	369.	1381.	670.	506.
Ave. Adult Peak Torso g	105.1	82.0	61.6	103.8	84.1	66.5
Child Peak Torso g	103.1	77.0	67.5	153.0	101.9	83.0

Since both models predict the same trends in injury indicies for the adult occupants, the divergence in results when the child occupant is simulated leads to the hypothesis that some element of data, developed from the scaling procedures discussed elsewhere, results in a different behavior in the CAL-3D than in the lumped mass model. It is believed that the dynamic coupling between the pelvis and upper torso is much more effective in accelerating the upper torso in the CAL-3D model, thus reducing the effect of the rib to door impact. This coupling was not simulated in the lumped mass model. In any case, it is apparent that additional study of the representations used for the child occupant is desirable in order to clarify the apparently inconsistent results from the two models.

Effects of Padding

The results of the parameter study clearly show that padding is of benefit in reducing occupant severity measures in lateral collisions. The average severity measures for all occupant sizes for 0, 3 and 6 inches of padding are shown in Table 7-2. Depending on the severity measure used, reductions for the first three inches of padding are obtained on the order of 12% to 30% for the CAL-3D model and 24% to 36% for the lumped mass model. Reductions for the second three inches of padding range from 11% to 23% for the CAL-3D and 20% to 23% for the lumped mass model. Thus, on the average, it appears that the first three inches of padding may offer more incremental benefit than the second three inches.

Additional benefit (reduction in severity measure) were seen by maintaining large gaps between the occupant and door in conjunction with padding. However, the magnitude of reductions were much less than the difference resulting from the padding itself.

Table 7-2

PREDICTED REDUCTIONS IN SEVERITY MEASURES WITH PADDING

	CAL-3D MODEL PADDING			LUMPED MASS MODEL PADDING		
	0"	3"	6"	0"	3"	6"
Average AIS	1.64	1.45	1.29	1.84	1.18	0.91
Ave. Reduction 0-3"		-11.6%			-35.9%	
Ave. Reduction 3-6"		-11.0%			-22.9%	
Average CSI	700	493	380	818	529	386
Ave. Reduction 0-3"		-29.6%			-35.3%	
Ave. Reduction 3-6"		-22.9%			-27.0%	
Average Peak Torso G	104.6	80.8	63.1	116.1	88.6	70.6
Ave. Reduction 0-3"		-23.6			-23.7	
Ave. Reduction 3-6"		-21.9			-20.3	

Occupant Size

In general, both models predict an increase in injury severity measures with decreasing adult occupant size. While differences in absolute values of severity measures between the two models are evident, as has been discussed previously, this trend is consistent and clear in both model irrespective of padding condition. It should be noted that results indicate that smaller adult occupants do indeed benefit from the presence of padding and perhaps moreso than larger occupants. This point is emphasized in Figure 7-1 in which it can be seen that the reduction in AIS or CSI when introducing 3 inches of padding is larger for the smaller adult occupant. This trend is also evident in the CSI measure for the child. A clear reduction in AIS level also occurs in the child occupant but uncertainty in the modeling representation of the child lead to uncertainty in the absolute severity measures for this occupant.

Impact Severity

The velocity of the striking vehicle at impact is clearly a strong indicator of the severity of the collision. Figure 7-2 illustrates the strong relationship between severity and impact speed for an unpadded vehicle.

Typically, accident studies have not, for many reasons, been successful in reconstructing large numbers of accidents to the point of having impact conditions available for analysis. Rather, procedures have been developed to estimate the velocity change experienced by the involved vehicles during the collision based on a rather limited amount of information. Hence, velocity change has been used as a principal measure of accident severity.

In the side impact situation, severity of accident injury has also been shown to be a strong function of velocity change of the struck vehicle. However, because the struck side occupant comes in direct contact with an

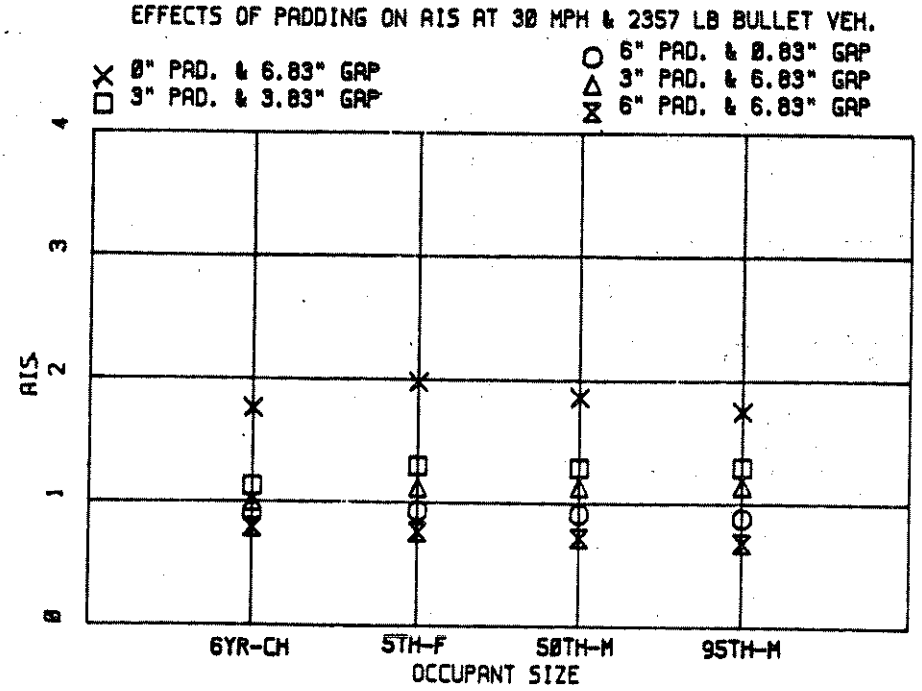

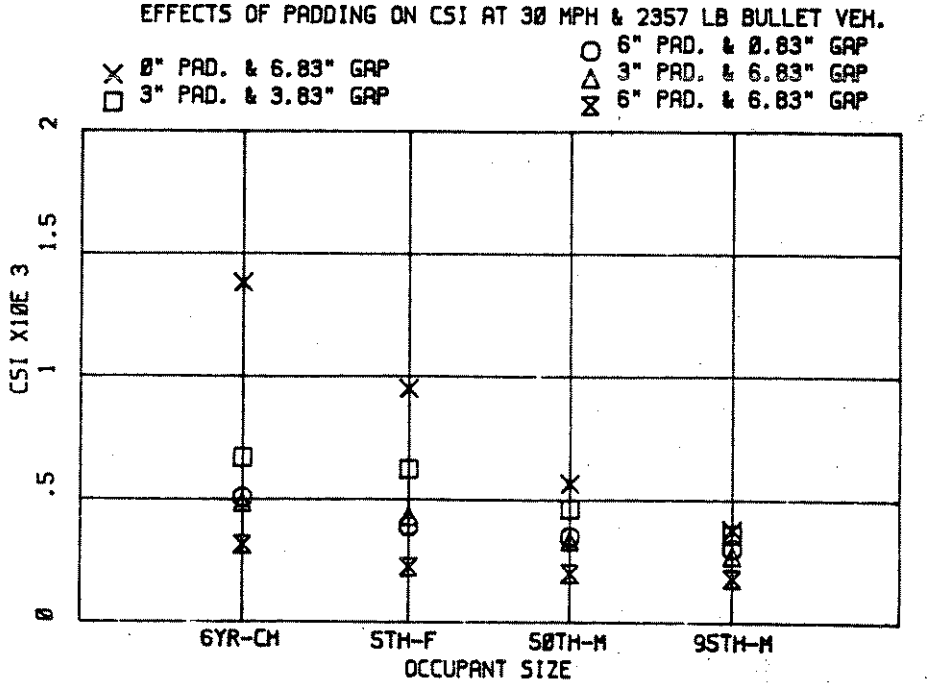

Figure 7-1 EFFECTS OF OCCUPANT SIZE ON INJURY MEASURES

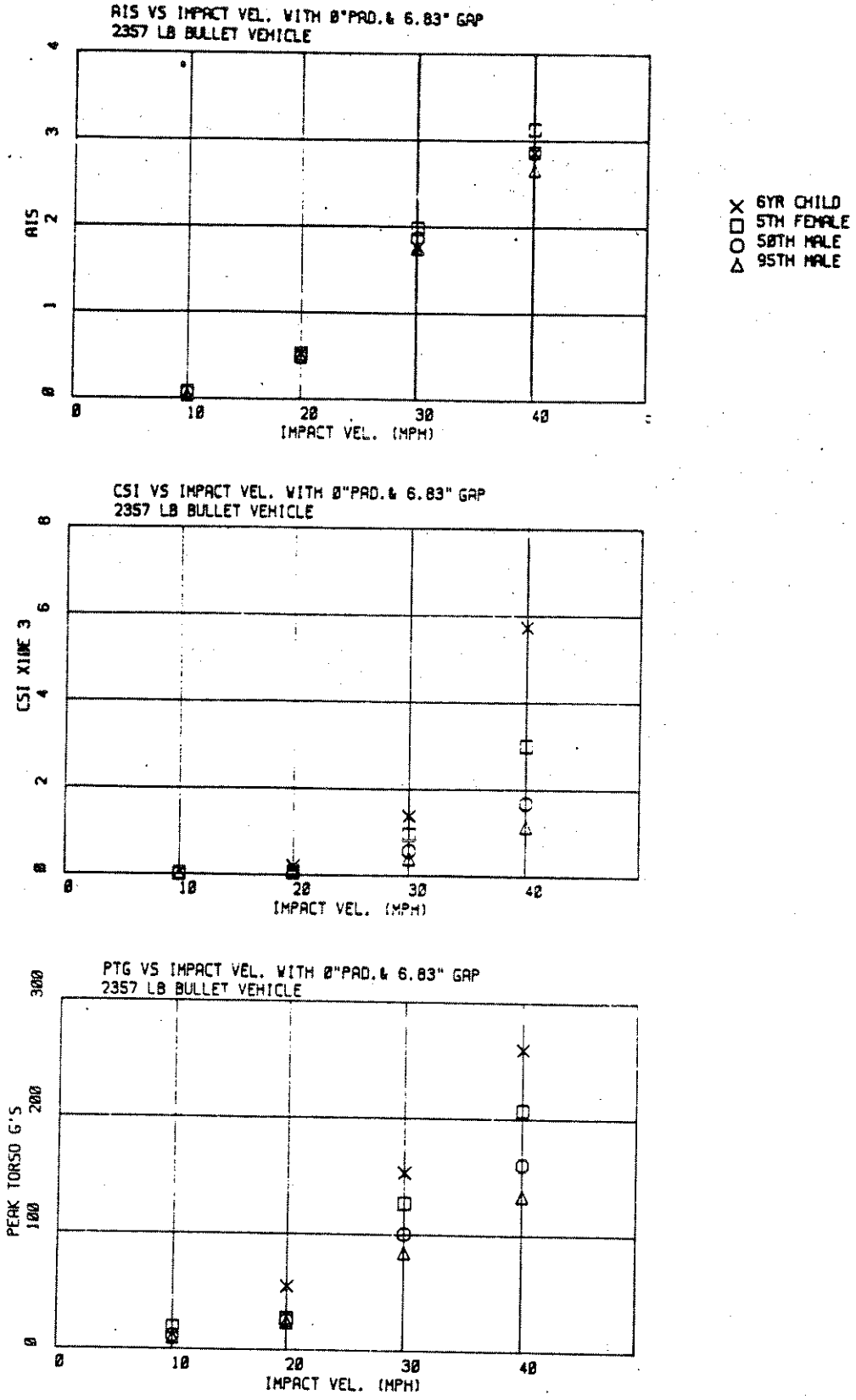

Figure 7-2 SIMULATED INJURY MEASURES FOR UNPADDED DOOR SURFACE

intruding door, the velocity of which is related to the velocity of the striking car, severity measures are also a function of striking vehicle speed.

Only a limited number of runs were made in the lumped mass parameter study to illustrate this effect as primary interest was on padding and occupant size. This does, however, appear to be an area that deserves additional attention in that there may be substantial implications on the interpretation of data contained in accident data bases.

Severity Measures

Although not a specific objective of this study, the substantial number of computer simulation runs made allowed looking at relationships between various severity measures over a rather broad range of impact conditions. Figure 7-3 presents plots of AIS versus CSI resulting from individual runs for both the lumped mass and CAL-3D models. Although data scatter is substantial in the lumped mass results, it is evident that the data tends to center about an AIS level of 2 at a CSI of 1000. This same trend is apparent in the CAL-3D results although fewer runs were made. Also note that in the lumped mass results, patterns in the data scatter are evident. That is, the stiffer door surfaces tend to be located at the top of the band while the more compliant surfaces (thicker padding) tend to be at the bottom of the band.

Figure 7-4 illustrates two additional cross plots of severity measures resulting from the lumped mass parameter study. As is seen, the scatter of peak torso acceleration versus CSI is quite narrow. Since CSI is equal to the integral of torso acceleration raised to the 2.5 power, it is reasonable to expect that the two measures are closely related. A cross plot of AIS versus peak torso acceleration exhibits substantially more scatter, however, a definite relationship exists.

The reader is referred to Section 2, page 4 for a concise summary of the conclusions and recommendations resulting from the study.

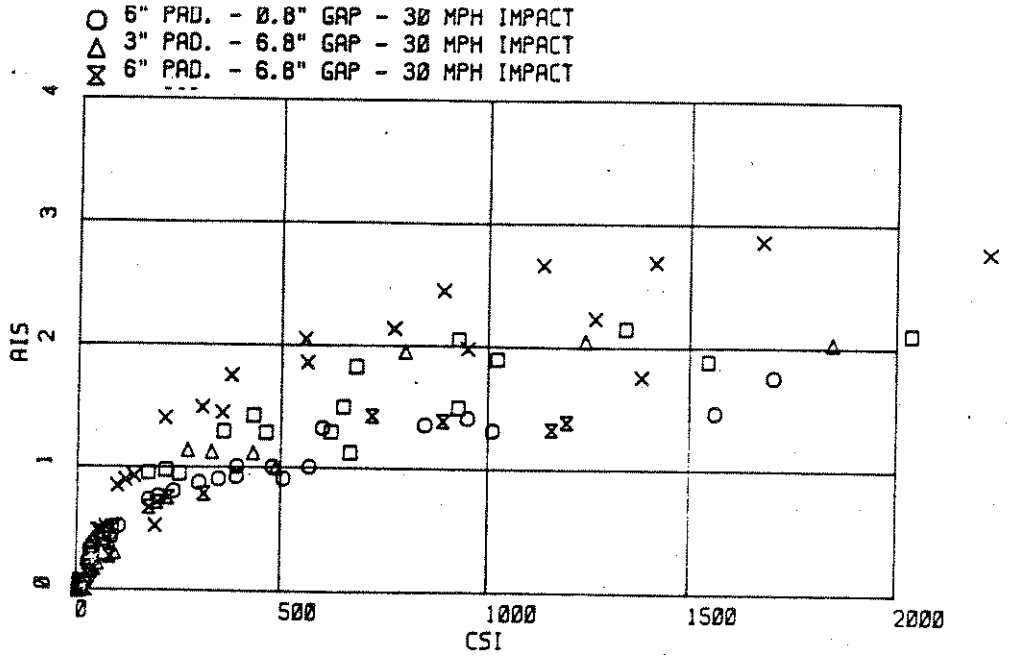

a) Lumped Mass Model Results

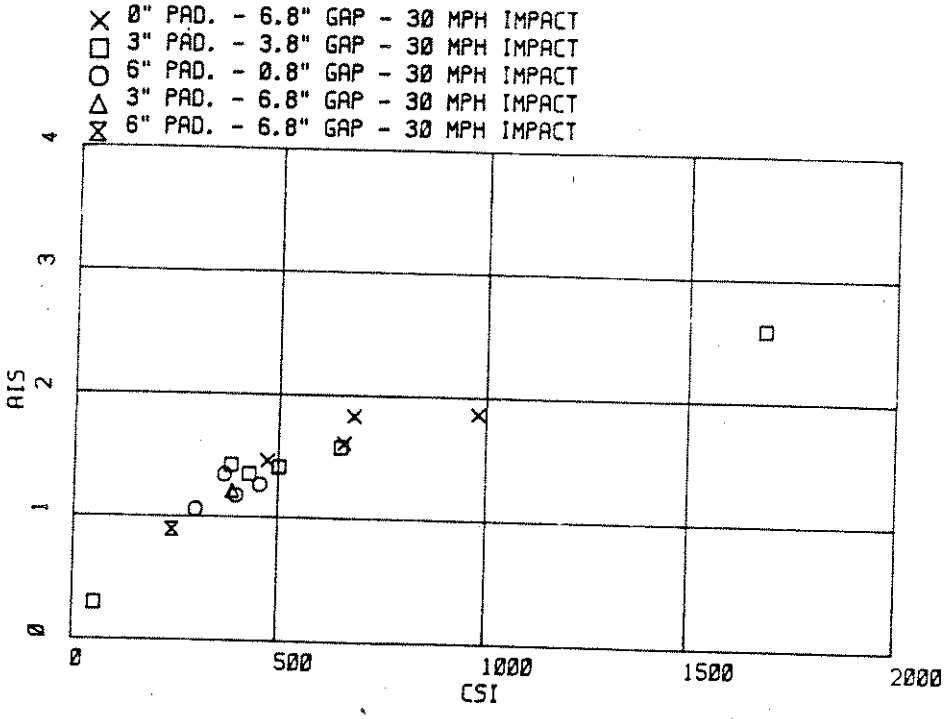

b) CAL-3D Model Results

Figure 7-3 RELATIONSHIP BETWEEN PREDICTED AIS AND CSI

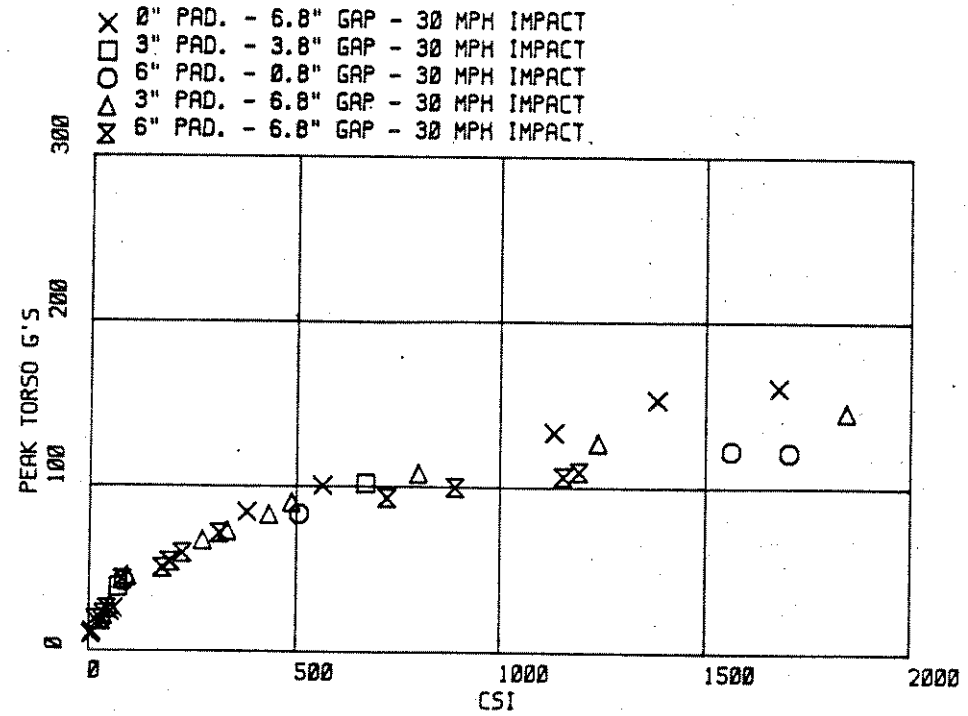

a) Relationship Between Peak Torso Acceleration and CSI

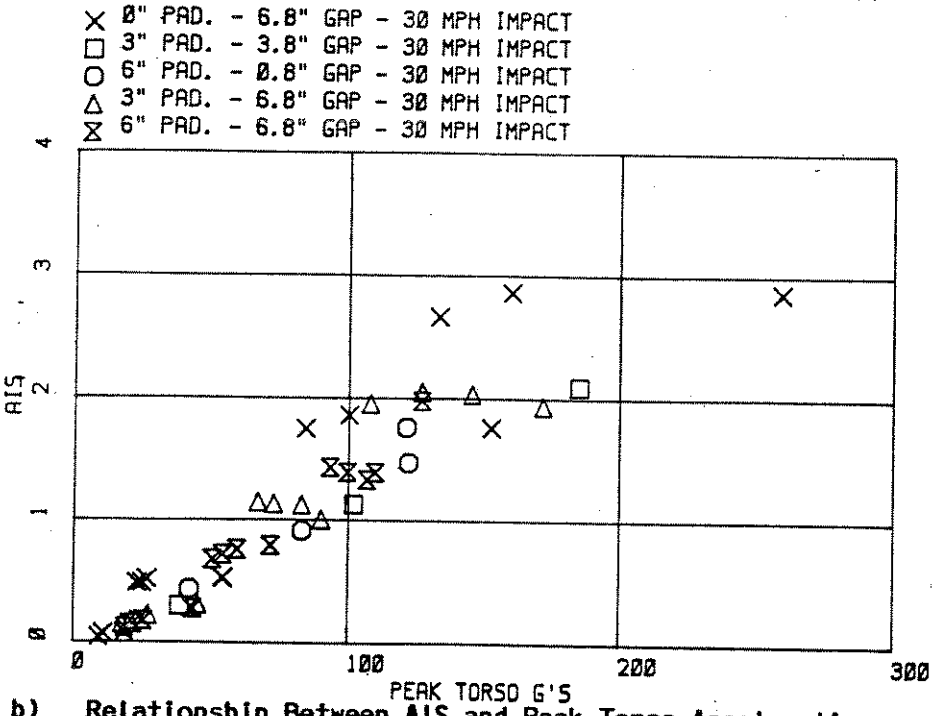

b) Relationship Between AIS and Peak Torso Acceleration

Figure 7-4 SEVERITY MEASURE CROSS PLOTS

8. REFERENCES

1. R. H. Eppinger and Han-Sun Chan, "Thoracic Injury Prediction via Digital Convolution Theory," SAE Paper No. 811010, Twenty-Fifth Stapp Car Crash Conference, Society of Automotive Engineers, Warrendale, PA.

2. M. Shaw, E. Knight, M. Rodack, A. Trudgen, and S. Davis, "Countermeasures for Side Impact, Final Report," Dynamic Science, Inc., DOT Report DOT-HS-806319 plus three appendix volumes: 806320, 806303 and 806304, August 1982.

3. M. W. Monk and L. K. Sullivan, "Side Impact Sled and Padding Development," Safety Research Laboratory, Report No. DOT-HS-805-889, February 1981.

4. M. T. McGrath and D. J. Segal, "CAL-3D User Convenience Package Version 2, Volume 1 - Users Manual," MGA Research Corporation, Contract No. DTNH22-82-A-37046, August 1983.

5. J. Wismans and J. Maltha, "Application of Three-Dimensional Mathematical Occupant Model for the Evaluation of Side Impacts," Proceedings of the 6th International IRCOBI Conference on the Biomechanics of Impacts, Salon de Provence, 1981.

6. J. Wismans and J. Wittebrood," Lateral Dummy Comparison: Theoretical Analysis," TNO Research Institute for Road Vehicles Report No. 700150015B, TNO-Complex, Zuidpolder, Schoemakerstaat 97, Postbus 237, Delft, Holland, August 1982.

APPENDIX A

LITERATURE REVIEW REPORT

COMPUTER MODELING OF SIDE IMPACT PENETRATION OF DUMMIES OF VARIOUS SIZES INTO PADDING - LITERATURE SURVEY

INTERIM TECHNICAL REPORT

BY

David J. Segal

September 1982

Contract No. DTNH22-82-C-07047

MGA Report No. G37-V-2

Prepared for:

U. S. Department of Transportation

NATIONAL HIGHWAY TRAFFIC SAFETY ADMINISTRATION

Washington, D. C. 20590

1. INTRODUCTION

The study of means for reducing injury severity in automobile side impacts has generally been restricted to consideration of fiftieth percentile male occupants. Substantial worldwide effort has been devoted to development of a side impact test device (anthropometric dummy) that allows interpretation of injury severity for this size occupant. Analytical procedures applied to the study of the side impact event have also concentrated on the same size occupant in paralleling and expanding experimental studies.

With combined experimental and analytical efforts, it is possible to optimize struck vehicle structural and interior door padding properties for a given (i.e. 50th percentile male) occupant at a given level of crash severity. However, the influence of such optimized vehicle properties on the injury potential of the remainder of the occupant population remains a question deserving of study. That is, does a side impact protective system optimized for a fiftieth percentile male occupant also provide optimum protective performance for the occupant population as a whole?

In an initial attempt to answer this question, the NHTSA contracted with MGA Research Corporation to study the effects of side impact padding on dummies of various sizes. The overall effort of this program was to develop and verify analytical models of different sized occupants in side impact situations and to estimate levels of protection provided for these occupants by various padding materials and surrounding structures at different crash exposures. Within the project, two different analytical models for side impact study are to be developed. The first is based on one-dimensional, lumped mass modeling procedures. The second will be a CAL-3D Crash Victim Simulation representation.

An initial task within the program involved a review of pertinent literature for the general purpose of assisting model development activities. This interim report covers the results of this literature review. In addition

to providing a general awareness of past and current side impact research activities, this review attempted to identify information applicable to the program within the four following categories:

- Modeling Approaches
- Model Development Test Data
- Modeling Parameters
- Model Verification Data

As a validated methodology for computer modeling of the side impact event has not been established to the same degree as for frontal collisions, the information obtained from this literature review is important in helping to define a fundamental basis for the thrust of this project; that is, development and use of side impact models. Thus, information in each of the above categories was reviewed with the intent of identifying data of value to the project, but also of identifying deficiencies that might affect the results.

A brief discussion of pertinent information uncovered within each of these categories is provided in the following section. One important remaining area that was not explicitly reviewed was that of side imapct injury criteria. The injury model to be used within the program was supplied by NHTSA. This is also described in the next section. A summary of important information sources then follows. Abstracts are then provided in chronological order, alphabetized by principle author within each year.

2. LITERATURE REVIEW SUMMARY

Four data bases were accessed in order to identify possible sources of information of value to the project. These were:

- Highway Safety Literature (HSL)
- Society of Automotive Engineers (SAE)
- National Technical Information Service (NTIS)
- Engineering Index (EI)

Keywords used in the automated searches of these data bases were lateral collision or impact and side collisions or impact. Abstracts containing these key words were printed and were reviewed for relevance to the project. Based on these abstracts, source documents were then reviewed to identify specific data or information that could be used. The following table summarizes the results of this review process for each data base.

Data Base	Number of Abstracts Reviews	Number of Relevant Sources
HSL	390	10
SAE	93	11
NTIS	98	3*
EI	103	none unique
other		7

It should be noted that while each of the above data bases contain a relatively large number of citations, a great deal of overlap existed, particularly in the HSL, SAE and EI files. Relevant sources in the "other"

*Does not include numerous test reports covering NHTSA sponsored side impact crash tests.

category included papers from the 8th ESV conference and reports supplied by the CTM which were not yet listed in any data base.

During review of source documents, efforts were made to categorize contents into one or more of the following categories:

- Modeling Approaches
- Model Development Test Data
- Modeling Parameters
- Model Verification

Since approaches toward modeling the side impact event, including modeling of occupant injury potential have not been developed to the same extent as has the frontal collision situation, a review of the various modeling efforts that have been reported was thought to be important in developing representations to be used in this study. The current study will use two different modeling procedures, namely, a simplified one-dimensional lumped mass representation and a CAL-3D CVS representation. Consequently, the review of previous side impact modeling effort was intended to identify basic representations which could be built upon to produce the modeling detail needed for reasonable injury prediction in this project.

Model development test data provides a basis for both selecting and confirming specific model representations. That is, elements of an overall model of the side impact event can be developed individually if suitable comparative test data are available to confirm submodel response predictions. In the current effort, emphasis has been placed on development of a rib and torso submodel so that accurate prediction of injury can be made. In order to successfully accomplish this submodel development, suitable test information must be available. Consequently, information sought for this category consisted of pendulum or sled test results for cadavers and side impact dummies in which both rib and spinal responses were available.

Information was also sought to aid in establishing model parameters. Requirements in this category include occupant data (mass elements, stiffness connectivity, etc.) and structural data for both striking and struck cars.

Finally, information was sought with which to verify the predictive capability of the complete developed models. Since the models developed will be used to study the total side impact event, verification of their predictive performance is necessary in that realm of operation. Both full scale crash tests and side impact sled simulations of lateral collisions were therefore reviewed in order to identify sources of test data with which model predictions could be compared.

A summary of important data sources for each of these categories follows later in this section. It should be noted that an important element of side impact modeling has not been rigorously addressed in this literature search. That is, an injury criteria or injury submodel.

The primary injury criteria to be used in the study will be used to predict torso injury level due to lateral loading. An excellent summary of injury criteria development has been developed by NHTSA personnel and provided to MGA Research for use on this project. A continuous injury criteria for side impact is suggested in the form:

$$AIS = .0768 \ \Delta V + .053 \ AGE - 1.89$$

where ΔV is the maximum velocity change of the struck rib versus the far side rib and AGE is the age (in years) of the occupant.

With this approach toward predicting injury level, the response of the far side rib is calculated by the digital convolution approach suggested by Eppinger (1981). Thus, only a representation of the struck side rib is needed for the injury submodel.

A summary discussion of information uncovered in each of the previously mentioned data categories follows.

Modeling Approaches

Various approaches to modeling side impact events have been tried, ranging from one-dimensional lumped mass models to complex three-dimensional models. Generally one-dimensional models have used very simple representations of the struck vehicle occupant--one or two masses representing the effective torso and pelvis masses. Structural representations generally contain a single mass for the striking vehicle, one for the struck vehicle door and one for the struck vehicle. This approach can provide an indirect indication of occupant injury potential through such measures as occupant velocity change and peak accelerations. Normally, this modeling approach has been used in conjunction with vehicle structure development or countermeasure development activities and thus little attention has been paid to detailed occupant response modeling.

More complex modeling approaches have also been applied to the side impact event. The MVMA two-dimensional occupant simulation has been used in a lateral mode but has neglected to consider intrusion of the inner door surface. Hoffman and Appel (1981) describe a model directed specifically toward side impact study. This model follows the traditional one-dimensional structure representation with a single striking vehicle mass, a struck vehicle door mass and the remainder of struck vehicle mass interconnected by structural force-deflection characteristics. The occupant is modeled as a pin jointed assembly of three masses representing the head, torso, and pelvis. Thus, the occupant is two-dimensional.

Padgaonkar and Prasad (1979) employed advanced features of the CAL-3D CVS to model the side impact phenomenon. They used four disjointed ellipsoidal segments to represent the struck vehicle, struck vehicle door,

striking vehicle and striking vehicle bumper. A three segment occupant was simulated in the struck vehicle. This effort thus allowed simulation of complete three-dimensional motion with a simplified occupant representation while at the same time allowed simulating the dynamic motion of the intruding door.

In 1980, Robbins, et al, reported on a generic vehicle representation for use with a modified version of the CAL-3D CVS inside impact studies. Results of a sample run using a fifteen segment occupant in a 90° impact are given. Intruding door motions were provided for through modifications to the CAL-3D which allow displacement time histories of vehicle contact panels to be input.

Very recently, Wismans and Wittebrood (1982) reported on a program involving simulation of four side impact dummies with the MADYMO computer simulation. Two-dimensional models of the ONSER, MIRA, APROD and DOT (SID) dummies were simulated. In addition, a three-dimensional representation of the DOT-SID was simulated. All models except that of the ONSER dummy included at least one rib element as distinct from the remainder of the torso mass. Supporting component test data are presented in an effort to quantify needed model parameters for the representations used.

Of particular interest is the fact that the authors felt that it was necessary to represent the SID thorax with, at a miniumum, both a struck side and far side rib in two-dimensions. A seven element, three-dimensional rib cage model was also attempted with good correlation with pendulum test results. This report provides an excellent source document for model development activities undertaken on the current project.

Model Development Test Data

Since the modeling approaches to be used in the study are semi-empirical in nature, test data are needed to develop and verify some model

parameters and responses. Two areas require information with which to develop and verify model representations. These are, the occupant representation and the struck vehicle structural representations.

The occupant model representation used must be consistent with the means used to evaluate injury potential. As noted elsewhere, this injury model is based on the maximum velocity change between the struck side and far side ribs. The implication of this means of predicting injury on model development activity is that the struck side rib must be modeled as a separate mass in order to obtain its dynamic response. The far side rib repsonse can then be predicted by the digital convolution procedure suggested by Eppinger (1981).

In order to confirm that the model representation used is acceptable in predicting rib response, impact test data must be available for comparisons. Available test data includes both pendulum and lateral sled impact data on cadavers and side impact dummies. With these data, model predictions of both rib response and torso response can be compared with test results to evaluate the suitability of model parameters.

Morgan, et al. (1981) provide an excellent summary of side impact cadaver test results. Data is presented as curves of the mean and $\pm$ one standard deviation accelerations of the impacted rib and the torso (at the T-12 location). Test data are summarized for 15 and 20 MPH sled tests with and without padding, and 14 and 20 fps pendulum tests. Corresponding results are available for the SID and APR side impact dummies. Individual test curves that make up the mean data are available elsewhere in the literature (e.g., Kallieris, 1981; Robbins, 1979; Eppinger, 1978) and/or the Biomechanics Data Base at NHTSA.

These test data will allow development of occupant model parameters and verification of model responses at a number of impact conditions.

Modeling Data

Data input to the models to be developed and used on the project fall into three general categories:

- Occupant data
- Structural data
- Padding data

A number of established occupant data sets are available for use with the CAL-3D CVS including 50th and 95th percentile male dummies and a six-year old child dummy representation. The GOOD program, recently made operational on the McAuto Timesharing System under Contract No. DTNH22-82-A-37046, Task Order 2, is also available for generating CAL-3D occupant data sets for any size adult occupant. Consequently, the basic occupant data for the CAL-3D model is readily available.

However, because it is necessary to model the struck side rib as an independent mass, it is necessary to define the interaction of the rib with the remainder of the system. Data on dynamic lateral force-deflection properties of cadaver chests is presented by Stalnaker, et al (1979). These data indicates a range of linear spring rates from about 135 lbs/in to 265 lbs/in for approximately the first 0.8 inches of deformation and were used to define a recommended corridor of side impact dummy characteristics. Tests on the APR dummy indicate that it falls within the recommended corridor. Comparative plots of the SID and APR dummy responses to pendulum and sled tests indicate that substantial differences in torso characteristics may be present. Hence, additional data on the SID dummy would be desirable.

Wismans (1982) provides some data which may be useful in defining the SID dummy. Static force-deflection properties of the external skin and padding and thorax stiffness relative to the spine are given. Results of dynamic tests on the SID thorax damper are also provided in terms of "average"

damping coefficients. In addition, dimensional and weight measurements are tabulated. This source appears to be the only available which provides such detailed data on the SID. Thus, it is expected to be of significant value to the study. It should, however, be pointed out that confirmation of some of this data is desirable. For example, the thorax damper characteristics, as measured by Wismans, were different from those reported by Melvin (1979). Furthermore, recent changes have been made to numerous components of the SID thorax by Calspan Corporation for the NHTSA. The effect of these changes on modeling parameters is not currently known. Thus, Wismans model data may not reflect the most recent SID design.

Information for quantifying the relationships between structural elements of both the striking and struck vehicles appears to be readily available. Shaw and Clark (1981) summarize the results of a project involving simulation of full scale lateral crash tests with a novel test device capable of accomplishing independent motion of a door panel and vehicle chassis. Comparative response plots indicate excellent agreement between the test device and crash tests. While the actual force-deflection characteristics acting between test device masses are not presented in this summary paper, they are presumably available in the project report. Alternately, they could be inferred from measured responses. Data from this project represents an excellent means of verifying occupant and padding model responses as structural properties are controlled and consistent. We, therefore, plan to use these results as a primary means of verifying modeling predictions.

Additional structural data are readily available in the literature for use in the modeling task. For example, Davis and Ragland (1981) summarize frontal force-deflection characteristics of a number of vehicles for both 0° and 30° impacts. Hollowell and Pavlick (1981) present side structural characteristics for modified and standard VW Rabbits. Seiffert (1979) also presents structural data for both the front and side of Rabbits. Rau (1972) provides data from a study of side stiffness in which static and dynamic characteristics are compared for both new and corroded vehicles.

Two principle sources of padding data are available. Monk, et al. (1980) report a comprehensive series of component test in which a body form consisting of an SID thorax was projected into various types of padding. Measurements of padding force-deflection characteristics are provided in both the summary paper and original source document.

The source document summarized by Shaw and Clark (1981) also contains results of padding tests in the form of stress-strain curves. This format can be very useful for extrapolating force-deflection properties to various sized dummies.

Model Verification Data

Data for verifying predictive capability of the models used in the project are available from a number of sources. Many crash tests have been conducted under NHTSA's efforts to upgrade FMVSS 214. Results for these crash tests are available both in the literature and on the NHTSA Crash Test Data base.

From the point of view of occupant model verification, it is desired to have carefully controlled and very repeatable test data. Thus, we feel that the extensive sled test program which was conducted in conjunction with the paper presented by Shaw and Clark (1981) provides an excellent data base with which to verify model predictions. These tests involved sled simulation of actual crash tests with controlled force-deflection characteristics acting between the bullet sled and target sled door and chassis. Furthermore, force-deflection data for various padding types is available and a variety of impact conditions and occupant initial spacings were simulated in the test program.

Data for verification of the model of the complete side impact event also appears to be available. Crash tests conducted in conjunction with the FMVSS 214 upgrade project (e.g., Hollowell and Pavlick, 1981) provide

extensive vehicle structural and occupant response measurements. Structural characteristics for the vehicles used in the testing are also available. Interior door and padding characteristics for the struck vehicle are available from Monk (1980). Consequently, one or more crash tests with a modified VW Rabbit side structure will provide a basis for verifying complete system response--both structural and occupant.

Summary

The results of the literature survey indicate that most of the information required to develop and verify the side impact model representations is readily available. One notable and important exception is information on the current SID thorax. Below, we summarize critical information needs and sources.

Model Development Data

• Cadaver pendulum and sled tests	Morgan, et al (1981) Kallieris, et al (1981)
• Dummy pendulum and sled tests	Morgan, et al (1981)

Model Approaches

• Single and multiple rib element models	Wismans (1982)

Modeling Data

• SID thorax properties	Wismans (1982), Melvin (1979)

- Additional data needed on current SID thorax properties

- Padding Data — Monk (1981); Shaw and Clark (1981)

- Structural properties — many available

Model Verification Data

- Side Impact Sled Simulation — Shaw & Clark (1981)

- Full Scale Crash Tests — Hollowell & Pavlick (1980)

Injury Criteria

- Supplied by NHTSA

Thus, the major problem uncovered in the literature review is that of modeling a separate rib element in the SID or occupant as is necessary to make use of the injury criteria. While this approach has been reported in the literature, the confidence with which reported data reflects the most recent SID thorax properties is low.

We have therefore recommended to the CTM that a SID be provided to MGA so that mass measurements can be made of the rib element and spinal structure and both static and dynamic force-deflection properties can be established for the device. Without such information, estimates of critical parameters will have to be made during model development and confidence in the results of the project will be severely compromised.

The following section provides detailed abstracts and other information on the data sources uncovered in this literature review.

3. REPORT SOURCES

The reports and papers reviewed in this literature survey and for which abstracts are given in Section 5, are generally available from a few sources as noted below:

The Stapp Conferences and other SAE reports may be obtained from the Society of Automotive Engineers, 400 Commonwealth Drive, Warrendale, Pennsylvania 15096.

TNO Reports may be obtained from the TNO Research Institute for Road Vehicles, TNO - Complex, Zuidpolder, Schoemakerstraat 97, Postbus 237, Delft, Holland.

The ESV Conference Reports and DOT Reports may be obtained from the National Technical Information Service, Springfield, Virginia 22161. The 8th International Technical Conference on Experimental Safety Vehicles ("ESV Conference") is DOT Report DOT HS 805 555, October, 1981. (The Conference was in Wolfsburg, Germany, in October, 1980). The 7th ESV Conference in Paris in June, 1979, is published as DOT Report DOT HS 805 199, December, 1979.

The HSRI Reports (the University of Michigan Highway Safety Research Institute) may be obtained from this institute, renamed in 1982 as the University of Michigan Transportation Research Institute (UMTRI), 2901 Baxter Road, Ann Arbor, Michigan 48109.

4. ALPHABETICAL AUTHOR INDEX

This section provides an index to all authors for those reports and papers abstracted in the subsequent section.

Clark, C.	See:	Shaw and Clark, 1981
Davis, S.	See:	Davis and Ragland, 1981 Beharrett, Johnson and Davis, 1980
Delmas, A.	See:	Terriere, Walfisch, Fayon, Rosey, Got, Patel and Delmas, 1979
Eppinger, R.	See:	Eppinger and Chan, 1981 Morgan, Marcus and Eppinger, 1981 Eppinger, Augustyn and Robbins, 1978 Kallieris, Mattern, Schmidt and Ep[pinger, 1981
Epron, L.	See:	Epron and Zaccariotto, 1981
Fayon, A.	See:	Fayon, Leung and Stalnaker, 1979 Stalnaker, Tarriere, Fayon, Walfisch, Buthazard, Masset, Got and Patel, 1979 Terriere, Walfisch, Fayon, Rosey, Got, Patel and Demas, 1979
Foust, D. R.	See:	Bowman, Schneider and Foust, 1975
Got, C.	See:	Stalnaker, Tarriere, Fayon, Wolfisch, Bathazard, Massett, Got and Patel, 1979 Tarriere, Wolfisch, Fayon, Rosey, Got, Patel and Delmas, 1979
Hackney, J. R.	See:	Burgett and Hackney, 1979
Herry-Martin, D.	See:	Cesari, Ramet, Herry-Martin, 1978

Ventre, D. See: Ventre, Provensal and Stcherbatcheff, 1979

Walfisch, G. See: Stainaker, Tarriere, Fayon, Walfische, Bathazard, Masset, Got and Patel, 1979
Tarriere, Walfische, Fayon, Rosey, Got Patel and Delmas, 1979

Wismans, J. S. See: Wismans and Witterbrood, 1982

Witterbrood, L. J. See: Wismans and Witterbrood, 1982

Zaccariotto, M. See: Epron and Zaccariotto, 1981

5. LITERATURE ABSTRACTS

Presented in this section are summaries of information sources that have been found to contain information relevant to the project. These summaries are in chronological order, alphabetized by principal author within each year. Contained on each summary are:

Year of publication
Title
Author
Affiliation
Publication source
Automated data base source
Abstract
Areas of relevance to project
Comments
Further Action Required

Year of Publication: 1982 Data Base: other
Title: "Predictions of Child Motion During Panic Braking and Impact"

Author(s): I. Kaleps and J. H. Marcus
Affiliation: AFAMRL, NHTSA
Publication: 1982 Stapp Conference (Draft)

ABSTRACT:

To study child motion during vehicle deceleration, 167 simulations were conducted using a large three-dimensional gross body motion model program in which seven initial body positions, 2.5-, 3- and 6-year-old body sizes, three levels of panic braking deceleration, cases of superimposed crash decelerations and several seat sliding friction coefficients were considered. Predicted head impact times and velocities of impact are given and three-dimensional motion graphics presented for a number of the simulations which illustrate body and vehicle interaction and gross three-dimensional body motion. Also included are comprehensive data sets for body dimensions, inertial properties and initial three-dimensional position descriptions.

Areas of Relevance to Project: Modeling Parameters

Comments: Contains CAL-3D data sets for 2.5, 3 and 6-year-old body sizes

Further Action Required: Contact author regarding joint torque properties

Year of Publication: 1982 Data Base: Other
Title: "Lateral Dummy Comparison: Theoretical Analysis"

Author(s): J. S. H. M. Wismans and L. J. J. Witterbrood
Affiliation: TNO
Publication: Report No. 700150015B

ABSTRACT:

The objective of this theoretical study was to contribute to the insight in the problem of mass distribution and rigidity, particularly concerning the chest and to contribute to the insight in the behaviour of the various side-impact dummies under several test conditions.

The mathematical analysis was conducted with the general purpose programme package MADYMO. A rough outline of the research programme is given below:

- literature review
- detailed analysis of the dummies and formulation of criteria for representation in a mathematical model
- if necessary, development of special subroutines for MADYMO to represent important construction details which cannot be simulated with the existing standard routines
- coordination with the dummy developing laboratories about aspects like general model setup and geometrical and material properties of the considered dummy
- analysis of geometrical and material properties provided by the developing laboratories and, if necessary, conducting additional measurements to achieve the relevant input characteristics
- preparation of model data sets
- selection of tests out of the experimental lateral dummy comparison programme which are suitable for validation of the developed models
- if necessary refinement and adjusting the models
- detailed evaluation of the effect of the four models on various padding and restraint types under different test conditions
- additional simulations to analyze problems which may rise during the experimental comparison programme

Areas of Relevance to Project: Modeling Approaches
Model Development Test Data
Modeling Parameters

Comments: Report on attempt to model four side impact dummies with MADYMO model. Contains measured dummy properties, dummy pendulum test responses and model comparisons.

Further Action Required: Contact author

Year of Publication: 1981 Data Base: Other
Title: "Development of a Deformable Side Impact Moving Barrier"

Author(s): Sol Davis, Carl Ragland
Affiliation: Dynamic Science, NHTSA
Publication: 8th ESV Conference Proceedings

ABSTRACT:

The National Highway Traffic Safety Administration and Dynamic Science, Inc. have developed a deformable moving barrier (Side Impactor) to evaluate passenger vehicle side structures in front-to-side collisions. Force-deflection properties for production vehicles at 0° and 30° frontal impacts were used to help establish the stiffness of the side impactor. Verification of side impactor stiffness was determined from load cell barrier testing and side impactor-to-car testing. Data from load cell barrier-to-car and car-to-car side impacts were used for comparative analysis. Repeatability tests will be conducted to determine the variability in performance parameters under "identical" test conditions.

Areas of Relevance to Project: Modeling Data

Comments: Summarizes project for development of deformable side impact barrier. Contains frontal stiffness data

Year of Publication: 1981 Data Base: SAE
Title: "Thoracic Injury Prediction via Digital Convolution Theory

Author(s): R. A. Eppinger, Han-Sun Chan
Affiliation: NHTSA
Publication: 25th Stapp Car Crash Conference, SAE No. 811010

ABSTRACT:

A dynamic characterization of the human thorax, in the form of a digital impulsive response signature, has been obtained which links the acceleration response of the struck side with the far side of the thorax under side impact conditions. This dynamic characterization was obtained by a unique combination of digital convolution theory, least squares approximation techniques, and a digital set of cadaver impact data. It has proven itself accurate in predicting the maximum relative acceleration, velocity and displacement between the left and the right lateral aspects of the thorax for a variety of impact conditions including lateral pendulum impacts, lateral rigid wall impacts at 15 and 20 MPH and lateral impacts into padded walls at 20 MPH.

Detailed discussions of the theory, the derivation of the various thoracic response signatures and their correspondence with actual data, the utilization of these response functions to predict injury, and the application of this technique to identify promising safety systems design strategies is presented.

Areas of Relevance to Project: Modeling Approaches

Comments: Describes procedure for relating far side rib response to struck side rib acceleration. Useful for prediction of injury based on maximum delta-V.

Year of Publication: 1981 Data Base: Other
Title: "Passenger Protection in a Lateral Collision--Non Destructive Mean Test Development for Lateral Collision Safety Device Study"

Author(s): Luc Epron and Moise Zaccariotto
Affiliation: Peugeot
Publication: 8th ESV Conference Proceedings

ABSTRACT:

In a collision in which one car is rammed from the side by another, the survival space is relatively limited, and it would seem that the only way to protect the occupant on the collision side, assuming the optimum realistically attainable rigidity of the passenger compartment, is by padding the inside surfaces of the sides of the vehicle (center pillars, door panels, rear side panels, and side boards) with materials having high energy-absorption properties (foams, combinations of sheet metal and foams, etc.).

To develop and optimize such materials, it is necessary to conduct a number of tests, with the possibility of varying the main parameters of the collision, in particular the velocity of the side of the vehicle.

To do this while holding down development costs, we have conceived an experimental setup that makes it possible to carry out dynamic tests without destroying the vehicle. This is the subject of our paper.

Areas of Relevance to Project: Modeling Approaches

Comments: Describes a one-dimensional model of perpendicular side impact: striking vehicle, struck vehicle, door and occupant masses.
Describes development of a side impact experimental sled device corresponding to mathematical model.
Door and struck vehicle connected by programmable force-deflection device.
Test results summarized in plots; however, stiffness data not given
Further Action Required: Contact authors

Year of Publication: 1981 Data Base: other
Title: "Mathematical Simulation of Side Impact--A Contribution to the Problem of Rigid/Deformable Barriers"
Author(s): J. Hofmann, H. Appel
Affiliation: NSU, Technical University of Berlin
Publication: 8th ESV Conference Proceedings

ABSTRACT:

The high proportion of side-on collisions and the very high injury risk in this type of accident led to the requirement for a dynamic test of the side structure by means of a barrier impact. It has still not been finally decided whether the cheaper rigid-type barrier or the more realistic deformable barrier will be specified in official test requirements. The following contribution employs a mathematical simulation model to investigate the basic differences between side impacts with a rigid barrier and a deformable barrier. The paper investigates whether it is possible to obtain a realistic simulation of a side impact by using a rigid moving barrier and reducing the collision speed.

Areas of Relevance to Project: Modeling Approaches

Comments: Describes two-dimensional perpendicular side impact model.
Striking vehicle: single mass
Struck vehicle: door mass and vehicle mass
Occupant: pelvis, torso, neck and head mass connected by pin joints
Representative force-deflection data given for front & side structures, combined door and pelvis, torso compliances
Data selected to match test results
Application of model: evaluation of deformable and rigid barriers

Further Action Required: Contact authors

Year of Publication: 1981 Data Base: other
Title: "Status of the Development of Improved Vehicle Side Structures for the Upgrade of FMVSS 214"
Author(s): W. T. Hollowell, M. Pavlick
Affiliation: NHTSA, The Budd Company
Publication: 8th ESV Conference Proceedings

ABSTRACT:

In its 1977 rulemaking plan, the National Highway Traffic Safety Administration established the upgrade of side impact protection as a top priority. This paper reports the progress to date on the developments to upgrade the design of vehicle side structures. Also presented is the philosophy used for these upgrades. Finally, the plan for integrating the upgraded vehicles into the other support areas for this rulemaking activity is discussed.

Areas of Relevance to Project: Modeling Parameters
Model Verification Data

Comments: Summarizes side structural development activities. Test reports available which document full scale crash test results. Side structure crush test data available.

Year of Publication: 1981 Data Base: SAE
Title: "Quantification of Side Impact Responses and Injuries"

Author(s): D. Kallieris, R. Mattern, G. Schmidt, R. H. Eppinger
Affiliation: U. of Heidelberg, NHTSA
Publication: 25th Stapp Car Crash Conference

ABSTRACT:

Side impacts have been shown to produce a large portion of both serious and fatal injuries within the total automotive crash problem. These injuries are produced as a result of the rapid changes in velocity an automobile occupant's body experiences during a crash. Any improvement to the side impact problem will be brought about by means which will ultimately modify the occupant's rapid body motions to such a degree that they will no longer produce injuries of serious consequence.

Accurate knowledge of both the body's motion and resulting injuries under a variety of impact conditions is needed to achieve this goal. Possession of this knowledge will then permit development of accurate anthropomorphic test devices and injury criteria which can be used to create effective injury countermeasures in vehicles.

Areas of Relevance to Project: Model Development Test Data

Comments: University of Heidlberg Cadaver Test Results. All sled tests:
H-80-011, H-80-014, H-80-017 - 15 MPH, rigid wall
H-80-024, H-81-002, H-81-004 - 20 MPH, rigid wall
H-80-018, H-80-020 - 20 MPH, APR pad
H-80-021, H-80-023 - 20 MPH, Fiberglas pad

Year of Publication: 1981 Data Base: NTIS
Title: "Side Impact Padding Integration Study"

Author(s): M. W. Monk, L. K. Sullivan
Affiliation: NHTSA
Publication: DOT-HS-805-957; SRL-27

ABSTRACT:

A study was conducted to design and fabricate producible padding materials suitable for side impact thoracic protection and for installation in a modified VW Rabbit. The fabricated materials were evaluated by three test procedures: component level testing at controlled temperatures, flammability testing and HYGE sled testing. The results of these tests are presented. Upon completion of testing, the padding materials were given an overall rating based on eight evaluation factors and the superior material was identified. The evaluation criteria are discussed and the results are presented.

Areas of Relevance to Project: Modeling Parameters

Comments: Contains padding force-deflection properties at different temperatures

Year of Publication: 1981 Data Base: SAE
Title: "Correlation of Side Impact Dummy/Cadaver Tests"

Author(s): R. M. Morgan, J. H. Marcus, R. H. Eppinger
Affiliation: NHTSA
Publication: 25th Stapp Car Crash Conference

ABSTRACT:

This paper is part of a four year study to systematically define side impact injury in terms of the kinetic response of a suitable anthropomorphic dummy. Last year a paper was presented at the Experimental Safety Vehicle Conference in Germany which analyzed side impact dummy response and injury prediction based on cadaver data generated by the Highway Safety Research Institute. These subjects were generally older than those discussed in the current paper. This paper includes data from a number of University of Heidelberg cadaver sled tests, including padding tests which we recently found to be (1) critical for a definitive analysis and (2) previously not available.

Two advanced dummies, whose design specifications are based upon biomechanical data, are currently being evaluated by the biomechanical community. The two dummies are (1) a Side Impact Dummy (SID) designed by the Highway Safety Research Institute (HSRI) and (2) the Association Peugeot-Renault (APR) dummy from France. The performance of these two candidate dummy designs is compared by a variety of techniques in seven identical tests using cadavers. These tests are chosen for use in evaluating biofidelity, repeatability, and dummy/padding interaction.

Among these techniques is a cumulative variance analysis--similar to a root-mean-square analysis--of the acceleration signal for the seven unique sled/pendulum tests where acceleration response data exists for APR dummy, SID, and cadavers. This cumulative variance approach allows an objective comparison of the response of each dummy design with respect to the cadaver data.

Areas of Relevance to Project: Model Development Test Data
Comments: Cadaver tests summarized by mean and ± 1 standard deviation curves corresponding dummy test results given

Speed	Type	Padding	Responses
20 MPH	Sled	APR	T12, LUR
20 MPH	Sled	SRL	T12, LUR
15 MPH	Sled	Rigid	T12, LUR
20 MPH	Sled	Rigid	T12, LUR
14 fps	Pendulum	Rigid	T12, LUR
20 fps	Pendulum	Rigid	T12, LUR
20 MPH	Sled	Minicars	T12, LUR

Year of Publication: 1981 Data Base: other
Title: "Side Impact Restraint Development and Evaluation Techniques"

Author(s): L. M. "Morrie" Shaw, Dr. Carl Clark
Affiliation: Dynamic Science, NHTSA
Publication: 8th ESV Conference

ABSTRACT:

The combination of vehicle and occupant kinematics in a side impact environment is a deceptively complex phenomenon involving the phasing of vehicle structural, restraint, and occupant dynamics and their interaction. Parameter sensitivity within this environment makes it difficult to economically develop and verify side impact countermeasures through full-scale crash testing. As a result, it was recognized that a more economical approach was needed to parametrically define a vehicle's lateral impact injury mechanisms.

This paper summarizes the results of a research program conducted by Dynamic Science, Inc. for the National Highway Traffic Safety Administration (NHTSA) of the U. S. Department of Transportation, to develop an economical sled test methodology for simulating the side impact environment. Sled test response characterization was defined from full-scale test data utilizing the Highway Safety Research Institute (HSRI) Side Impact Prototype Dummy (SID). The development of the methodology, vehicle side impact response characterization, sled methodology validation, and parametric results are presented and discussed.

The sled test methodology proved to be an accurate and low-cost test approach for characterization of a vehicle's side impact response for parametric analysis and countermeasure development.

Areas of Relevance to Project: Model Development Test Data
Modeling Parameters
Model Verification Data

Comments: Describes development of side impact sled test device. Comparisons between crash test and sled test door and vehicle responses are presented for validation purposes. Dummy accelerations and velocities are also compared. Contains summary results of experimental parameter study.

Year of Publication: 1980 Data Base: NTIS
Title: "Test Device and Test Procedure to Assess Side Structures - Phase I Final Report"
Author(s): J. Beharrell, N. Johnson, S. Davis
Affiliation: Dynamic Science, Inc.
Publication: Report No. DOT-HS-805-491

ABSTRACT:

The purpose of this report is to document the results of studies and tests performed under Phase I of the Side Structures Evaluation program. This contract involves the development of a test device which will simulate the effect of a bullet car in car-to-car side impacts. The test device described herein consists of a layered aluminum honeycomb energy-absorbing (E/A) face mounted on a wheeled bogey vehicle. The stiffness and geometry of the E/A face are based upon weighted averages of test data and frontal geometric characteristics of a representative selection of late-model cars.

Three series of crash tests were conducted, along with a series of static honeycomb component tests. The crash tests were conducted to provide frontal stiffness data, to measure the E/A face stiffness, and to compare the effect of the Side Impactor with that of a bullet car in car-to-car side impacts.

Areas of Relevance to Project: Modeling Parameters

Comments: Contains frontal force-deflection data on various automobiles developed from barrier impacts. Contains side structure force-deflection data for 1976 Plymouth Volare.

Year of Publication: 1980 Data Base: SAE
Title: "Evaluation of Pelvic Fracture Tolerance in Side Impact"

Author(s): D. Cesari, M. Ramet, P. Clair
Affiliation: ONSER
Publication: 24th Stapp Car Crash Conference

ABSTRACT:

Pelvic fracture is a typical lesion sustained by the occupant of a vehicle involved in a lateral impact collision who is seated on the impact side. If this fracture is generally not severe by itself, it is nevertheless often associated with severe abdominal lesions.

Study of injury mechanisms in lateral impact collisions shows that there are two ways of ensuring a better protection of the occupant in this type of accident: first by preventing intrusion so that the contact velocity "occupant/inner door" is decreased, secondly by absorbing the shock of the occupant against the inner door, especially at pelvis and thorax levels.

It is necessary to have a good knowledge of human tolerance to fracture of the considered body segment in order to determine the mechanical properties of the padding material.

The aim of this study is to determine the tolerance of the human pelvis. This study takes into account results of 36 impact tests against the pelvis of 10 cadavers and proposes injury criteria values to characterize the risk of pelvic fracture.

Areas of Relevance to Project: Model Development Test Data

Comments: Recommended Pelvic Injury Criteria as 5000 N or 100 N.S.

FurRelevance to Project: Model Development Test Data

Comments: Recommended Pelvic Injury Criteria as 5000 N or 100 N.S.

Further Action Required: Contact Authors

Year of Publication: 1980 Data Base: SAE
Title: "Side Impact Sled and Padding Development"

Author(s): M. W. Monk, R. M. Morgan, L. K. Sullivan
Affiliation: NHTSA
Publication: 24th Stapp Car Crash Conference

ABSTRACT:

In a one-year laboratory study, a side impact sled was designed, built, and validated. Using the sled and a newer generation of side impact dummy, a number of energy-absorbing materials were tested and superior materials identified.

Initially this study concentrated on the crash test data for a number of V.W. Rabbits crashed in a previously completed study. The crashed vehicles were obtained, and interior crush tests were performed with a specially designed body form. This was done to determine how the effective stiffness (as seen by the occupant of the struck vehicle) of the interior door increases as the bullet vehicle presses against the interior door trim from the opposite side.

An acceleration-type sled buck was then designed and built with an "interior door" mounted to mimic the interior stiffness determined from the crush tests. The sled was dynamically tested with a Haversine sled pulse similar to the door crash pulse. The sled was validated by reproducing the crash environment of a car-to-car collision. The criteria considered for matching the two were: (1) acceleration-time curve of the interior door, (2) the velocity-time curve of the interior door, (3) kinematics of the Part 572 surrogate, and (4) accelerations on the surrogate.

Areas of Relevance to Project: Modeling Parameters

Comments: Contains results of side impact padding tests. Padding force-deflection curves given

Year of Publication: 1980 Data Base: NTIS
Title: "Accident Data Simulation Pedestrian and Side Impact - 3D"

Author(s): D. H. Robbins, J. M. Becker, R. O. Bennett, B. M. Bowman
Affiliation: HSRI
Publication: Report No. UM-HSRI-80-75

ABSTRACT:

The objective of this study has been to provide practical baseline data sets to describe a vehicle occupant in side impacts and to describe a pedestrian in frontal impacts. This report describes the baseline vehicle geometry in Part 2. The occupant and pedestrian, along with their contact interactions with the vehicle, are described in Parts 3 and 4. The baseline data sets and a sampling of the resulting computer program output are given in Part 5. A summary of information about the HSRI version of the Calspan occupant dynamics program is given in Part 6.

Areas of Relevance to Project: Modeling Parameters

Comments: Describes nominal vehicle geometry for side impact studies. Data developed for HSRI version of CAL-3D CVS. Sample run presented.

Year of Publication: 1979 Data Base: HSL
Title: "Status of the National Highway Traffic Safety Administration's Research and Rulemaking Activities for Upgrading Side Impact Protection"
Author(s): A. Burgett, J. R. Hackney
Affiliation: NHTSA
Publication: 7th ESV Conference Proceedings

ABSTRACT:

In the National Highway Traffic Safety Administration's 1977 Rulemaking Plan, improvement in Side Impact Protection was formally established as a top priority. This plan calls for a notice of proposed rulemaking (NPRM) on an upgrade of Federal Motor Vehicle Safety Standard 214 in 1980. Research projects are underway to generate data on how occupant compartment integrity can be improved and how occupant injuries can be reduced by changes to the side structure and by modification of the interior of the vehicle. The upgrade program contains four major areas of activity: development of a moving barrier impactor; development of a dummy and associated performance criteria; development of vehicles that can be used to demonstrate performance; and analysis of accident data to support the other three activities. Progress to date in these areas is reported; and cost, weight, and leadtime studies are briefly discussed. A schedule of the total program is provided, with anticipated dates for dummy, barrier impactor, and rule NPRM's.

Areas of Relevance to Project: general review
Comments: Paper presents a general review of the NHTSA activities to upgrade FMVSS 214. Much of this activity has been changed as a result of the new administration. More data should be obtained on the following NHTSA contracts:

Contract No.	Title	Organization
DOT-HS-8-01933	Test Device and Test Procedures to Assess Side Structures	Dynamic Science
DOT-HS-7-01758	Development of a Test Methodology for Evaluating Crash Compatibility and Aggressiveness	Dynamic Science
DOT-HS-6-01296	Calibration Procedures of Test Dummies for Side Impact Testing	HSRI
DOT-HS-4-00921	Quantification of Thoracic Response and Injury	HSRI
DOT-HS-7-01588	Lightweight Subcompact Side Structure Program	The Budd Co.
DOT-HS-7-01664	Identification of Superior Energy Absorbing Materials for School Bus Interiors	

Paper also indicates that a padding study similar to the school bus (above) is underway.

Year of Publication: 1979 Data Base: HSL
Title: "Presentation of a Frontal Impact and Side Impact Dummy, Defined from Human Data and Realized from a "Part 572" Basis
Author(s): A. Fayon, Y. C. Leung, R. L. Stalnaker
Affiliation: Renault
Publication: 7th ESV Conference Proceedings

ABSTRACT:

Research is described for improving the human response characteristics of the part 572 dummy in side and frontal impacts. Biomechanical data were obtained in free-fall, side impact experiments using human cadavers in order to determine the force/deflection characteristics of the human chest. Using the experimental data, the Part 572 dummy's thorax was redesigned for improved response during side impact conditions. Modifications were made to the Part 572's shoulder assembly to give it the range of motions observed for cadavers in vehicle crashes. Modifications were also made to the part 572 arm, in order to improve its deformation characteristics. Results of dynamic testing of the redesigned dummy are described: frontal impact tests were comapred with those of the Part 572 dummy, and side impact tests with those of the human cadavers. Frontal impact tests using Part 572 dummies and cadavers, both restrained by three-point belts, indicated dissimilarities in their submarining behavior. Differences between the Part 572 and human being pelvic areas, and some modifications to the dummy pelvis to align its submarining behavior to human response are described.

Areas of Relevance to Project: Model Development Test Data
Modeling Parameters

Comments: Developed modifications to Part 572 dummy force-deflection corridor for laterally loaded chest presented based on cadaver test results. Dynamic force-deflection curves for APR side impact dummy.

Further Action Required: Contact authors

Year of Publication: 1979 Data Base: HSL
Title: "Response of Belt Restrained Subjects in Simulated Lateral Impact"

Author(s): J. D. Horsch, D. C. Schneider, C. K. Kroell, F. D. Raasch
Affiliation: Univ. of Calif.
Publication: 23rd Stapp Car Crash Conference Proceedings

ABSTRACT:

Far-side lateral impacts were simulated using a Part 572 dummy and human cadavers (embalmed and unembalmed) to compare responses for several belt restraint configurations. Sled tests were conducted with a velocity change of 35 KPH at a 10 g deceleration level. From field data, it was estimated that this velocity change of the laterally struck vehicle represents about an 80th percentile level for injury-producing lateral collisions. Subjects restrained by a three-point belt system with an outboard-anchored, diagonal shoulder belt (i.e., positioned over the shoulder opposite the side of impact) rotated out of the shoulder belt and onto the seat. The subject received some lateral restraint due to interaction with the shoulder belt and seatback. The subjects restrained by a three-point belt system with an inboard-anchored, diagonal shoulder belt (i.e., positioned over the shoulder on the side of impact) remained essentially upright due to shoulder belt interaction with the neck and/or head. Kinematic responses of the Part 572 dummy were generally similar to those of the cadaver subjects. Injuries were found in cadavers restrained by both shoulder belt configurations, but were more extensive to the cervical region for those subjects receiving direct neck and/or head loading from the belt. Limitations in the cadaver model and test environment, as well as the preliminary nature of the experiments, do not permit definitive conclusions on the significance or applicability of the injury data obtained to real accident situations. Appended is a discussion of the effect of age on intervertebral disc structure.

Areas of Relevance to Project: Model Verification Data

Comments: Far side lateral impacts at 35 km/hr. Sled testing with both dummies and cadavers to compare responses. Limited test data are available for the following tests - Dummy 1152, 1151, & 1150. Cadaver 057, 047, 051, 052, 046, 053 & 049. Acceleration responses and photos provided in text.

Year of Publication: 1979 Data Base: HSL
Title: "Experimental Application of Advanced Thoracic Instrumentation Techniques to Anthropomorphic Test Devices"

Author(s): J. W. Melvin, D. H. Robbins, J. B. Benson
Affiliation: Univ. of Michigan, HSRI
Publication: 7th International Tech. Conf. on Experimental Safety Vehicles

ABSTRACT:
A 12 accelerometer instrumentation array developed for use in cadaver experiments on thoracic injury has been adapted for ATD (Anthropmorphic Test Device) installation. Accelerometers around the periphery of the Part 572 chest register different acceleration signatures for different directions, levels, and time durations of impact. A series of modifications has been made to the ATD to improve the side impact response of the thoracic regions. These modifications ranged from slight changes in structure to radical altering of the thoracic lateral dynamic stiffness, mass distribution, and rib linkages. When a series of side impact tests was conducted using the modified ATD's, their response was similar to the mean cadaver-based response. The modified thoracic structures are prototype designs which are intended for lateral impact use only. The use of injury-predictive models to predict thoracic injury levels using kinematic data from the modified ATD test indicates that this is a promising approach to injury assessment.

Areas of Relevance to Project: Model Development Test Data
Modeling Parameters

Comments: Provides general description of SID. Limited data on torso weight and damper properties given. Comparison of responses with cadaver test results given in terms of acceleration plots.

Year of Publication: 1979 Data Base: HSL
Title: "Simulation of Side Impact Using the CAL-3D Occupant Simulation Model"

Author(s): A. J. Padgaonkar, P. Prasad
Affiliation: Ford Motor Co.
Publication: 23rd Stapp Car Crash Conference Proceedings

ABSTRACT:

By applying some advanced features of the CAL-3D occupant simulation model, a single model incorporating the vehicle structure and a simplified occupant were developed for studying the sensitivity of occupant response to parameter changes in perpendicular, vehicle-to-vehicle side impacts, not involving vehicle rotation. Results of the model show qualitative agreement with published experimental results. Occupant responses are sensitive to the initial clearance between the occupant and the door inner surface, the stiffnesses of the front structure of the impacting vehicle, and the side structure of the impacted vehicle. Although door intrusion is an important factor affecting occupant response, it is hypothesized that the occupant response is more sensitive to the kinematics of the door than to peak intrusion. Door intrusion seems to affect the efficiency of the padding between door and occupant, i.e., thicker padding will be required to limit peak occupant responses to preselected levels for vehicles with lower side structure stiffness.

Areas of Relevance to Project: Modeling Approaches

Comments: Use of CAL-3D CVS for side impact simulation
- 3 segment occupant
- 4 disjointed ellipsoid segments representing struck vehicle, door striding vehicle, bumper
- capable of simulating door intrusion

Further Action Required: Contact authors

Year of Publication: 1979 Data Base: HSL
Title: "Prediction of Thoracic Injuries as a Function of Occupant Kinematics"
Author(s): D. H. Robbins, R. J. Lehman, K. Augustyn
Affiliation: Univ. of Mich., HSRI
Publication: 7th Interational Tech. Conf. on Experimental Safety Vehicles

ABSTRACT:

Injury-predictive models of the severity of blunt thoracic trauma have been developed using the data gathered in a series of impact tests utilizing 18 cadaver subjects. Two classes of tests were conducted to generate various levels of injury: tests on an impact sled where the subjects interacted with padded or rigid side door structures in side impact; and controlled energy impacts delivered to the side of the thorax using a flat-faced pendulum impactor. The instrumentation which was designed to monitor kinematics consisted of a matrix of accelerometers surgically placed on the bony exterior structure of the thorax. The active axes of the accelerometers were chosen to represent the three orthogonal axes, and hence, to provide information on direction of impact. After the tests, autopsies were performed to obtain a level of injury reported as an abbreviated injury scale (AIS) number. The injury-predictive models have the AIS number, the number of rib fractures, or derivatives thereof, as the dependent variable and various features of the time-dependent acceleration traces as the independent variables. The features which show the greatest correlation with the level of injury, and hence, which hold the greatest potential for building injury-predictive models have been found to be quantities related to velocities or integrals of acceleration pulses. After quantities such as these were derived from the accelerometer traces, those with the highest correlation to injury measures were selected as candidate independent variables. The predictive models, were then generated using regression software.

Areas of Relevance to Project: Model Development Test Data

Comments: Cadaver test results summarized mean and $\pm$ one standard deviation curves presented for four pendulum tests

Year of Publication: 1979 Data Base: SAE
Title: "Lateral Impact-Considerations for Vehicle Development"

Author(s): U. W. Seiffert
Affiliation: Volkswagen
Publication: SAE Paper 790709

ABSTRACT:

A number of accident analyses involving lateral (side-on) impacts is steadily increasing. An accident simulation test procedure that is applicable worldwide must first be established in order to significantly improve the safety features of vehicles.

Factors to be considered in studying lateral impacts are: the mass, structural design, and rigidity of the vehicles involved in the collision; the point and angle of impact; impact speeds; vehicle interior and design; and the use of restraints.

Areas of Relevance to Project: Modeling Data

Comments: Contains front and side overall force-deflection curves for VW Rabbit

Further Action Required: Contact author

Year of Publication: 1979 Data Base: HSL
Title: "Modification of Part 572 Dummy for Lateral Impact According to Biomechanical Data"
Author(s): R. L. Stalnaker, C. Tarriere, A. Fayon, G. Walfisch, M. Balthazard, J. Masset, C. Got, A. Patel
Affiliation: APR
Publication: 23rd Stapp Car Crash Conference Proceedings

ABSTRACT:

The Part 572 dummy was modified in order to improve its performance in lateral impact studies. The rib cage, arms, and shoulders of the dummy were modified so its impact performance more closely simulates that of a human. Based on biomechanical data obtained on cadavers during lateral collision tests, the Part 572 arm was modified by reducing the size of the structural members and increasing the padding, and the mobility of the shoulder was increased in both forward and upward directions. The shoulder was modified to become transversely collapsible to a certain degree. The rib cage was redesigned to give a more realistic deformation. The measurement of lateral chest deflection was also incroporated into the rib cage design, while frontal impact characteristics were left unchanged. Results of freefall and full-scale crash tests, both frontal and lateral impacts, are compared for the modified dummy and cadavers. Preliminary results are encouraging; further developments are expected.

Areas of Relevance to Project: Modeling Parameters
Model Development Test Data

Comments: Reports on program to (1) determine force deflection characteristics of human body (cadaver) and modify Part 572 dummies to provide thorax of similar regularity. Provides force-deflection characteristics for rigid impact and padded impacts. A force-deflection corridor is also provided. Information may be helpful in defining force-deflection properties for thorax components in model.

Year of Publication: 1979 Data Base: HSL

Title: "Synthesis of Human Tolerances Obtained from Lateral Impact Simulations"

Author(s): C. Tarriere, G. Walfisch, A. Fayon, J. P. Rosey, C. Got, A. Patel, A. Delmas

Affiliation: APR

Publication: 7th International Technical Conference on Experimental Safety Vehicles

ABSTRACT:

Results are summarized from biomechanical experiments using fresh, unembalmed cadavers to study human tolerances to side impacts. The findings are the most recent from free-fall tests performed over the past few years. In studies of head impact, no relationship was found between head injury criterion (HIC) and abbreviated injury scale values. For these lateral skull impacts, only a slight likelihood of serious injury was found. No constant relationship was found between the accelerations measured on a dummy and those on a cadaver in these head impacts. No positive conclusions can be drawn concerning the protection provided in car-to-car side collisions unless the dummy's behavior yields a head impact velocity close to that of the human head, which does not occur when the shoulder acts as a brace and when the chest deflects insufficiently. HIC 1500 can be determined in impacts using a separate head rather than the complete dummy. For chest side impact experiments, the injuries found were essentially rib fractures. The number of fractures can be an injury level indicator. Correlations were made between the number of fractures and the force applied to the chest, and also the relative deflection of the chest and the thoracic acceleration. Chest protection criteria can be established when an appropriate anthropo-dynamic dummy has been developed and tested. On the basis of pelvis impact experiments and other studies, 80 to 90 G/3msec to the pelvis seem to be a conservative level of human tolerance. For a Part 572 dummy protection criterion, a level of 90-100 G/3msec could be considered. For the experimental condition of the side wall stopping the thorax without head impact, it is concluded that there is no need for a neck protection criterion.

Areas of Relevance to Project: Model Development Data

Comments: Description of cadaver test results. Provides summary of subjects. Proposes lateral thorax injury criteria based on percent relative deflection. Also recommends a pelvic tolerance level. No detailed test data.

Year of Publication: 1979
Data Base: SAE
Title: "Development of Protection Systems for Lateral Impacts"

Author(s): P. Ventre, J. Provensal, G. Stcherbatcheff
Affiliation: Renault
Publication: SAE Paper 790710

ABSTRACT:

A series of 21 experimental car-to-car collisions were produced. The accelerations on the thorax and the pelvis of the dummy exposed to the impact were analyzed and related to the parameters linked to the vehicles. Two lateral collisions of a rigid, mobile barrier with a car were produced and compared to the car-to-car collisions. The parameters of the relative stiffness and of the mass of impacting vehicles and impacted vehicles were examined. The protective measures were developed for the impacted vehicle and tested in different configurations.

Areas of Relevance to Project: Model Verification Data

Comments: Reports on 21 experimental side impact crashes. Test summary results provided as response measures versus impact velocity, intrusion, door panel speed, mass ratio. May be useful for evaluating model trends. A first phase model developed.

Year of Publication: 1978 Data Base: SAE
Title: "Injury Mechanisms in Side Impact"

Author(s): D. Cesari, M. Ramet, D. Herry-Martin
Affiliation: ONSER
Publication: 22nd Stapp Car Crash Conference

ABSTRACT:

Side impact accidents are the most severe and second frequent traffic accident configuration. By a comparison of results of tests with and without intrusion, this paper shows that the severity of side impact for the occupant seated near the impacted side is mainly due to intrusion of the side wll inside the car compartment of the struck car. Without intrusion, injury criteria recorded on a dummy are much lower than when there is intrusion.

The influence of intrusion can be explainted by the deformation speed of the side wall of the struck car. The velocity change of different parts of cars and of dummy have been determined in two tests conducted at 40 and 50 KPH. The diagrams of these velocity changes indicate that the door and the frame seat of the struck car sustain a velocity change higher than the car floor. The pelvis of the dummy seated near the impacted side sustains a velocity change in the same order of magnitude as the door, whereas its chest has a lower velocity change.

This paper concludes that preventing from intrusion will decrease the severity of side impact and the seat can be used to participate in this stiffening. A padding should also be necessary but the determination of its characteristics needs a better knowledge of human tolerance to side impact.

Areas of Relevance to Project: Model Verification Data

Comments: Summarizes results from two side impact crash tests at 40 KPH and 50 KPH. Contains vehicle and dummy velocity and displacement time history curves.

Year of Publication: 1978 Data Base: SAE
Title: "Development of a Promising Universal Thoracic Trauma Prediction Methodology"

Author(s): R. H. Eppinger, K. Augustyn, D. Robbins
Affiliation: NHTSA, Adaptronics, Inc., HSRI
Publication: 22nd Stapp Car Crash Conference

ABSTRACT:

Analysis of experimental acceleration time history data obtained from a thoracic instrumentation array has been performed. The data were generated under test conditions which include realistic frontal impacts in belt, air bag, and steering column systems and side impacts with rigid and padded door structures. Data from frontal and lateral pendulum impacts were also included.

The results demonstrate that the instrumentation array captures sufficient information from the impact event to allow prediction of resulting thoracic trauma, defined either as thoracic AIS or total number of thoracic fractures, using a single function for each injury measure.

Each function is universal in the sense that it is valid for all test modes and directions of impact.

A strategy for developing a surrogate thorax to implement this injury predictive methodology is discussed and preliminary specifications are presented.

Areas of Relevance to Project: Model Development Test Data

Comments: Contains side impact cadaver test data. Rigid side and pendulum tests conducted at HSRI. Much of this data is available and summarized in other sources. However, this paper contains additional response curves (sternal, T1, upper and lower ribs).

Year of Publication: 1978 Data Base: SAE
Title: "Mathematical Modeling of Occupant Biomechanical Stress Occurring During a Side Impact"

Author(s): W. Schmid
Affiliation: Daimler-Benz AG
Publication: SAE Paper 780670

ABSTRACT:

After the frontal impact, the side impact is the next most dangerous frequently occurring accident mode, accounting for approximately 25% of all injuries and fatalities. Safety Research, therefore, endeavors to determine those parameters of the side impact event, which have a decisive influence on the risk of injury to the occupants. Two parameters are the structural rigidity of the impacting vehicle and of the impacted vehicle. Using a very simple mathematical model, the possibilities of vehicle compatibility in side impacts are being investigated in order to reduce the likelihood of injury to the lowest possible level.

Areas of Relevance to Project: Modeling Approaches
Modeling Data

Comments: Reports on side impact model and parameter study. Used one-dimensional four mass model. Single mass for occupant. Force-deflection curves for side structure, front structure and occupant/padding given.

Further Action Required: Contact author

Year of Publication: 1975 Data Base: HSL
Title: "Simulated Occupant Response to Side-Impact Collisions"

Author(s): B. M. Bowman, L. W. Schneider, D. R. Foust
Affiliation: Univ. of Michigan, HSRI
Publication: 19th Stapp Car Crash Conference Proceedings

ABSTRACT:

Occupant response to side-impact collisions is studied with a mathematical vehicle/occupant model to investigate head-torso relative motion and neck forces and moments. Computer simulations were performed in conjunction with a study on properties of the neck in lateral motion involving 96 subjects divided into groups by age and sex (18-24 years, 35-44 years, and 62-74 years old, male and female). Subject data were collected on head-neck lateral bend range of motion, sternomastoid muscle group strength, reflect time, and anthropometry. For the various subject groups, the series of computer simulations investigated 10 and 30 MPH car-to-car impacts, the effect of muscle reflex with muscle tension buildup, and the effect of varying degrees of pre-impact constant tension. It is determined that neck muscle contraction may significantly lessen the likelihood of hard tissue injury resulting from excessive lateral flexion. The lesser muscular strength of female and elderly crash victims indicates greater susceptibility of neck injury for these groups.

Areas of Relevance to Project: Modeling Approaches

Comments: Describes use of MVMA 2-D CVS in modeling side impacts. Emphasis on neck/head motion and muscular contraction low speed (DV = 10 MPH) simulations. No interior door panel motion simulated.

Year of Publication: 1972 Data Base: SAE
Title: "Investigation of Vehicle Side Impact Stiffness-Comparison of Static and Dynamic Tests"

Author(s): Hartmut Rau
Affiliation: Institute for Automobile Engineering Technical Uni
Publication: SAE Paper 720224

ABSTRACT:

The purpose of this investigation on vehicle side-impact stiffness and the comparison of the static and dynamic tests was to contribute guidelines for a final test procedure with two advantages: to be, on the one hand, simply practicable and reproducible and, on the other hand, to provide results corresonding as close as possible to real accidents. Additionally, the investigation emphasized testing of side parts significant to the objectives of the test: door only, door and sill, or door, sill and roof. New cars as well as heavily rusted vehicles were used for the test. Therefore, this paper also treats the question of what degree a test of only new cars will be useful, without considering the state of corrosion of older vehicles.

Areas of Relevance to Project: Modeling Data

Comments: Contains data on static and dynamic force-deflection of vehicle side structures. Thirty-six tests of model years 1960 through 1970 vehicles test curves given.

Further Action Required: Contact author

Year of Publication: 1972 Data Base: HSL
Title: "Door Crashworthiness Criteria"

Author(s): J. H. McElhaney, R. L. Stalnaker, V. L. Roberts, R. G. Snyder
Affiliation: Univ. of Michigan, HSRI
Publication: 15th Stapp Car Crash Conference Proceedings

ABSTRACT:

Results of animal studies, cadaver studies, and anthropometric dummy tests have been combined to produce injury criteria for lateral impacts to the head, thorax, and abdomen. Full-scale crash simulations were performed on an impact sled to verify results of the more specialized tests and analyses, scaling relationships for various species of animals have been developed and extrapolated to man. Significant differences in right and left side tolerances to imapct were noted and detailed. Critical impact velocities for various body sites have been developed for several categories of impact.

Areas of Relevance to Project: Modeling Approaches

Comments: Addresses scaling laws for primate to human scaling. May be useful in scaling from 50th percentile to other occupant sizes. Emphasis on head injury. Scaling developed for head criteria. Mechanical impedance of head addressed and model developed. Body impact criteria primarily concerned with upper abdomenal region. 19 psi average pressure recommended.

APPENDIX B

LUMPED MASS PARAMETER
STUDY DATA SUMMARY

RUN #	PEAK RIB Gy	PEAK TORSO Gy	PEAK PELVIC Gy	PEAK HEAD Gy	AIS	CSI	MAX RIB del V (fps)	MAX TORSO del V (fps)	DOOR VEL AT CONTACT (fps)
1	18.68	11.39	23.05	19.38	0.07	7.89	12.57	11.13	10.32
2	36.46	25.42	39.71	31.99	0.49	60.36	24.56	25.41	21.21
3	132.05	100.27	100.92	31.15	1.86	564.60	34.46	29.85	37.40
4	214.87	160.48	166.15	28.76	2.86	1679.81	48.13	39.82	48.23
5	16.94	9.53	19.83	17.14	0.04	4.93	11.19	9.79	8.68
6	35.16	23.65	37.47	31.65	0.49	51.49	23.28	24.10	20.35
7	121.91	84.14	94.09	30.15	1.75	378.15	33.10	25.64	38.01
8	190.53	133.37	146.32	29.27	2.66	1134.40	45.78	35.12	46.67
9	22.71	19.16	30.19	21.36	0.08	13.56	12.83	12.25	11.18
10	42.37	27.29	46.23	32.20	0.52	71.60	25.26	25.72	17.66
11	145.16	126.98	111.71	27.89	1.98	949.37	34.24	34.63	34.71
12	258.56	207.03	203.93	31.87	3.13	3004.73	50.64	50.20	49.79
13	9.09	8.15	19.91	14.54	0.00	5.03	12.44	12.69	7.27
14	29.95	17.78	30.19	31.98	0.30	33.34	23.38	24.26	22.90
15	85.83	82.57	73.33	30.56	1.29	462.83	33.98	34.02	39.25
16	137.41	131.78	120.57	28.57	2.15	1339.41	45.78	45.85	43.55
17	9.45	7.48	16.63	14.12	0.00	4.06	11.46	11.81	6.53
18	30.33	17.66	28.82	31.21	0.29	32.58	22.79	23.60	20.14
19	79.98	74.83	71.56	30.10	1.30	360.60	30.69	30.91	41.27
20	126.18	114.36	111.41	28.71	2.06	926.34	39.55	39.35	42.77
21	10.27	24.20	12.45	14.52	0.00	8.67	14.06	14.99	6.83
22	25.88	17.60	36.22	32.58	0.33	33.10	24.31	25.27	23.37
23	88.84	94.99	87.34	29.67	1.30	623.01	36.56	37.01	36.72
24	157.92	151.87	131.66	29.57	2.11	2035.88	55.95	56.74	45.89
25	9.27	10.38	14.47	9.38	0.00	5.84	12.52	13.53	14.27
26	28.70	28.16	31.84	30.94	0.38	39.94	20.88	21.39	27.05
27	69.22	66.65	61.62	29.85	0.91	347.93	35.20	35.38	27.24
28	100.80	102.91	96.52	29.68	1.42	949.70	49.08	49.45	30.58
29	7.70	8.13	13.71	8.38	0.00	3.89	12.06	12.88	0.05
30	26.51	25.86	29.61	30.68	0.35	40.36	22.04	22.90	0.11
31	66.70	61.78	55.53	30.30	0.88	300.20	34.07	34.08	0.16
32	87.37	86.40	83.54	28.94	1.33	601.20	40.98	40.99	0.22
33	13.01	15.09	18.01	11.75	0.00	9.36	13.26	14.48	9.66
34	39.66	32.80	37.56	31.75	0.43	50.88	21.27	22.21	27.67
35	72.56	71.08	68.70	32.24	0.93	391.88	35.89	36.29	38.68
36	128.39	122.21	114.58	30.92	1.47	1562.89	58.16	58.89	40.30
37	22.63	21.40	26.64	32.11	0.18	36.03	22.53	23.46	21.21
38	69.65	72.54	66.54	30.13	1.13	331.26	30.40	30.44	37.40
39	18.07	18.10	23.65	31.78	0.15	30.48	21.95	22.82	20.35
40	71.14	66.84	62.89	30.47	1.14	271.54	28.53	28.48	38.01
41	28.34	27.62	32.41	32.41	0.22	51.63	24.19	25.21	17.66

RUN #	PEAK RIB Gy	PEAK TORSO Gy	PEAK PELVIC Gy	PEAK HEAD Gy	AIS	CSI	MAX RIB del V (fps)	MAX TORSO del V (fps)	DOOR VEL AT CONTACT (fps)
42	75.07	82.82	78.60	29.13	1.12	432.05	32.29	32.73	34.71
43	21.83	22.28	24.52	32.08	0.15	34.94	22.54	23.49	21.21
44	55.75	54.09	49.49	30.33	0.72	197.41	28.75	28.90	37.40
45	19.55	19.10	21.89	31.68	0.12	28.81	21.86	22.72	20.35
46	51.44	50.38	45.71	29.73	0.68	176.91	28.37	28.38	38.01
47	26.91	25.83	29.26	32.69	0.18	44.64	23.68	24.72	17.66
48	62.12	59.23	53.47	31.72	0.76	223.83	29.21	29.64	34.71
49	78.72	54.28	84.46	14.83	0.53	194.10	24.96	24.99	13.55
50	165.66	152.97	144.35	13.93	1.76	1380.80	37.21	38.86	34.21
51	41.81	38.79	45.73	14.50	0.30	72.05	23.32	23.38	18.72
52	105.24	101.90	108.15	14.39	1.13	669.67	37.50	38.97	36.06
53	52.17	42.24	47.32	15.09	0.44	85.71	22.62	23.93	24.27
54	123.74	82.96	82.19	13.84	0.91	505.87	37.19	38.66	37.69
55	54.45	45.18	46.66	14.96	0.31	92.67	18.60	19.08	13.55
56	104.24	90.08	96.19	13.70	1.00	486.55	33.40	34.88	34.21
57	58.67	43.33	42.04	14.60	0.28	80.82	18.43	17.59	13.55
58	82.86	71.47	69.99	15.18	0.79	312.40	31.46	33.09	34.21
59	35.10	33.67	27.79	30.97	0.38	58.11	19.96	20.63	13.34
60	101.54	79.01	74.61	30.00	1.49	307.50	29.47	22.54	33.87
61	201.04	150.25	153.42	27.86	2.69	1414.44	45.74	37.72	48.22
62	17.47	20.58	28.46	21.63	0.00	16.38	13.99	14.51	9.06
63	59.46	49.98	53.01	29.74	0.90	119.44	23.89	24.86	23.30
64	154.58	116.51	118.75	32.12	2.14	773.03	37.94	32.47	39.56
65	19.20	17.18	23.67	22.50	0.08	19.85	18.88	19.75	21.46
66	57.18	64.06	60.85	30.12	0.98	218.17	24.94	23.91	36.00
67	121.70	117.80	107.08	28.88	1.90	1020.86	42.26	42.41	43.55
68	16.80	14.21	21.20	21.88	0.03	9.63	13.54	14.07	9.17
69	33.75	37.05	38.77	30.90	0.48	67.73	23.31	24.29	23.01
70	96.17	94.96	84.79	31.66	1.50	651.80	39.24	39.42	41.28
71	23.11	18.57	27.46	30.13	0.25	28.83	20.43	20.93	26.78
72	52.92	56.52	51.79	29.53	0.77	199.72	26.79	26.95	27.21
73	97.42	97.68	91.72	29.08	1.36	847.02	46.37	46.43	30.56
74	15.13	15.21	17.34	11.88	0.00	9.48	14.66	15.37	14.53
75	42.00	38.38	35.75	30.98	0.46	80.22	22.17	22.94	23.10
76	76.67	72.82	67.33	30.51	1.01	478.95	41.09	41.49	27.26
77	27.73	27.22	23.26	30.92	0.28	40.27	19.15	19.65	18.40
78	96.04	66.68	73.75	29.59	1.40	216.99	28.55	21.33	36.02
79	172.43	121.72	132.71	29.57	2.45	890.11	42.62	32.27	46.67
80	15.80	17.55	24.06	22.85	0.00	12.22	13.48	12.85	7.41
81	54.47	44.61	46.63	30.75	0.85	99.74	24.02	24.89	22.19
82	144.02	100.36	110.66	28.53	2.05	558.99	37.46	28.20	38.94

RUN #	PEAK RIB Gy	PEAK TORSO Gy	PEAK PELVIC Gy	PEAK HEAD Gy	AIS	CSI	MAX RIB del V (fps)	MAX TORSO del V (fps)	DOOR VEL AT CONTACT (fps)
83	17.43	16.56	21.67	21.57	0.08	17.29	18.16	19.00	19.38
84	55.00	57.29	54.78	30.70	0.96	175.92	25.13	22.90	40.10
85	110.39	101.64	98.86	31.68	1.83	682.58	36.37	35.92	42.77
86	21.33	15.94	16.67	20.94	0.01	10.24	13.37	12.80	7.34
87	30.64	34.46	36.51	30.75	0.47	63.01	23.99	24.87	20.99
88	85.35	81.13	78.33	29.35	1.43	431.79	33.85	34.05	41.61
89	21.55	17.66	24.91	28.39	0.23	26.23	19.64	20.02	0.11
90	48.32	52.86	48.01	29.71	0.74	177.17	25.65	26.22	0.16
91	87.30	86.40	83.53	28.91	1.33	600.70	40.49	40.39	0.22
92	12.28	13.70	15.94	10.97	0.00	7.55	14.03	14.78	0.05
93	38.28	35.74	33.55	30.61	0.42	69.82	21.81	22.54	0.11
94	68.35	69.02	63.11	29.43	1.01	392.12	38.43	38.84	0.16
95	46.50	42.77	41.24	31.64	0.51	89.35	20.94	21.33	10.38
96	104.76	90.16	90.23	31.14	1.45	357.84	28.10	23.55	30.64
97	227.44	181.86	174.64	32.13	2.78	2229.48	46.01	45.29	47.91
98	23.03	24.96	37.07	20.25	0.00	25.16	16.53	17.36	11.83
99	70.25	56.81	63.36	32.38	0.93	140.87	24.41	25.05	20.83
100	169.33	144.08	126.37	28.70	2.23	1264.88	39.44	39.85	37.76
101	21.09	19.87	27.68	27.56	0.06	24.66	20.55	21.50	18.49
102	68.60	69.41	70.31	31.35	0.95	251.83	25.21	25.54	34.87
103	149.18	136.49	119.65	28.29	1.89	1545.40	49.14	49.38	45.89
104	16.07	12.67	28.71	22.24	0.08	10.62	15.41	16.70	6.62
105	46.56	41.80	44.09	30.81	0.52	85.23	23.48	24.56	25.81
106	109.88	109.43	97.74	32.40	1.50	926.12	43.14	43.66	38.94
107	23.37	19.23	32.12	32.58	0.26	33.46	21.73	22.78	26.10
108	71.71	61.66	56.19	32.74	0.81	237.37	27.70	28.17	38.36
109	106.34	104.33	100.83	32.67	1.32	1010.81	48.48	49.06	40.30
110	19.48	19.63	18.60	16.60	0.00	15.18	15.48	16.70	10.03
111	45.56	44.13	41.36	31.05	0.53	103.23	22.38	23.03	28.80
112	86.67	78.24	77.78	30.30	1.01	568.74	42.40	42.78	38.39
113	120.78	109.72	118.25	14.81	1.39	1194.21	53.28	54.64	48.41
114	119.24	106.79	102.72	30.04	1.33	1155.74	52.31	52.97	49.79
115	101.28	99.56	93.61	29.41	1.39	889.97	47.92	48.31	48.23
116	87.76	93.10	66.21	28.97	1.43	721.20	43.10	42.99	46.67
117	170.35	172.14	160.81	13.07	1.94	2533.81	58.85	60.10	48.41
118	143.51	145.69	127.20	32.52	2.03	1845.31	54.23	54.96	49.79
119	132.38	127.03	115.75	31.90	2.05	1239.56	45.09	45.06	48.23
120	118.55	108.08	105.37	29.48	1.95	798.32	38.00	37.69	46.67
121	313.53	259.38	209.84	11.61	2.86	5728.94	63.52	64.82	48.41
122	248.67	185.30	168.09	13.87	2.10	3143.63	61.76	62.89	49.01
123	130.17	121.34	132.44	13.36	1.76	1706.61	59.69	61.12	44.33

APPENDIX C

CAL-3D SIDE IMPACT OCCUPANT DATA SETS

1 CRASH VICTIM EST. PART 572 DUMMY 17 SEGMENTS 16 JOINTS

CARD 8.1

CARDS 8.2

T	SEGMENT SYM	PLOT	WEIGHT (LBS)	PRINCIPAL MOMENTS OF INERTIA (LBS-SEC**2-INCH) X	Y	Z	SEGMENT CONTACT ELLIPSOID SEMIAXES (INCH) X	Y	Z	CENTER (INCH) X	Y	Z	PRINCIPAL AXES (DEG) YAW	PITCH	ROLL
1	HT	5	35.750	1.7600	1.1400	1.7100	4.340	6.940	6.000	-.400	0.000	-.900	0.00	0.00	0.00
2	CT	4	9.330	.3250	.3140	.1490	4.650	5.800	6.000	2.130	0.000	-3.550	0.00	0.00	0.00
3	UT	3	16.750	1.1600	.8250	.6650	4.650	5.470	5.200	.500	3.470	1.250	0.00	0.00	0.00
4	N	2	1.500	.0400	.0400	.0066	2.570	2.280	3.280	-.570	0.000	0.000	0.00	0.00	0.00
5	H	1	10.200	.2590	.3110	.2000	4.000	3.100	4.700	.400	0.000	0.000	0.00	0.00	0.00
6	RUL	6	19.400	.7270	.7030	.1540	3.350	3.740	11.000	0.000	0.000	-1.700	0.00	0.00	0.00
7	RLL	7	6.900	.4400	.4420	.0190	2.100	2.230	9.500	0.000	0.000	-.500	0.00	0.00	0.00
8	RF	8	2.800	.0383	.0434	.0132	1.500	1.800	5.200	0.000	0.000	.850	0.00	0.00	0.00
9	LHL	9	19.400	.7270	.7030	.1540	3.350	3.740	11.000	0.000	0.000	-1.700	0.00	0.00	0.00
10	LLL	A	6.900	.4400	.4420	.0150	2.100	2.230	9.500	0.000	0.000	-.500	0.00	0.00	0.00
11	LF	B	2.800	.0383	.0434	.0132	1.500	1.800	5.200	0.000	0.000	.850	0.00	0.00	0.00
12	RUA	C	4.800	.1640	.1660	.0141	2.070	1.640	7.050	0.000	0.000	.550	0.00	0.00	0.00
13	RLA	D	4.800	.2550	.2550	.0115	1.300	1.110	6.000	0.000	0.000	-1.650	0.00	0.00	0.00
14	LUA	E	4.800	.1640	.1660	.0141	2.070	1.640	7.050	0.000	0.000	.550	0.00	0.00	0.00
15	LLA	F	4.800	.2550	.2550	.0115	1.300	1.110	6.000	0.000	0.000	-1.650	0.00	0.00	0.00
16	RIB	P	15.000	1.1600	.8250	.6650	4.650	4.270	5.200	0.000	-4.270	0.000	0.00	0.00	0.00
17	PNL	G	1.000	1.0000	1.0000	1.0000	1.000	1.000	1.000	0.000	0.000	0.000	0.00	0.00	0.00

CARDS 8.3

J	JOINT SYM	PLOT	JNT	PIN	LOCATION(INCH) - SEG(JNT) X	Y	Z	LOCATION(INCH) - SEG(J+1) X	Y	Z	PRIN. AXIS(DEG) - SEG(JNT) YAW	PITCH	ROLL	PRIN. AXIS(DEG) - SEG(J+1) YAW	PITCH	ROLL
1	P	O	1	-2	-2.200	0.000	-3.750	0.000	0.000	1.050	0.00	0.00	0.00	0.00	0.00	0.00
2	W	D	2	-2	0.000	0.000	-1.050	-1.400	0.000	10.520	0.00	0.00	0.00	0.00	0.00	0.00
3	NP	M	3	-2	1.250	0.000	-3.780	0.000	0.000	1.770	0.00	0.00	0.00	0.00	0.00	0.00
4	HP	M	4	-2	0.000	0.000	-1.780	.100	0.000	2.350	0.00	0.00	0.00	0.00	15.00	0.00
5	RH	J	1	0	-.100	4.450	.900	0.000	0.000	-8.810	0.00	0.00	0.00	0.00	0.00	0.00
6	RK	R	6	1	0.000	0.000	6.790	0.000	0.000	-8.000	0.00	0.00	0.00	0.00	-84.00	5.72
7	RA	S	7	-2	0.000	0.000	8.200	1.700	0.000	-2.200	0.00	0.00	0.00	0.00	75.00	0.00
8	LH	T	1	0	-.100	-4.450	.900	0.000	0.000	-8.810	0.00	0.00	0.00	0.00	-80.00	0.00
9	LK	U	8	1	0.000	0.000	6.790	0.000	0.000	-8.000	0.00	0.00	0.00	0.00	-84.00	-5.72
10	LA	V	10	-2	0.000	0.000	8.200	1.700	0.000	-2.200	0.00	0.00	0.00	0.00	75.00	0.00
11	RS	W	3	-2	-.150	7.600	-.930	0.000	0.000	-5.000	0.00	0.00	0.00	0.00	-80.00	0.00
12	RE	X	12	-1	0.000	0.000	6.100	0.000	0.000	-6.650	0.00	0.00	0.00	0.00	-55.00	10.19
13	LS	Y	3	-2	-.150	-7.600	-.930	0.000	0.000	-5.000	0.00	0.00	0.00	0.00	-72.50	0.00
14	LE	Z	14	-1	0.000	0.000	6.100	0.000	0.000	-6.650	0.00	0.00	0.00	0.00	-55.00	-10.19
15	RTRH	H	3	1	-4.150	0.000	1.500	-4.650	0.000	0.000	0.00	0.00	90.00	0.00	-72.50	0.00
16	NN		0	0	0.000	0.000	0.000	0.000	0.000	0.000	0.00	0.00	0.00	0.00	0.00	90.00

1 CRASH VICTIM 50 LB. CHILD 17 SEGMENTS 16 JOINTS CARD NO.1

CARDS 8.2

I	SEGMENT SYM	PLOT	WEIGHT (LBS)	PRINCIPAL MOMENTS OF INERTIA (LBS-SEC**2-INCH) X	Y	Z	SEGMENT CONTACT ELLIPSOID SEMIAXES (INCH) X	Y	Z	CENTER (INCH) X	Y	Z	PRINCIPAL AXES (DEG) YAW	PITCH	ROLL
1	LT	5	10.740	.2030	.1280	.1710	2.950	4.700	3.800	0.000	0.000	0.000	0.00	0.00	0.00
2	CT	4	2.823	.0540	.0450	.0340	2.900	3.900	4.700	0.000	0.000	0.000	0.00	0.00	0.00
3	UT	3	5.040	.0460	.0330	.0550	2.900	1.730	2.200	0.000	1.730	0.000	0.00	0.00	0.00
4	N	2	.450	.0010	.0010	.0015	1.670	1.670	3.950	0.000	0.000	0.000	0.00	0.00	0.00
5	H	1	7.190	.0882	.1050	.0770	3.550	2.850	3.950	0.000	0.000	0.000	0.00	0.00	0.00
6	RUL	6	5.100	.1590	.1590	.0251	2.180	2.180	7.450	0.000	0.000	0.000	0.00	0.00	0.00
7	RLL	7	1.960	.0486	.0486	.0046	1.500	1.500	6.750	0.000	0.000	0.000	0.00	0.00	0.00
8	RF	8	.747	.0059	.0055	.0011	1.000	1.350	3.650	0.000	0.000	0.000	0.00	0.00	0.00
9	LUL	9	5.100	.1590	.1590	.0251	2.180	2.180	7.450	0.000	0.000	0.000	0.00	0.00	0.00
10	LLL	A	1.960	.0486	.0486	.0046	1.500	1.500	6.750	0.000	0.000	0.000	0.00	0.00	0.00
11	LF	B	.747	.0059	.0055	.0011	1.000	1.350	3.650	0.000	0.000	0.000	0.00	0.00	0.00
12	RUA	C	.863	.0100	.0100	.0011	1.100	1.100	4.600	0.000	0.000	0.000	0.00	0.00	0.00
13	RLA	D	.956	.0209	.0209	.0012	1.100	1.100	6.400	0.000	0.000	0.000	0.00	0.00	0.00
14	LUA	E	.863	.0100	.0100	.0011	1.100	1.100	4.600	0.000	0.000	0.000	0.00	0.00	0.00
15	LLA	F	.956	.0209	.0209	.0012	1.100	1.100	6.400	0.000	0.000	0.000	0.00	0.00	0.00
16	RIB	R	4.200	.0460	.0330	.0540	2.900	2.230	2.200	0.000	-2.230	-1.000	0.00	0.00	0.00
17	PNL	G	1.000	1.0000	1.0000	1.0000	1.000	1.000	1.000	0.000	0.000	0.000	0.00	0.00	0.00

CARDS 8.3

J	JOINT SYM	PLOT	JNT	PIN	LOCATION(INCH) - SEG(JNT) X	Y	Z	LOCATION(INCH) - SEG(J+1) X	Y	Z	PRIN. AXIS(DEG) - SEG(JNT) YAW	PITCH	ROLL	PRIN. AXIS(DEG) - SEG(J+1) YAW	PITCH	ROLL
1	P	P	1	0	0.000	0.000	-2.080	0.000	0.000	2.080	0.00	0.00	0.00	0.00	0.00	0.00
2	W	O	2	0	0.000	0.000	-2.880	0.000	0.000	2.880	0.00	0.00	0.00	0.00	0.00	0.00
3	NP	N	3	0	0.000	0.000	-1.620	0.000	0.000	1.620	0.00	0.00	0.00	0.00	15.00	0.00
4	HP	M	4	0	0.000	0.000	-2.500	0.000	0.000	2.500	0.00	0.00	0.00	0.00	0.00	0.00
5	RH	Q	1	U	0.000	2.540	1.600	0.000	0.000	-5.250	0.00	0.00	0.00	0.00	-84.00	5.72
6	RK	R	6	1	0.000	0.000	5.856	0.000	0.000	-5.150	0.00	0.00	0.00	0.00	75.00	0.00
7	RA	S	7	0	0.000	0.000	5.750	1.000	0.000	-1.650	0.00	0.00	0.00	0.00	-80.00	0.00
8	LH	T	1	0	0.000	-2.540	1.600	0.000	0.000	-5.250	0.00	0.00	0.00	0.00	-84.00	-5.72
9	LK	T	9	1	0.000	0.000	5.850	0.000	0.000	-5.150	0.00	0.00	0.00	0.00	75.00	0.00
10	LA	V	10	0	0.000	0.000	5.750	1.000	0.000	-1.650	0.00	0.00	0.00	0.00	-80.00	0.00
11	RS	W	3	0	0.000	4.250	-1.100	0.000	0.000	-3.500	0.00	0.00	0.00	0.00	-55.00	10.15
12	RE	X	12	1	0.000	0.000	3.360	0.000	0.000	-5.160	0.00	0.00	0.00	0.00	-72.50	0.00
13	LS	Y	3	0	0.000	-4.250	-1.100	0.000	0.000	-3.500	0.00	0.00	0.00	0.00	-55.00	-10.19
14	LE	Z	14	1	0.000	0.000	3.360	0.000	0.000	-5.160	0.00	0.00	0.00	0.00	-72.50	0.00
15	RIBH	H	3	1	-2.900	0.000	0.000	-2.900	0.000	0.000	0.00	0.00	90.00	0.00	0.00	90.00
16	NN		0	0	0.000	0.000	0.000	0.000	0.000	0.000	0.00	0.00	0.00	0.00	0.00	0.00

"1 CRASH VICTIM STOCSTH 17 SEGMENTS 16 JOINTS

CARD 8.1

SEGMENT			WEIGHT	PRINCIPAL MOMENTS OF INERTIA (LBS-SEC**2-INCH)			SEGMENT CONTACT ELLIPSOID SEMI-AXES (INCH)			SEGMENT CONTACT ELLIPSOID CENTER (INCH)			CARDS 8.2 PRINCIPAL AXES (DEG)		
I	SYM	PLOT	(LBS)	X	Y	Z	X	Y	Z	X	Y	Z	YAW	PITCH	ROLL
1	LT	5	47.250	2.6400	1.5200	2.7300	5.420	7.620	6.590	-.440	0.000	-.990	0.00	0.00	0.0
2	CT	4	12.410	.4150	.5000	.2370	2.160	4.370	4.590	2.240	0.000	-3.900	0.00	0.00	0.0
3	UT	3	22.150	1.8500	1.3100	1.0600	5.100	3.810	5.710	-.550	3.810	1.370	0.00	0.00	0.0
4	NK	2	1.080	.0640	.0640	.0110	2.220	3.500	3.660	-.636	0.000	0.000	0.00	0.00	0.0
5	HD	1	13.490	.4120	.6940	.3190	4.200	3.400	5.160	.440	0.000	0.000	0.00	0.00	0.0
6	PIL	6	24.340	1.1500	1.1200	.2450	3.660	4.110	12.070	0.000	0.000	-1.870	0.00	0.00	0.0
7	RLL	7	6.130	.7010	.7040	.0300	2.210	2.450	10.630	0.000	0.000	-.550	0.00	0.00	0.0
8	RF	8	3.700	.0610	.0650	.0210	1.650	1.960	5.710	0.000	0.000	.933	0.00	0.00	0.0
9	LUL	9	24.340	1.1500	1.1200	.2450	3.660	4.110	12.070	0.000	0.000	-1.870	0.00	0.00	0.0
10	LFL	A	6.130	.7010	.7040	.0300	2.210	2.450	10.630	0.000	0.000	-.559	0.00	0.00	0.0
11	LF	B	3.700	.0610	.0650	.0210	1.650	1.960	5.710	0.000	0.000	.933	0.00	0.00	0.0
12	RUA	C	6.350	.2610	.2650	.0225	2.270	1.800	7.730	0.000	0.000	.604	0.00	0.00	0.0
13	RLA	D	6.350	.4060	.4130	.0193	1.430	1.220	6.590	0.000	0.000	-1.910	0.00	0.00	0.0
14	LUA	E	6.350	.2610	.2650	.0225	2.270	1.800	7.730	0.000	0.000	.604	0.00	0.00	0.0
15	LLA	F	5.350	.4060	.4130	.0193	1.430	1.220	6.590	0.000	0.000	-1.811	0.00	0.00	0.0
16	RIB	G	19.840	1.6500	1.3150	1.0600	5.100	4.690	5.710	0.000	-4.690	-1.370	0.00	0.00	0.0
17	PNL	G	1.000	1.0000	1.0000	1.0000	1.000	1.000	1.000	0.000	0.000	0.000	0.00	0.00	0.0

JOINT					LOCATION(INCH) - SEG(JNT)			LOCATION(INCH) - SEG(J+1)			PRIN. AXIS(DEG) - SEG(JNT)			CARDS 8.3 PRIN. AXIS(DEG) - SEG(J+		
J	SYM	PLOT	JNT	PTH	X	Y	Z	X	Y	Z	YAW	PITCH	ROLL	YAW	PITCH	ROL
1	P		1	-2	-2.410	0.000	-4.120	0.000	0.000	1.150	0.00	0.00	0.00	0.00	0.00	0.0
2	W		2	-3	0.000	0.000	-1.150	-1.540	0.000	11.550	0.00	0.00	0.00	0.00	0.00	0.0
3	NP		3	-5	1.370	0.000	-4.150	0.000	0.000	1.640	0.00	0.00	0.00	0.00	0.00	0.0
4	HP		4	-2	0.000	0.000	-1.150	.110	0.000	2.580	0.00	0.00	0.00	0.00	15.00	0.0
5	RH		1	0	-.110	4.880	.955	0.000	0.000	0.000	0.00	0.00	0.00	0.00	0.00	0.0
6	PK		6	1	0.000	0.000	7.450	0.000	0.000	-9.670	0.00	0.00	0.00	0.00	-84.00	90.0
7	PA		7	-2	0.000	0.000	9.000	0.000	0.000	-8.790	0.00	0.00	0.00	0.00	75.00	0.0
8	LH		1	0	-.110	-4.880	.955	1.666	0.000	-2.410	0.00	0.00	0.00	0.00	-80.00	0.0
9	LK		9	1	0.000	0.000	7.450	0.000	0.000	-9.670	0.00	0.00	0.00	0.00	-84.00	90.0
10	LA		10	-3	0.000	0.000	9.000	0.000	0.000	-8.790	0.00	0.00	0.00	0.00	75.00	0.0
11	RS		3	-2	-.164	6.240	-1.020	1.666	0.000	-2.410	0.00	0.00	0.00	0.00	-80.00	0.0
12	PE		12	-1	0.000	0.000	-6.660	0.000	0.000	-5.488	0.00	0.00	0.00	0.00	-55.00	10.0
13	LS		3	-2	-.164	-6.240	-1.020	0.000	0.000	-7.300	0.00	0.00	0.00	0.00	-72.50	0.0
14	LE		14	-1	0.000	0.000	-5.696	0.000	0.000	-5.488	0.00	0.00	0.00	0.00	-55.00	-10.0
15	RTSH		3	-1	-4.550	0.000	1.640	0.000	0.000	-7.300	0.00	0.00	0.00	0.00	-72.50	0.0
16	NN		0	0	0.000	0.000	0.000	-5.104	0.000	0.000	0.00	0.00	90.00	0.00	0.00	90.0
								0.000	0.000	0.000	0.00	0.00	0.00	0.00	0.00	0.0

1 CRASH VICTIM SID5THFEMALE 17 SEGMENTS 16 JOINTS

CARD F.1

CARDS F.2

I	SEGMENT SYM	PLOT	WEIGHT (LBS)	PRINCIPAL MOMENTS OF INERTIA (LBS-SEC**2-INCH) X	Y	Z	SEGMENT CONTACT ELLIPSOID SEMIAXES (INCH) X	Y	Z	CENTER (INCH) X	Y	Z	PRINCIPAL AXES (DEG) YAW	PITCH	ROLL
1	LT	5	22.600	.8290	.5310	.7970	4.240	5.960	5.150	-.343	0.000	-.772	0.00	0.00	0.00
2	PT	4	5.930	.1510	.1460	.0690	3.990	4.980	5.150	1.830	0.000	-3.047	0.00	0.00	0.00
3	UT	3	10.590	.5400	.3940	.3100	3.990	2.980	4.460	-.429	2.980	1.073	0.00	0.00	0.00
4	N	2	.348	.0180	.0160	.0030	2.200	1.960	2.820	-.490	0.000	0.000	0.00	0.00	0.00
5	H	1	6.450	.1210	.1450	.0930	3.430	2.660	4.030	.343	0.000	0.000	0.00	0.00	0.00
6	PUL	6	11.630	.3360	.3270	.0720	2.875	3.210	9.440	0.000	0.000	-1.460	0.00	0.00	0.00
7	PLL	7	4.360	.2050	.2060	.0088	1.802	1.910	8.150	0.000	0.000	-.429	0.00	0.00	0.00
8	RF	8	1.770	.0178	.0202	.0060	1.287	1.540	4.460	0.000	0.000	.730	0.00	0.00	0.00
9	LHL	9	11.630	.3390	.3270	.0720	2.970	3.210	9.440	0.000	0.000	-1.460	0.00	0.00	0.00
10	LLL	A	4.360	.2050	.2060	.0088	1.902	1.910	8.150	0.000	0.000	-.430	0.00	0.00	0.00
11	LF	B	1.770	.0178	.0202	.0060	1.287	1.540	4.460	0.000	0.000	.730	0.00	0.00	0.00
12	RUA	C	3.030	.0764	.0770	.0066	1.770	1.400	6.050	0.000	0.000	.470	0.00	0.00	0.00
13	RLA	D	3.030	.1190	.1206	.0054	1.116	.950	5.150	0.000	0.000	-1.410	0.00	0.00	0.00
14	LUA	E	3.030	.0764	.0770	.0066	1.770	1.400	6.050	0.000	0.000	.470	0.00	0.00	0.00
15	LLA	F	3.030	.1190	.1206	.0054	1.116	.950	5.150	0.000	0.000	-1.410	0.00	0.00	0.00
16	RIB	R	9.490	.5400	.3840	.3100	3.990	3.660	4.460	0.000	-3.660	-1.073	0.00	0.00	0.00
17	PNL	G	1.000	1.0000	1.0000	1.0000	1.000	1.000	1.000	0.000	0.000	0.000	0.00	0.00	0.00

CARDS F.3

J	JOINT SYM	PLOT	JNT	PIN	LOCATION(INCH) - SEG(JNT) X	Y	Z	LOCATION(INCH) - SEG(J+1) X	Y	Z	PRIN. AXIS(DEG) - SEG(JNT) YAW	PITCH	ROLL	PRIN. AXIS(DEG) - SEG(J+1) YAW	PITCH	ROLL
1	P	P	1	-2	-1.888	0.000	-3.219	0.000	0.000	.901	0.00	0.00	0.00	0.00	0.00	0.00
2	M	M	2	-2	0.000	0.000	-.901	-1.200	0.000	5.030	0.00	0.00	0.00	0.00	0.00	0.00
3	HP	N	3	-2	1.073	0.000	-3.240	0.000	0.000	1.520	0.00	0.00	0.00	0.00	0.00	0.00
4	RH	O	4	-2	0.000	0.000	-1.530	.086	0.000	2.020	0.00	0.00	0.00	0.00	15.00	0.00
5	RK	R	1	0	-.086	3.820	.770	0.000	0.000	-7.560	0.00	0.00	0.00	0.00	0.00	0.00
6	RA	S	6	1	0.000	0.000	5.830	0.000	0.000	-6.860	0.00	0.00	0.00	0.00	-94.00	5.72
7	LH	T	7	-2	0.000	0.000	7.040	1.460	0.000	-1.888	0.00	0.00	0.00	0.00	75.00	0.00
8	LK	U	8	0	-.086	-3.820	.770	0.000	0.000	-7.560	0.00	0.00	0.00	0.00	-80.00	0.00
9	LA	V	9	1	0.000	0.000	5.830	0.000	0.000	-6.860	0.00	0.00	0.00	0.00	-84.00	-5.72
10	LB	W	10	-2	0.000	0.000	7.040	1.460	0.000	-1.888	0.00	0.00	0.00	0.00	75.00	0.00
11	RS	X	11	-2	-.129	6.520	-.800	0.000	0.000	-4.290	0.00	0.00	0.00	0.00	-80.00	0.00
12	LS	Y	12	-2	0.000	0.000	5.240	0.000	0.000	-5.708	0.00	0.00	0.00	0.00	-55.00	10.15
13	LRISH	Z	13	-2	-.129	-6.520	-.800	0.000	0.000	-4.290	0.00	0.00	0.00	0.00	-72.50	0.00
14	LC	H	14	-1	0.000	0.000	5.240	0.000	0.000	-5.708	0.00	0.00	0.00	0.00	-55.00	-10.15
15	RISH				-3.540	0.000	1.290	-3.990	0.000	0.000	0.00	0.00	90.00	0.00	-72.50	0.00
16	NN		3	0	0.000	0.000	0.000	0.000	0.000	0.000	0.00	0.00	0.00	0.00	0.00	90.00
																0.00

APPENDIX D

LUMPED MASS PROGRAM LISTING

```
      INTEGER*1 INFILE(11),OUTFIL(11),DAT(3)
      INTEGER*4 LBL1(17),LBL2(17),ITTLE(20)
      DIMENSION SRIB(45),TRNF(45),DVRIB(200)
      COMMON F(20,30),S(20,30),L(30),
     1    N(20,3),UK1(20),UF1(20),UK2(20),UF2(20),UK3(20),
     2    XREL(20),VREL(20),IUNLD(20),DEFLP(20),FUNLMX(20),SPRFRC(20),
     3    DEFLMX(20),A(30),AP(30),XP(30),IH(20,30),K1(30),V(30),
     4    R9(20),DYNFC(20),C9(20,6),
     5    WM(30),X(30),ACCMX(30),FMULT(20),CLR(30),IFLAG,
     6    TIME,TINC,NPRNT,NFOUT,TPRNT,TFOUT,ITIME
      DATA TRNF/0.46193,-0.71032, 0.10809, 0.46534,-0.11179,
     1          0.02809,-0.38776, 0.32800, 0.29154,-0.01035,
     2         -0.08155,-0.04710, 0.16269, 0.14598, 0.10515,
     3         -0.02970, 0.01949, 0.03948, 0.13491, 0.10206,
     4          0.08549, 0.00164,-0.02334, 0.08463, 0.07260,
     5          0.04146, 0.00164,-0.04284,-0.03330, 0.04419,
     6          0.02379,-0.00313,-0.00831,-0.04094,-0.00038,
     7          0.02501, 0.00253,-0.01502,-0.02452,-0.02127,
     8          0.00518, 0.00676,-0.02821,-0.03638,-0.02782/
      DATA LBL1/4H    ,4H    ,4H  FO,4HRCE ,4H    ,4H    ,
     1          4HDISP,4HL   ,4H  UN,4HLD F,4HORCE,4H 1  ,4H    ,
     2          4HUNLD,4H FOR,4HCE 2,4H    /
      DATA LBL2/4H  TI,4HME  ,4H   S,4HPR  ,4H  FO,4HRCE ,
     1          4H  DY,4HN FA,4HC   ,4HX RE,4HL   ,4HM   ,4H X A,
     2          4HBS  ,4H VEL,4H   A,4HCCEL/
      DATA DAT/1HD,1HA,1HT/
      LF=Z'0A'
      DO 1 I=1,11
      INFILE(I)=1H
    1 OUTFIL(I)=1H
      WRITE(3,970)
  970 FORMAT(/'  ENTER INPUT FILE NAME :')
      READ(3,971)(INFILE(I),I=1,8)
  971 FORMAT(8A1)
      WRITE(3,972)
  972 FORMAT(/'  ENTER OUTPUT FILE NAME :')
      READ(3,971)(OUTFIL(I),I=1,8)
      DO 2 I=9,11
      INFILE(I)=DAT(I-8)
    2 OUTFIL(I)=DAT(I-8)
      CALL OPEN(3,INFILE,0)
      CALL OPEN(4,OUTFIL,0)
      CSI=0.0
      ITIME=0
      DVSRIB=0.0
      DVTRX=0.0
      IDRVL=0
      DRVEL=0.0
      DO 99 I=1,20
      SPRFRC(I)=0.0
      FUNLMX(I)=0.0
      DEFLP(I)=0.0
      DEFLMX(I)=0.0
      XREL(I)=0.0
      VREL(I)=0.0
```

```
      UK1(I)=0.0
      UK2(I)=0.0
      UK3(I)=0.0
      UF1(I)=0.0
      UF2(I)=0.0
      FMULT(I)=1.0
      DYNFC(I)=0.0
      IUNLD(I)=0
      DO 98 J=1,3
   98 N(I,J)=0
      DO 97 J=1,30
      F(I,J)=0.0
      S(I,J)=0.0
   97 IH(I,J)=0
      DO 96 J=1,6
   96 C9(I,J)=0.0
   99 CONTINUE
      DO 95 I=1,30
      L(I)=0
      A(I)=0.0
      AP(I)=0.0
      XP(I)=0.0
      V(I)=0.0
      K1(I)=0
      X(I)=0.0
      WM(I)=0.0
      ACCMX(I)=0.0
   95 CLR(I)=0.0
      DO 94 I=1,45
   94 SRIB(I)=0.0
      FRIBP=0.0
      ICNT=1
      DVRMX=0.0
      VFRIB=0.0
      READ(3,1001)ITTLE
      READ(3,1002)TINC,TEND,NFOUT,NPRNT,NMASS,NSPRG
 1001 FORMAT(20A4)
      NMP1=NMASS+1
 1002 FORMAT(2F8.0,4I4)
      WRITE(4,5001)LF,ITTLE
 5001 FORMAT(A1,20A4)
      WRITE(4,5000)LF,NMP1,TINC,TEND
 5000 FORMAT(A1,I4,2E14.5)
      WRITE(2,1003)ITTLE
 1003 FORMAT(1X,20A4)
      WRITE(2,1010)TINC,TEND,NPRNT,NFOUT
 1010 FORMAT(' DT= ',F8.5,' TEND = ',F8.5,' NPRNT = ',I3,' NFOUT = ',
     1   I3/)
      WRITE(2,1020) NMASS,NSPRG
 1020 FORMAT(' NMASS = ',I3,' NSPRG = ',I3/)
      TIME=0.0
 1030  FORMAT(3X,'MASS NO.'5X,'WEIGHT',10X,'X(0)',10X,'V(0)')
      WRITE(2,1030)
      DO 5 K5=1,NMASS
      READ(3,1040)JMASS,WM5,X5,V5
```

```
1040 FORMAT(I4,3F8.0)
     WM(JMASS)=WM5
     V(JMASS)=V5
     X(JMASS)=X5
     WRITE(2,1050)JMASS,WM5,X5,V5
1050 FORMAT(2X,I3,4X,F12.2,6X,F8.2,6X,F8.2)
     V(JMASS)=V(JMASS)*17.6
     XP(JMASS)=X(JMASS)
     A(JMASS)=0.0
   5 CONTINUE
     DO 10 K5=1,NSPRG
     WRITE(2,1250)
1250 FORMAT(//3X,'SPR NO.',4X,'M1',6X,'M2',11X,'UNLD K1',6X,
    1   'UNLD K2',6X,'UNLD K3'/)
 610 READ(3,611)JSP
 611 FORMAT(I4)
 612 FORMAT(2F8.0)
 613 FORMAT(3I4,5F8.0)
     READ(3,612)FMULT(JSP),CLR(JSP)
     READ(3,613)N(JSP,1),N(JSP,2),N(JSP,3),UK1(JSP),UF1(JSP),
    1     UK2(JSP),UF2(JSP),UK3(JSP)
     READ(3,614)(C9(JSP,I7),I7=1,6)
 614 FORMAT(6F8.0)
     IUNLD(JSP)=0
 135 FORMAT(5X,I3,5X,I3,5X,I3,3X,I3,3X,F9.2,4X,F9.2,4X,F9.2//)
     WRITE(2,135)JSP,N(JSP,1),N(JSP,2),N(JSP,3),UK1(JSP),UK2(JSP),
    1     UK3(JSP)
 140 FORMAT(1X,17A4/)
     WRITE(2,140)LBL1
 815 N9=N(JSP,3)
     DO 20 J=1,N9
     READ(3,141)F(JSP,J),S(JSP,J)
 141 FORMAT(2F8.0)
     F(JSP,J)=F(JSP,J)*FMULT(JSP)
     IF(J.GT.1) GO TO 200
     WRITE(2,145)F(JSP,1),S(JSP,1),UF1(JSP),UF2(JSP)
     GO TO 20
 145 FORMAT(10X,F9.2,3X,F8.2,5X,F9.2,10X,F9.2)
 150 FORMAT(10X,F9.2,3X,F8.2)
 200 WRITE(2,150)F(JSP,J),S(JSP,J)
  20 CONTINUE
 205 FORMAT(/' FORCE LEVELS HAVE BEEN MULTIPLIED BY A FACTOR OF ',
    1   F6.2)
     WRITE(2,205)FMULT(JSP)
 210 FORMAT(/1X,'SPRING CLEARANCE = ',F8.2)
     WRITE(2,210)CLR(JSP)
     WRITE(2,160)(C9(JSP,I7),I7=1,6)
 160 FORMAT(' DAMPING FACTORS :'/6F10.2)
  10 CONTINUE
     CALL INSPRG(NSPRG,DEFLMX,CLR)
     WRITE(2,170)LBL2
 170 FORMAT(//1X,17A4/)
     DO 25 I=1,NSPRG
     DO 30 K5=1,2
     J5=N(I,K5)
```

```
      L(J5)=L(J5)+1
      LLL=L(J5)
      IH(LLL,J5)=I
   30 CONTINUE
   25 CONTINUE
      CALL SPRIN(NSPRG)
      IF(IFLAG.EQ.1) GO TO 215
      CALL ACCEL(NMASS)
      CALL OUTPT(NSPRG,NMASS)
 1370 CONTINUE
      ITIME=ITIME+1
      TIME=TIME+TINC
      DO 35 J=1,NMP1
      AP(J)=A(J)*386.4
      XP(J)=X(J)
      X(J)=X(J)+V(J)*TINC+AP(J)*TINC*TINC/2.0
   35 CONTINUE
      CALL SPRIN(NSPRG)
      IF(IFLAG.EQ.1) GO TO 215
      CALL ACCEL(NMASS)
      DO 40 J=1,NMASS
      V(J)=V(J)+(A(J)*386.4+AP(J))*TINC/2.0
   40 CONTINUE
      DVSRIB=AMAX1(DVSRIB,V(4))
      DVTRX=AMAX1(DVTRX,V(6))
      IF(IDRVL.NE.0) GO TO 401
      IF(XREL(3).LE.0.0) GO TO 401
      DRVEL=V(2)
      IDRVL=1
  401 CONTINUE
      DO 43 K=1,44
      KK=45-K
   43 SRIB(KK+1)=SRIB(KK)
      SRIB(1)=A(4)*386.4
      FRIB=0.0
      DO 44 K=1,45
   44 FRIB=FRIB+TRNF(K)*SRIB(K)
      V(NMP1)=V(NMP1)+(FRIB+FRIBP)*TINC/2.0
      A(NMP1)=FRIB/386.4
      DVRIB(ICNT)=(V(4)-V(NMP1))/12.0
      DVRMX=AMAX1(DVRMX,DVRIB(ICNT))
      ICNT=ICNT+1
      FRIBP=FRIB
      CSI=CSI+(ABS(A(6))**2.5)*TINC
 1520 CALL OUTPT(NSPRG,NMASS)
      IF(TIME.LE.TEND) GO TO 1370
  175 FORMAT(6X,'SPR. NO.',8X,'MAX. DEFL.'/)
  215 WRITE(2,175)
      DO 45 I=1,NSPRG
  180 FORMAT(8X,I2,10X,F8.2)
      WRITE(2,180)I,DEFLMX(I)
   45 CONTINUE
      WRITE(2,185)
  185 FORMAT(6X,'MASS NO.',9X,'MAX. G'/)
      DO 50 I=1,NMASS
```

```
      WRITE(2,190)I,ACCMX(I)
  190 FORMAT(8X,I2,10X,F9.2)
   50 CONTINUE
      AIS=0.0768*DVRMX+0.053*30.0-1.89
      WRITE(2,6000)DVRMX,AIS
 6000 FORMAT(//,'  MAX REL RIB DELTA V = ',F8.2,' FPS'5X,'AIS = ',F8.2)
      WRITE(2,6002)CSI
 6002 FORMAT(/'  CSI = ',F8.2)
      DVSRIB=DVSRIB/12.0
      DVTRX=DVTRX/12.0
      DRVEL=DRVEL/12.0
      WRITE(2,6005) DVSRIB,DVTRX,DRVEL
 6005 FORMAT(/'  STRUCK RIB DELTA V = ',F8.2,' FPS',
     1       /'       THORAX DELTA V = ',F8.2,' FPS',
     2       /' DOOR VEL AT CONTACT = ',F8.2,' FPS')
      KK=3*NMASS
      TLST=-9999.0
      WRITE(4,6001)(TLST,J=1,KK)
 6001 FORMAT(10E13.6)
      ENDFILE 3
      ENDFILE 4
      END
      SUBROUTINE SPRIN(NSPRG)
C-----------------------------------------------------------------------
      COMMON F(20,30),S(20,30),L(30),
     1    N(20,3),UK1(20),UF1(20),UK2(20),UF2(20),UK3(20),
     2    XREL(20),VREL(20),IUNLD(20),DEFLP(20),FUNLMX(20),SPRFRC(20),
     3    DEFLMX(20),A(30),AP(30),XP(30),IH(20,30),K1(30),V(30),
     4    R9(20),DYNFC(20),C9(20,6),
     5    WM(30),X(30),ACCMX(30),FMULT(20),CLR(30),IFLAG,
     6    TIME,TINC,NPRNT,NFOUT,TPRNT,TFOUT,ITIME
      IFLAG=0
      DO 1 I=1,NSPRG
      F3=0.0
      NS1=N(I,1)
      NS2=N(I,2)
      U1=X(NS1)-X(NS2)-CLR(I)
      IF(U1.LE.DEFLMX(I)) GO TO 15
      DEFLMX(I)=U1
   15 XREL(I)=U1
      VREL(I)=(V(NS1)-V(NS2))
      IF(IUNLD(I).EQ.1) GO TO 20
      DEFLP(I)=XP(NS1)-XP(NS2)-CLR(I)
      FUNLMX(I)=-SPRFRC(I)
      IF(U1.LT.0.0) GO TO 60
   20 IF(U1.LT.DEFLP(I)) GO TO 30
      IUNLD(I)=0
      NI=N(I,3)
   25 IIND=0
      DO 2 K5=2,NI
      IF(IIND.NE.0) GO TO 2
      IF(U1.GE.S(I,K5)) GO TO 2
      S1=S(I,K5-1)
      S2=S(I,K5)
      F1=F(I,K5-1)
```

```
      F2=F(I,K5)
      F3=F1+(U1-S1)*(F2-F1)/(S2-S1)
      IIND = 1
    2 CONTINUE
      IF(IIND.NE.0) GO TO 60
      WRITE(2,1000)I
 1000 FORMAT(' COORDINATE EXCEEDED IN SPRING NO. ',I2)
      IFLAG=1
      RETURN
   30 IUNLD(I)=1
      IF(FUNLMX(I).GT.UF1(I)) GO TO 40
      S3=DEFLP(I)-FUNLMX(I)/UK1(I)
      S4=S3
      GO TO 45
   40 S3=DEFLP(I)-(FUNLMX(I)-UF1(I))/UK1(I)
      S4=S3-(UF1(I)-UF2(I))/UK2(I)
   45 IF(U1.GE.S3) GO TO 50
      IF(U1.GE.S4) GO TO 55
      F3=UF2(I)-UK3(I)*(S4-U1)
      GO TO 60
   55 F3=UF1(I)-UK2(I)*(S3-U1)
      GO TO 60
   50 F3=FUNLMX(I)-UK1(I)*(DEFLP(I)-U1)
   60 SPRFRC(I)=-F3
    1 CONTINUE
      RETURN
      END
      SUBROUTINE ACCEL(NMASS)
C-----------------------------------------------------------------------
      COMMON F(20,30),S(20,30),L(30),
     1    N(20,3),UK1(20),UF1(20),UK2(20),UF2(20),UK3(20),
     2    XREL(20),VREL(20),IUNLD(20),DEFLP(20),FUNLMX(20),SPRFRC(20),
     3    DEFLMX(20),A(30),AP(30),XP(30),IH(20,30),K1(30),V(30),
     4    R9(20),DYNFC(20),C9(20,6),
     5    WM(30),X(30),ACCMX(30),FMULT(20),CLR(30),IFLAG,
     6    TIME,TINC,NPRNT,NFOUT,TPRNT,TFOUT,ITIME
      DO 1 J=1,NMASS
      DG=0.0
      LJ=L(J)
      DO 2 K5=1,LJ
      I4=IH(K5,J)
      CALL DYNLO(I4)
      IF(J.EQ.N(I4,1)) GO TO 15
      DG=DG-SPRFRC(I4)-DYNFC(I4)
      GO TO 2
   15 DG=DG+SPRFRC(I4)+DYNFC(I4)
    2 CONTINUE
      A(J)=DG/WM(J)
      IF(ABS(A(J)).LE.ACCMX(J)) GO TO 1
      ACCMX(J)=ABS(A(J))
    1 CONTINUE
      RETURN
      END
      SUBROUTINE OUTPT(NSPRG,NMASS)
C-----------------------------------------------------------------------
```

```
      DIMENSION VO(30)
      COMMON F(20,30),S(20,30),L(30),
     1    N(20,3),UK1(20),UF1(20),UK2(20),UF2(20),UK3(20),
     2    XREL(20),VREL(20),IUNLD(20),DEFLP(20),FUNLMX(20),SPRFRC(20),
     3    DEFLMX(20),A(30),AP(30),XP(30),IH(20,30),K1(30),V(30),
     4    R9(20),DYNFC(20),C9(20,6),
     5    WM(30),X(30),ACCMX(30),FMULT(20),CLR(30),IFLAG,
     6    TIME,TINC,NPRNT,NFOUT,TPRNT,TFOUT,ITIME
      LF=Z'0A'
      NMP1=NMASS+1
      K5=1
      IF(MOD(ITIME,NPRNT).NE.0) GO TO 25
      TPRNT=TPRNT+TINC*FLOAT(NPRNT)
      V9=V(1)/17.6
      WRITE(2,100)TIME,K5,SPRFRC(1),DYNFC(1),XREL(1),K5,X(1),V9,A(1)
  100 FORMAT(/1X,F6.4,4X,I2,1X,F10.1,1X,F8.1,1X,F7.2,3X,I2,1X,3F8.2)
      NMX=AMAX0(NMP1,NSPRG)
      NMN=AMIN0(NMP1,NSPRG)
      DO 1 K5=2,NMX
      V8=V(K5)/17.6
      IF(K5.GT.NMN) GO TO 120
      WRITE(2,105)K5,SPRFRC(K5),DYNFC(K5),XREL(K5),K5,X(K5),V8,A(K5)
  105 FORMAT(11X,I2,1X,F10.1,1X,F8.1,1X,F7.2,3X,I2,1X,3F8.2)
      GO TO 1
  120 IF(K5.GT.NSPRG) GO TO 200
      WRITE(2,110)K5,SPRFRC(K5),DYNFC(K5),XREL(K5)
  110 FORMAT(11X,I2,1X,F10.1,1X,F8.1,1X,F7.2)
      GO TO 1
  200 WRITE(2,115)K5,X(K5),V8,A(K5)
    1 CONTINUE
  115 FORMAT(44X,I2,1X,3F8.2)
   25 IF(MOD(ITIME,NFOUT).NE.0) GO TO 30
      DO 600 I=1,NMP1
  600 VO(I)=V(I)/17.6
      WRITE(4,499)TIME
  499 FORMAT(F8.5)
      WRITE(4,500)(A(I),I=1,NMP1)
  500 FORMAT(10E13.6)
      WRITE(4,500)(VO(I),I=1,NMP1)
      WRITE(4,500)(X(I),I=1,NMP1)
   30 RETURN
      END
      SUBROUTINE DYNLO(I)
C-----------------------------------------------------------------------
      COMMON F(20,30),S(20,30),L(30),
     1    N(20,3),UK1(20),UF1(20),UK2(20),UF2(20),UK3(20),
     2    XREL(20),VREL(20),IUNLD(20),DEFLP(20),FUNLMX(20),SPRFRC(20),
     3    DEFLMX(20),A(30),AP(30),XP(30),IH(20,30),K1(30),V(30),
     4    R9(20),DYNFC(20),C9(20,6),
     5    WM(30),X(30),ACCMX(30),FMULT(20),CLR(30),IFLAG,
     6    TIME,TINC,NPRNT,NFOUT,TPRNT,TFOUT,ITIME
      IF(VREL(I).GT.C9(I,5)) GO TO 10
      DYNFC(I)=C9(I,1)*(VREL(I)-C9(I,5))+C9(I,2)*C9(I,5)
      GO TO 40
   10 IF(VREL(I).GT.0.0) GO TO 20
```

```
      DYNFC(I)=C9(I,2)*VREL(I)
      GO TO 40
   20 IF(VREL(I).GT.C9(I,6)) GO TO 30
      DYNFC(I)=C9(I,3)*VREL(I)
      GO TO 40
   30 DYNFC(I)=C9(I,3)*C9(I,6)+C9(I,4)*(VREL(I)-C9(I,6))
   40 DYNFC(I)=-DYNFC(I)
      RETURN
      END
      SUBROUTINE INSPRG(NSPRG,AA,BB)
C-----------------------------------------------------------------------
C          INITIALIZES PREVIOUS SPRING DEFLECTION TO ACCOUNT FOR CLEARENCE
      DIMENSION AA(1),BB(1)
      DO 10 J=1,NSPRG
      AA(J)=-BB(J)
   10 CONTINUE
      RETURN
      END
```

```
RUN NO. 3     050 P1 S3 V1
0.001    0.1        200    2    7    6
    1 2357.   0.0      30.0
    2 165.0   0.0      0.0
    3 2248.   0.0      0.0
    4 20.0    0.0      0.0
    5 79.0    0.0      0.0
    6 32.0    0.0      0.0
    7 10.2    0.0      0.0
    1
1.0      0.0
    1    2    5250000. 2000.    250000. 0.0       0.00
0.0      0.0      0.0      0.0      0.0      0.0
0.0      0.0
2000.0   2.50
33000.   4.2
33000.   9.7
33000.   30.0
   2
1.0      0.0
    2    3    3 250000.2500.    5000.    0.        5000.
0.0      0.0      0.0      0.0      0.0      0.0
0.0      0.0
29000.   3.0
29000.   30.0
   3
1.0      6.83
    2    4   22 2680.   200.     78.0     0.0       0.0
0.0      0.0      0.0      0.0      0.0      0.0
0.0      0.0
16.3     1.21
26.9     1.78
79.6     2.63
103.0    2.85
111.4    2.94
148.7    3.28
181.0    3.57
187.7    3.60
231.0    3.72
272.5    3.82
322.8    3.97
366.0    4.06
374.9    4.08
418.8    4.14
467.2    4.21
503.1    4.265
512.0    4.274
527.1    4.29
1092.0   4.76
2450.0   5.515
6862.0   7.160
   4
1.0      8.33
    2    5   1723000.  100.     100.     0.0       0.0
0.0      0.0      0.0      0.0      0.0      0.0
```

```
0.0      0.0
13.2     .214
28.3     .434
47.0     .671
69.9     .95
94.9     1.14
137.6    1.29
202.4    1.37
276.1    1.44
325.9    1.46
1350.0   1.63
1640.0   1.79
2630.0   2.57
3505.0   2.87
4565.0   3.41
5895.0   4.05
15195.0  5.96
   5
1.0      0.0
   4    6  13 23000.  100.     100.     0.0      0.0
5.03     5.03     5.03     5.03     -1000.   1000.
0.0      0.0
33.0     0.6
57.0     1.1
115.     1.46
167.     1.56
220.     1.66
291.     1.73
359.     1.77
422.     1.78
493.     1.81
520.     1.82
547.     1.83
4716.0   3.83
   6
1.0      0.0
   6    7  131000.    200.     190.     0.0      0.0
0.0      0.0      0.0      0.0      0.0      0.0
0.0      0.0
3.3      .148
37.9     .392
117.9    .779
328.1    1.31
198.6    1.77
193.7    2.17
153.8    2.54
118.4    2.9
98.6     3.28
82.2     3.68
71.7     4.07
70.0     40.0
```

```
   8
0.0      0.0
20.0     0.15
20.0     0.6
25.0     1.2
35.0     1.8
70.0     2.4
150.0    2.64
250.0    2.7
```

8

0.0	0.0
1350.0	0.084
1640.0	0.22
2630.0	0.90
3505.0	1.11
4565.0	1.55
5895.0	2.055
15895.0	3.1

```
100 DIM X1(45),X(90),T(45)
110 FOR I=1 TO 45
111 READ T(I)
112 NEXT I
120 DATA 0.46193, -0.71032,  0.10809,  0.46534, -0.11179
130 DATA 0.02809, -0.38776,  0.32800,  0.29154, -0.01035
140 DATA -0.08155, -0.04710,  0.16269,  0.14598,  0.10515
150 DATA -0.02970,  0.01949,  0.03948,  0.13491,  0.10206
160 DATA 0.08549,  0.00164, -0.02334,  0.08463,  0.07260
161 DATA 0.04146,  0.00164, -0.04284, -0.03330,  0.04419
162 DATA 0.02379, -0.00313, -0.00831, -0.04094, -0.00038
163 DATA 0.02501,  0.00253, -0.01502, -0.02452, -0.02127
170 DATA 0.00518,  0.00676, -0.02821, -0.03638, -0.02782
180 FOR I=1 TO 45
190 X1(I)=0!
200 NEXT I
201 FOR I=1 TO 90
210 TIME=.001*I
220 IF I>30 GOTO 250
230 X=0!
240 GOTO 300
250 IF I>39 GOTO 280
260 X=170!*(I-30!)/9!
270 GOTO 300
280 IF I>46 GOTO 230
290 X=170!-170!*(I-39!)/7!
300 FOR J=1 TO 44
305 L=45-J
310 X1(L+1)=X1(L)
320 NEXT J
330 X1(1)=X
340 Y=0!
350 FOR J=1 TO 45
360 Y=Y+T(J)*X1(J)
370 NEXT J
380 PRINT I,TIME,X,Y
390 NEXT I
400 END
```

```
100 DIM X1(45),X(90),T(45),Y(90)
110 FOR I=1 TO 45
111 READ T(I)
112 NEXT I
120 DATA 0.46193, -0.71032,  0.10809,  0.46534, -0.11179
130 DATA 0.02809, -0.38776,  0.32800,  0.29154, -0.01035
140 DATA -0.08155, -0.04710,  0.16269,  0.14598,  0.10515
150 DATA -0.02970,  0.01949,  0.03948,  0.13491,  0.10206
160 DATA 0.08549,  0.00164, -0.02334,  0.08463,  0.07260
161 DATA 0.04146,  0.00164, -0.04284, -0.03330,  0.04419
162 DATA 0.02379, -0.00313, -0.00831, -0.04094, -0.00038
163 DATA 0.02501,  0.00253, -0.01502, -0.02452, -0.02127
170 DATA 0.00518,  0.00676, -0.02821, -0.03638, -0.02782
171 INPUT N3
172 FOR I=1 TO N3
173 INPUT X(I),Y(I)
174 NEXT I
175 YF=0!
180 FOR I=1 TO 45
190 X1(I)=0!
200 NEXT I
201 FOR I=1 TO 90
210 TIME=.001*I
220 N1=2
230 IF I>X(N1) GOTO 270
240 AP=A
250 A=Y(N1-1)+(I-X(N1-1))*(Y(N1)-Y(N1-1))/(X(N1)-X(N1-1))
260 GOTO 305
270 N1=N1+1
280 REM
290 IF N1>N3 GOTO 440
300 GOTO 230
305 FOR J=1 TO 44
310 L=45-J
320 X1(L+1)=X1(L)
330 NEXT J
340 X1(1)=A
350 YP=YF
360 YF=0!
370 FOR J=1 TO 45
380 YF=YF+T(J)*X1(J)
390 NEXT J
400 VSR=VSR+32.2*(A+AP)*.001/2!
410 VFR=VFR+32.2*(YF+YP)*.001/2!
420 LPRINT I,TIME,A,YF,VSR,VFR,VSR-VFR
430 NEXT I
440 STOP
450 END
```

```
      INTEGER*1 F1NAM(11),F2NAM(11),F3NAM(11),DAT(3)
      DIMENSION FD1(50),DD1(50),FD2(50),DD2(50),FD3(50),DD3(50)
      DATA DPR/57.29578/
      DATA DAT/1HD,1HA,1HT/
      DATA F3NAM/1HF,1HD,1HM,1HU,1HT,1HU,1HA,1HL,1HD,1HA,1HT/
      LF=X'0A'
      DO 1 I=1,11
      F1NAM(I)=1H
    1 F2NAM(I)=1H
      WRITE(3,5000)
 5000 FORMAT('   INPUT FILE 1 NAME : ')
      READ(3,5001)(F1NAM(I),I=1,8)
 5001 FORMAT(8A1)
      WRITE(3,5002)
 5002 FORMAT(/'   INPUT FILE 2 NAME :')
      READ(3,5001)(F2NAM(I),I=1,8)
      DO 2 I=9,11
      F1NAM(I)=DAT(I-8)
    2 F2NAM(I)=DAT(I-8)
      CALL OPEN(7,F1NAM,0)
      CALL OPEN(8,F2NAM,0)
      CALL OPEN(9,F3NAM,0)
      READ(7,1000)NFD1
 1000 FORMAT(I4)
      WRITE(3,1000)NFD1
      DO 10 I=1,NFD1
      READ(7,1010) FD1(I),DD1(I)
      WRITE(3,1010) FD1(I),DD1(I)
   10 CONTINUE
      ENDFILE 7
 1010 FORMAT(2F12.0)
      READ(8,1000)NFD2
      WRITE(3,1000)NFD2
      DO 20 I=1,NFD2
      READ(8,1010)FD2(I),DD2(I)
      WRITE(3,1010)FD2(I),DD2(I)
   20 CONTINUE
      ENDFILE 8
      CALL MUTFUN(FD1,DD1,NFD1,FD2,DD2,NFD2,FD3,DD3,NFD3)
      WRITE(9,1100)NFD3,LF
 1100 FORMAT(1X,I4,A1)
      WRITE(3,9001)
 9001 FORMAT('      MUTUAL FORCE-DEFLECTION FUNCTION'/
     1   '       FORCE        DEFLECTION'//)
      DO 300 I=1,NFD3
      WRITE(3,9000)FD3(I),DD3(I)
 9000 FORMAT(2F12.2)
  300 WRITE(9,1110)FD3(I),DD3(I),LF
 1110 FORMAT(2F12.3,A1)
      STOP
      END
      SUBROUTINE MUTFUN(A1,D1,N1,A2,D2,N2,FM,DM,NM)
      DIMENSION A1(1),D1(1),A2(1),D2(1),FM(1),DM(1)
      NM=2
      FM(1)=0.0
```

```
      DM(1)=0.0
       I1=2
       I2=2
       K1=2
       K2=2
  160  IF(A1(I1)-A2(I2))170,180,190
  170  Y0=A1(I1)
       X1=D1(I1)
       X2=D2(I2-1)+(D2(I2)-D2(I2-1))
      1      *(A1(I1)-A2(I2-1))/(A2(I2)-A2(I2-1))
       I1=I1+1
       K1=K1+1
       GO TO 200
  180  Y0=A1(I1)
       X1=D1(I1)
       X2=D2(I2)
       I1=I1+1
       I2=I2+1
       K1=K1+1
       K2=K2+1
       GO TO 200
  190  Y0=A2(I2)
       X2=D2(I2)
       X1=D1(I1-1)+(D1(I1)-D1(I1-1))
      1     *(A2(I2)-A1(I1-1))/(A1(I1)-A1(I1-1))
       I2=I2+1
       K2=K2+1
  200  DM(NM)=X1+X2
       FM(NM)=Y0
       NM=NM+1
       IF(K1.GT.N1.OR.K2.GT.N2) GO TO 500
       GO TO 160
  500  NM=NM-1
       RETURN
       END
```

16	
0.0	0.0
16.3	1.1
26.9	1.6
79.6	2.1
111.4	2.2
148.7	2.3
187.7	2.4
231.0	2.47
272.5	2.52
322.8	2.6
374.9	2.65
418.8	2.69
467.2	2.73
503.1	2.76
527.1	2.77
4188.0	3.77

11

0.0	0.0
13.2	0.213
28.3	0.432
47.0	0.668
69.9	0.945
94.95	1.13
137.6	1.28
202.4	1.36
276.1	1.42
325.9	1.44
10326.0	2.44

```
      INTEGER*1 IFDR(11),IFPD(11),IFBD(11),IFOT(11),IDAT(3)
      DIMENSION FDR(50),DDR(50),PPAD(50),DPAD(50),FBDY(50),DBDY(50),
     1          FOUT(50),DOUT(50),FT(50),DT(50)
      DATA DPR/57.29578/
      DATA IDAT/1HD,1HA,1HT/
      LF=X'0A'
      DO 1 I=1,11
      IFDR(I)=1H
      IFPD(I)=1H
      IFBD(I)=1H
    1 IFOT(I)=1H
      WRITE(3,2000)
 2000 FORMAT('   INPUT DOOR F-D DATA FILE :')
      READ(3,2001)(IFDR(I),I=1,8)
 2001 FORMAT(8A1)
      WRITE(3,2002)
 2002 FORMAT(/'   INPUT PADDING P-D DATA FILE :')
      READ(3,2001)(IFPD(I),I=1,8)
      WRITE(3,2003)
 2003 FORMAT(/'   INPUT BODY F-D DATA FILE :')
      READ(3,2001)(IFBD(I),I=1,8)
      WRITE(3,2004)
 2004 FORMAT(/'   INPUT OUTPUT F-D DATA FILE :')
      READ(3,2001)(IFOT(I),I=1,8)
      DO 2 I=9,11
      IFDR(I)=IDAT(I-8)
      IFPD(I)=IDAT(I-8)
      IFBD(I)=IDAT(I-8)
    2 IFOT(I)=IDAT(I-8)
      CALL OPEN(7,IFDR,0)
      CALL OPEN(8,IFPD,0)
      CALL OPEN(9,IFBD,0)
      CALL OPEN(10,IFOT,0)
      READ(7,1000)NUPD
 1000 FORMAT(I4)
      WRITE(2,3000)(IFDR(I),I=1,11)
 3000 FORMAT('    DOOR COMPLIANCE - FILE : ',11A1,/
     1  '   FORCE   DEFLECTION'//)
      WRITE(2,1000)NUPD
      DO 10 I=1,NUPD
      READ(7,1010) FDR(I),DDR(I)
      WRITE(2,2999) FDR(I),DDR(I)
   10 CONTINUE
 2999 FORMAT(2F10.2)
 1010 FORMAT(2F8.0)
      READ(8,1000)NPAD
      WRITE(2,3001) (IFPD(I),I=1,11)
 3001 FORMAT(///' PADDING PROPERTIES - FILE : ',11A1,/
     1  '   FORCE    DEFLECTION'//)
      WRITE(2,1000)NPAD
      DO 20 I=1,NPAD
      READ(8,1010)PPAD(I),DPAD(I)
      WRITE(2,2999)PPAD(I),DPAD(I)
   20 CONTINUE
      READ(9,1000)NBDY
```

```
      WRITE(2,3002)(IFBD(I),I=1,11)
 3002 FORMAT(///'  BODY COMPLIANCE - FILE : ',11A1,/
     1  '   FORCE    DEFLECTION'//)
      WRITE(2,1000)NBDY
      DO 30 I=1,NBDY
      READ(9,1010)FBDY(I),DBDY(I)
      WRITE(2,2999)FBDY(I),DBDY(I)
   30 CONTINUE
      WRITE(3,1020)
 1020 FORMAT(' ENTER BODY CYLINDER RADIUS : ')
      READ(3,1030)BRAD
 1030 FORMAT(F8.0)
      WRITE(3,1040)
 1040 FORMAT(' ENTER BODY CYLINDER LENGTH : ')
      READ(3,1030)BLEN
      FOUT(1)=0.0
      DOUT(1)=0.0
      DMAX=DPAD(NPAD)
      NDEFL=((DMAX+.01)/0.5)
      DO 100 INC=1,NDEFL
      DEFL= INC*0.5
      IF(DEFL.GE.BRAD) GO TO 110
      B=SQRT(BRAD*BRAD-(BRAD-DEFL)**2)
      ANG=ATAN(B/(BRAD-DEFL))
      GO TO 120
  110 ANG=1.5707963
  120 NANG= ANG*DPR+1
      ANGINC=ANG/NANG
      DO 150 IANG=1,NANG
      CANG=ANGINC*(IANG-1)
      DEFINC=DEFL-BRAD*(1-COS(CANG))
      CALL PRES(DEFINC,PPAD,DPAD,NPAD,P)
      FINC=BRAD*ANGINC*COS(CANG)*P*BLEN
      FOUT(INC+1)=FOUT(INC+1)+2.0*FINC
  150 CONTINUE
      DOUT(INC+1)=DEFL
  100 CONTINUE
      NDEFL1=NDEFL+1
      WRITE(2,3010)
 3010 FORMAT(///'  CALCULATED PADDING PROPERTIES'/
     1  '   FORCE    DEFLECTION'//)
  771 WRITE(2,7771) (FOUT(J),DOUT(J),J=1,NDEFL1)
 7771 FORMAT(2F10.2)
      CALL MUTFUN(FOUT,DOUT,NDEFL1,FDR,DDR,NUPD,FT,DT,NT)
      WRITE(2,3015)
 3015 FORMAT(///'   COMBINED PADDING AND DOOR PROPERTIES'/
     1  '   FORCE    DEFLECTION'//)
  772 WRITE(2,7771)(FT(J),DT(J),J=1,NT)
      CALL MUTFUN(FT,DT,NT,FBDY,DBDY,NBDY,FOUT,DOUT,NOUT)
  230 CONTINUE
      WRITE(2,3020)(IFOT(I),I=1,11),NOUT
 3020 FORMAT(///'   COMPLETE COMPOSITE CHARACTERISTIC - FILE : ',11A1/
     1  ' NO. POINTS = ',I4,/'   FORCE    DEFLECTION'//)
      WRITE(10,7773)NOUT,LF
 7773 FORMAT(I4,A1)
```

```
      DO 300 I=1,NOUT
      WRITE(10,7772)FOUT(I),DOUT(I),LF
 7772 FORMAT(2F8.2,A1)
      WRITE(2,7771)FOUT(I),DOUT(I)
  300 CONTINUE
      WRITE(2,7778)
 7778 FORMAT(' '////)
      STOP
      END
      SUBROUTINE MUTFUN(A1,D1,N1,A2,D2,N2,FM,DM,NM)
      DIMENSION A1(1),D1(1),A2(1),D2(1),FM(1),DM(1)
      NM=2
      FM(1)=0.0
      DM(1)=0.0
      I1=2
      I2=2
      K1=2
      K2=2
  160 IF(A1(I1)-A2(I2))170,180,190
  170 Y0=A1(I1)
      X1=D1(I1)
      X2=D2(I2-1)+(D2(I2)-D2(I2-1))
     1      *(A1(I1)-A2(I2-1))/(A2(I2)-A2(I2-1))
      I1=I1+1
      K1=K1+1
      GO TO 200
  180 Y0=A1(I1)
      X1=D1(I1)
      X2=D2(I2)
      I1=I1+1
      I2=I2+1
      K1=K1+1
      K2=K2+1
      GO TO 200
  190 Y0=A2(I2)
      X2=D2(I2)
      X1=D1(I1-1)+(D1(I1)-D1(I1-1))
     1     *(A2(I2)-A1(I1-1))/(A1(I1)-A1(I1-1))
      I2=I2+1
      K2=K2+1
  200 DM(NM)=X1+X2
      FM(NM)=Y0
      NM=NM+1
      IF(K1.GT.N1.OR.K2.GT.N2) GO TO 500
      GO TO 160
  500 NM=NM-1
      RETURN
      END
      SUBROUTINE PRES(D,PF,DF,NF,P)
      DIMENSION PF(1),DF(1)
      IND=0
      IF(D.LE.DF(1)) GO TO 100
      IF(D.GT.DF(NF)) GO TO 200
      NF1=NF-1
      DO 10 I=1,NF1
```

```
      IF(D.LT.DF(I)) GO TO 10
      IND=I+1
   10 CONTINUE
      I1=IND-1
      P=(PF(IND)-PF(I1))*(D-DF(I1))/(DF(IND)-DF(I1))+PF(I1)
      RETURN
  100 P=0.0
      RETURN
  200 P=PF(NF)
      RETURN
      END
```